Sustainable dry hard turning of AISI 52100 hard steel with new coating material (HSN^2) on carbide insert and simulation of forces

A thesis submitted
in partial fulfillment of the requirements
for the degree of

Doctor of Philosophy

By

Anupam Alok
Roll No.-136103033

Department of Mechanical Engineering

Indian Institute of Technology Guwahati

Guwahati, India

April 2019

Department of Mechanical Engineering
Indian Institute of Technology Guwahati
Guwahati-781039
INDIA

CERTIFICATE

It is certified that the work contained in the thesis entitled "**Sustainable dry hard turning of AISI 52100 hard steel with new coating material (HSN^2) on carbide insert and simulation of forces**", submitted by **Anupam Alok**, Roll No. 136103033 to the Indian Institute of Technology Guwahati for the degree of Doctor of Philosophy has been carried out under my supervision in the Department of Mechanical Engineering, Indian Institute of Technology Guwahati. This work has not been submitted elsewhere for the award of any other degree or diploma.

Dr. Manas Das

Date:

Department of Mechanical Engineering

Indian Institute of Technology Guwahati

Guwahati-781039, Assam, India

Declaration

I declare that this written submission represents my ideas in my own words and where others' ideas or words have been included, I have adequately cited and referenced the original sources. I also declare that I have adhered to all principles of academic honesty and integrity and have not misrepresented or fabricated or falsified any idea/data/fact/source in my submission. I understand that any violation of the above will be cause for disciplinary action by the Institute and can also evoke penal action from the sources which have thus not been properly cited or from whom proper permission has not been taken when needed.

Date:

Anupam Alok
Roll No. 136103033

DEDICATED

TO

MY PARENTS AND FAMILY

ACKNOWLEDGEMENT

"Starting something can be easy; it is finishing that is the highest hurdle". The journey of doctoral study is always a difficult and challenging task. Throughout this long journey, I have gained a lot by learning to persevere despite hardship. I would never have successfully completed this thesis without the assistance of numerous people who I am indebted to. Their direction, advice, support and contributions have proved invariable along the way.

First and foremost, I would like to express my special appreciation and respect to my supervisor, Dr. Manas Das, who has been a tremendous mentor for me. I appreciate all his contributions of time, ideas and funding to make my PhD experience productive and stimulating. I am also thankful to him for the excellent example he has provided as a successful research scientist and professor. The joy and enthusiasm he has for his research were contagious and motivational for me, even during the tough times in my PhD pursuit. A very special gratitude goes to him for encouraging my research. I thank him for his advice on my research, my career, as well as my personal life, which was always been priceless.

I offer my sincere thanks to my doctoral committee members, Dr. R. Ganesh Narayanan, Dr. Pankaj Biswas and Prof. Subrata K. Majumder for their insightful comments and encouragement, and also for the hard questions which incented me to widen my research from various perspectives.

My sincere gratefulness to past and present departmental heads Prof. A. K. Dass and Prof. S. K. Dwivedy for their kind permission for enrollment, registration and several important supports at IIT Guwahati. I am also grateful to all the faculty members of Mechanical Engineering Department for giving me a comfortable and friendly environment for pursuing my research.

I would like to express my special sense of gratitude to Mr. Jitesh Gosalia for providing the facility of PVD coating in his lab.

Next, I would like to express my special sense of gratitude to Mr. Nandan Kanan Das, assistant workshop superintendent and all the staffs of the workshop specially Mr. Dhaneswar Khaklary, Mr. Mrinal Sarma, Mr. Dilip Chetri, Mr. Chandan Banikya, Mr. Ali, Mr. Bijoy Kumar Choudhury, Mr. Upen Gohain and Mr. Minesh Ch. Medhi for extending their help in fabrication of experimental setup and various other experimental work. I sincerely acknowledge the assistance received from Mr. Saiffuddin Ahmed, Mr. Sanjib Sarma, Mr. Jiten Basumatary and Mr. Pranjol Paul in various experimental proceedings. I also wise to express my gratitude to the Central Instruments Facility, IIT Guwahati for providing technical support.

"A good friend is like a four leaf clover hard to find and lucky to have", I have been fortunate to be surrounded myself by some amazing friends, Jitendra Kumar, Anwesa Barman, Kelli Durga Prasad, Abhinav Kumar, Kishor Kumar Gajani, Manjesh Kumar, Ambrish Singh, Kuldeep Dewangan, Vikash Kumar, Arvind Kumar Agarwal, Kamal Kumar Basumatary, Soumya Ranjan Nanda, R. Vignesh Babu, Firdausa Ahmed, Nitashree Gogoi, Hirok Basumatary. Thank you all for your support and encouragement. I am also thankful to internship students for their support. It is my pleasure to acknowledge the help provided by my seniors, juniors and internship students, and all other lab members from our lab.

"The love of a family is life's greatest blessings". In this precious moment of my life, I would like to express my deep sense of gratitude to my parents, Mr. Satyanarayan Prasad Saday and Mrs. Sangyan Saday for their love, blessings and constant encouragement throughout my life. I would like to thank my brother Amit Alok and sisters Pratibha Rashmi, Prerna Rashmi for their love and best wishes. I want to offer my sincere gratitude to all extended members of my family. You have always been inspiring, supporting and teaching me to understand the true value of human life.

Anupam Alok

ABSTRACT

The low cost machining of britle materials is a challenging job for any industries. EN 31 (AISI 52100, hardness 55 HRC) is one of the difficult-to-cut steel alloys and it is commonly used in shafts and bearings. Nowadays, it is becoming a challenge to develop a cutting tool insert material for economical machining of extremely tough and hard steels. Generally, CBN and PCBN tools are used for machining of hardened steel. However, machining cost using these tools becomes higher due to high tool cost. For this purpose, carbide tool using selective coatings is best substitute having comparable tool life while its cost is approximately one-tenth of CBN tool. In this work, a newly developed 2nd generation TiAlxN super nitride (i.e. HSN^2) is selected for PVD coating on carbide tool insert and further characterized using TGA and DSC for oxidation and thermal stability at high temperature. Later, HSN^2 coated carbide inserts are successfully tested for their sustainability to expected tool life for turning AISI 52100 steel. In the present study, forces, surface finish and tool wear are used as a measure to appraise the performance of hard turning process. Experimentally, it is found that speed, feed and depth of cut have considerable impact on forces, tool wear and surface roughness of the machined surface. Further, a relationship is built between input process parameters i.e. cutting speed, feed and depth of cut with output responses i.e. main cutting, radial and feed forces, maximum flank wear and surface quality of work piece. Statistical design of experiment is used to examine the consequence of cutting parameters on machinability prospects. Also, the regression models are developed to correlate between input process parameters with output responses. Further, the cutting parameters are optimized using response surface method and validated using confirmation tests. From confirmation test, it is observed that the percentage error for main cutting force, radial force, feed force, surface roughness and flank wear are 4.3%, 3.33%, 6.8%, 6.2% and 0.05%, respectively. The maximum value of the observed tool wear is 292 µm which is acceptable as per ISO Standard 3685. It is found that the cutting speed is the most effective parameter among all output responses.

In the field of hard turning, the study of white layer is most interesting research topic among scientific community. White layer is one of the main reasons for cutting tool insert failure or excess insert wear. Also, the machined surface quality is affected due to the white layer. Hence, in the present thesis an attempt has been made to examine the development of white layer in hard turning at different cutting speeds. All the experiments are executed on AISI 52100 grade steel (having hardness 55 HRC) with newly developed HSN^2 coated carbide insert having fresh edge for each experiment. Field emission scanning electron microscope, optical microscope and X-ray diffraction are used to analyze white layer at different cutting conditions on

machined surface as well as bulk material. In addition, micro hardness of the machined surfaces is measured. Also, workpiece surface and chip temperatures are studied. Based on analysis of white layers at different cutting speeds, it is observed that low cutting speed is more dominant factor for the formation of white layer during hard turning of AISI 52100 steel. The thickness of white layer reduces with increased cutting speed and its maximum thickness (6.5 µm) is found at lowest cutting speed of 100 m/min and their relationship is justified from analysis of X-ray diffraction peaks. Also, weight percentage of retained austenite in machined surface is calculated from XRD analysis and its highest value of 28.5 % is observed at lowest cutting speed of 100 m/min and it's value reduces with higher cutting speed as compared to base material (6.5%).

In the present study, hard turning operation of AISI 4340 work piece is simulated using finite element based software package ABAQUS® while subjected to given loads or boundary conditions to accurately determine the responses. The model created is an idealization of the real physical system to yield accurate solutions. This advancement in technology helps in fast creation, analyze and production of products satisfying demands. It is difficult to obtain output responses at the deformation zone through practical experiments. In the present work, the cutting force and temperature for the orthogonal cutting of AISI 4340 steel with Al_2O_3 coated tungsten-based cemented carbide cutting inserts are predicted for different cutting speeds with a fixed feed and depth of cut. To study the plastic deformations that occur into the workpiece, Johnson-cook materials model is used.

TABLE OF CONTENTS

LIST OF FIGURES VII

LIST OF TABLES IX

NOMENCLATURE XI

Chapter 1 Introduction to hard turning process 1

1.1 Introduction 1

1.2 Hard turning 2

1.2.1 Environmental concerns during machining 2

1.2.2 Complications in hard turning 3

1.2.3 Cutting tool materials 3

1.2.4 Cutting tool coatings 5

1.2.5 Coating techniques 7

1.3 White layer formation 8

1.4 Simulation of hard turning 9

Chapter 2 Literature survey 11

2.1 Introduction 11

2.1.1 Forces, tool life, and surface roughness 11

2.1.2 White layer 18

2.1.3 Force modeling 19

2.2 Gaps in the literature 21

2.3 Motivation for the present thesis 21

2.4 Objectives of the thesis 21

2.5 Organization of the thesis 22

Chapter 3 Preliminary experimental investigation 25

3.1 Introduction 25

3.2 Experimental investigation 27

3.3 Workpiece material 28

3.4 PVD coating of tool insert 28

3.4.1 Characterization of the coating 29

3.4.2 Physical-chemical properties of coating 30

3.5 Preliminary experiments 31

3.6 Statistical one variable at a time (OVAT) Experiments 32

3.7 Results and discussion 33

3.7.1 Forces 33

3.7.2 Surface roughness 34

3.7.3 Maximum flank wear (VB_{max}) 36

3.8 Chip analysis 39

3.8.1 Geometry of the chip 40
3.8.2 Results and Discussion 42
3.8.2.1 Chip thickness 42
3.8.2.2 Chip reduction ratio 43
3.8.2.3 Shear angle 43

3.9 Summary 44

Chapter 4 Statistical design of experiments 45

4.1 Introduction 45

4.2 Experimental investigation 49
4.2.1 Work piece material, tool and its geometry 49

4.3 Design of experiments 50

4.4 Results and discussion 51
4.4.1 ANOVA study 51
4.4.2 Validation of the present model 54
4.4.3 Forces 55
4.4.4 Surface roughness 60
4.4.5 Maximum flank wear (V_{Bmax}) 62

4.5 Multi-objective optimization of process parameters 64

4.6 Confirmation tests 65

4.7 Summary 66

Chapter 5 White layer analysis 67

5.1 Introduction 67
5.1.1 Formation of white layers 68

5.2 Details of experiments 70
5.2.1 Work piece material, tool and its geometry 70

5.3 Sample preparation for white layer characterization 71

5.4 Results and discussion 72
5.4.1 Workpiece and chip temperature 72
5.4.2 Depth of white layer 74
5.4.3 XRD analysis of white layer 75
5.4.4 Microhardness 78

5.5 Summary 79

Chapter 6 Simulation of orthogonal hard turning operation 81

6.1 Introduction 81

6.2 Materials and method 82
6.2.1 2D FEM formulation of orthogonal cutting 82
6.2.2 Boundary conditions 83
6.2.3 Element formulation 83
6.2.4 Material model 84
6.2.5 Contact properties 86
6.2.6 Explicit dynamic analysis 86

6.2.7 Arbitrary Lagrangian Eulerian 86

6.3 Results and discussion 86

6.3.1 Validation of cutting force model 87

6.4 Summary 88

Chapter 7 Conclusions and scope for future work 89

7.1 Conclusions 89

7.1.1 Preliminary experimental investigation 89

7.1.2 Statistical design of experiments 90

7.1.3 White layer analysis 91

7.1.4 Simulation of orthogonal hard turning operation 92

7.2 Scope for future work 92

REFERENCES 93

PUBLICATIONS 109

LIST OF FIGURES

Fig. 1.1 *Growth of production in the German machine industry (Cselle et al., 2009)* _____6
Fig. 1.2 *Standard coatings develop in last three decades (Cselle et al., 2009)* _____6
Fig. 2.1 *Representation of the factors influencing machining performance (Jawahir, 1988)* 12
Fig. 3.1 *Hard turning experimental set up* _____28
Fig. 3.2 *(a) Ultrasonic bath, (b) fixture for tool insert, and (c) PVD CC800®/9 ML set up* _29
Fig. 3.3 *Elemental analysis of (a) HSN^2 coated carbide insert, and (b) uncoated carbide insert* _____29
Fig. 3.4 *Thermogravimetric analysis (TGA) and Differential Scanning Calorimetry (DSC) plots at different temperature for HSN^2 coating in air* _____30
Fig. 3.5 *Effect of cutting speed on (a) flank wear and work piece surface roughness and (b) mesured forces comaring two different coating thickness* _____31
Fig. 3.6 *comparison between maximum flank wear of two different coating thickness (a) 12 micron (b) 8 micron at 288 m/min cutting speed* _____32
Fig. 3.7 *Effect of (a) cutting speed (f=0.1 mm/rev, d=0.08mm), (b) feed (V_c=170 m/min, a_p=0.08 mm), and (c) depth of cut (V_c=170 m/min, f=0.1 mm/rev) on cutting tool forces* __34
Fig. 3.8 *Effect of (a) cutting speed (f=0.1 mm/rev, d=0.08mm), (b) feed (V_c=170 m/min, d=0.08 mm), and (c) depth of cut (V_c=170 m/min, f=0.1 mm/rev) on surface roughness (R_a) of the workpiece* _____35
Fig. 3.9 *Flank wear of the tool at different cutting speeds; (a) 100 m/min, (b) 130 m/min, (c) 170 m/min,(d) 222 m/min, and (e) 288 m/min for f= 0.1 mm/rev and a_p =0.8 mm* _____37
Fig. 3.10 *Flank wear of the tool at different feed rates; (a) 0.06 mm/rev, (b) 0.08 mm/rev, (c) 0.12 mm/rev,and (d) 0.14 mm/rev for V_c =170 m/min and a_p = 0.8 mm depth* _____38
Fig. 3.11*Flank wear of the tool at different depth of cut; (a) 0.04 mm, (b) 0.06 mm, (c) 0.1 mm, and (d) 0.12 mm for V_c=170 m/min and f= 0.1 mm/rev* _____38
Fig. 3.12 *Effect of (a) cutting speed (f=0.1 mm/rev, d=0.08 mm), (b) feed (V_C=170 m/min, d=0.08mm), and (c) depth of cut (V_C=170 m/min, f=0.1 mm/rev) on flank wear of the tool* _39
Fig. 3.13 *Schematic diagram of chip generation during turning* _____41
Fig. 3.14 *Chip morphology at V_c = 130 m/min, f = 0.1 mm/rev and a_p= 0.08 mm* _____42
Fig. 3.15 *Variation of chip thickness at different (a) cutting speed and (b) feed* _____42
Fig. 3.16 *Variation of chip reduction ratio at different (a) cutting speed and (b) feed rate* _43
Fig. 3.17 *Variation shear angle at different (a) V_c and (b) f* _____44
Fig. 4.1 *Photograph of hard turning experimental set up* _____49
Fig. 4.2 *Validation tests to compare between experimental Vs. predicted responses (with % error) for (a) forces F_f, F_p, F_c and maximum flank wear (VB_{max}) and (b) Ra value* _____55
Fig. 4.3 *(a) Effect of cutting speed at different feed rate on (a) main cutting force (Fc), (b) radial force (Fp) and (c) feed force Ff* _____56
Fig. 4.4 *Effect of feed rate on (a) F_c, (c) F_p and (e) F_f at different cutting speed; 3D surface plots showing combined effect of feed and cutting speed on (b) F_c, (d) F_p and (f) F_f* _____57
Fig. 4.5 *Effect of depth of cut on (a) main cutting force (Fc), (c) radial force (Fp) and (e) feed force Ff) at different feed; 3D surface plots as combined effect of depth of cut and cutting speed on (b) F_c (d) F_p and (f) F_f* _____58

Fig. 4.6 *Effect of (a) cutting speed, (b) feed and (c) depth of cut on total cutting force (F_m)* 59
Fig. 4.7 *Effect of (a) cutting speed, (b) feed and (d) depth of cut on work piece surface roughness; 3D surfaceplots showing combined effect of (c) feed and cutting speed and (e) depth of cut and cutting speed on work piece surface roughness.* 61
Fig. 4.8 *(a) Crater and flank wear, (b) Flank-wear area (A_f), width of flank wear (VB) and VB_{max} in zone B, notch wear (VN) in zone N, and nose wear (VC) in zone C (Trejo-Hernandez et al., 2010).* 62
Fig. 4.9 *Effect of (a) cutting speed, (b) feed and (d) depth of cut on maximum flank wear ; 3D surface plots of combined effect of (c) feed and cutting speed and (e) depth of cut and cutting speed on VB_{max}.* 63
Fig. 5.1 *EDX analysis of AISI 52100 steel workpiece before machining* 71
Fig. 5.2 *Schematic diagram showing preparation of sample from hard turned bar* 72
Fig. 5.3 *Temp. plot of machined surface along with chip with time at 100 m/min cutting speeds* 73
Fig. 5.4 *Temperature plot of machined surface along with chip at different cutting speeds* 73
Fig. 5.5 *(a) FESEM micrograph at 100 m/min cutting speed, and optical images of white layer at (b) 100, (c) 171 and (d) 288 m/min cutting speeds* 74
Fig. 5.6 *White layer thickness variation plot at different cutting speeds* 75
Fig. 5.7 *Comparison of diffractograms between base material and machined surfaces at (a) 100, (b) 131, (c) 171, (d) 220 and (e) 288 m/min cutting speeds* 76
Fig. 5.8 *Microhardness plot along radially below machined at different cutting speeds* 78
Fig. 6.1 *2D computational domain of hard turning with mesh configuration and dimensions* 82
Fig. 6.2 *Boundary conditions on cutting tool and workpiece* 83
Fig. 6.3 *Simulated main cutting and feed force plots with time at 100 m/min cutting speed* 87
Fig. 6.4 *Effect of cutting speed on (a) main cutting force and (b) feed force* 87
Fig. 6.5 *Effect of feed rate on (a) main cutting force and (b) feed force* 88

LIST OF TABLES

Table 3.1 *Process parameters during hard turning* _____ *33*
Table 3.2 *Process parameters during hard turning* _____ *40*
Table 4.1 *Elemental composition (wt %) of AISI 52100 steel* _____ *50*
Table 4.2 *Cutting parameters with ranges* _____ *50*
Table 4.3 *Experimental table based on CCRD and measured responses* _____ *51*
Table 4.4 *ANOVA for forces F_f, F_p, F_c* _____ *52*
Table 4.5 *ANOVA for Ra and VB_{max}* _____ *54*
Table 4.6 *Experimental conditions for validation tests.* _____ *55*
Table 4.7 *Tool failure criteria as per ISO standard 3685 (Mia et al. 2016).* _____ *62*
Table 4.8 *Constraints for optimization* _____ *64*
Table 4.9 *Optimization of the process parameters.* _____ *65*
Table 4.10 *Confirmation tests* _____ *65*
Table 5.1 *Process parameters and their range for experimentation* _____ *70*
Table 5.2 *Comparison between base material and machined surfaces at different cutting speeds in terms of FWHM and retained austenite content (wt. %)* _____ *77*
Table 6.1 *Hard turning process parameters* _____ *82*
Table 6.2 *Johnson-Cook parameters for AISI 4340 (Ucun and Aslantas, 2010)* _____ *85*
Table 6.3 *Material properties of AISI 4340 workpiece, carbide tool and Al_2O_3 coating (Ucun and Aslantas, 2010)* _____ *85*
Table 6.4 *Thermal conductivity of carbide tool and Al_2O_3 coating (Ucun and Aslantas, 2010)* _____ *85*

NOMENCLATURES

F_m	Total machining force
δ	Degree of segmentation
$\bar{\sigma}$	Equivalent flow stress
$\dot{\bar{\varepsilon}}$	Plastic strain rate
$\bar{\varepsilon}$	Equivalent plastic strain
$\dot{\bar{\varepsilon}}_0$	Reference strain rate
$\theta_{melting}$	Melting temperature
θ	Process temperature
θ_{room}	ambient temperature
$\Delta\bar{\varepsilon}$	Increment of equivalent plastic strain
$\bar{\varepsilon}_f$	Equivalent strain at failure
$\emptyset$	Shear angle
A	Initial yield stress
A_f	Flank-wear area
B	Hardening modulus
C	Strain rate dependency coefficient
d	Pitch of serrated chip
D	Damage parameter
d_{ch}	Segment distance
E	Elastic modulus
f	Feed
F_c	Main cutting force
F_f	Feed force
F_p	Radial force
m	Thermal softening coefficient
n	Work hardening coefficient
p	Length
P	Hydrostatic pressure
t_{max}	Maximum chip thickness
t_{min}	Minimum chip thickness
TW	Tool wear

V_B	Flank wear
VB_{max}	Maximum flank wear
V_c	Cutting speed
VC	Nose wear in zone C
VN	Notch wear
α	Thermal expansion coefficient
θ_{melt}	Melting temperature
θ_{room}	Room temperature
ν	Poisson's ratio
ρ	Density

ACRONYM

Al_2O_3	Aluminum oxide
ALE	Arbitrary Lagrangian Eulerian
ANOVA	Analysis of variance
BCC	Body center cubic
CBN	Cubic boron nitride
CCRD	Central composite rotatable design
Cr	Chromium
CrN	Chromium nitride
CrTiAlN	Chromium titanium aluminium nitride
CVD	Chemical vapour deposition
DOE	Design of experiments
EDX	Energy dispersive X-ray
FCC	Face center cubic
FEM	Finite element method
FESEM	Field emission scanning electron microscope
FWHM	Full width half maxima
HiPIMS	High power impulse magnetron sputtering
HSS	High speed steel
IR	Infrared
MRR	Material removal rate

MT-CVD	Medium Temperature CVD
PCBN	Polycrystalline cubic boron nitride
PCD	Polycrystalline diamond
PVD	Physical vapour deposition
RSM	Response surface methodology
Si_3N_4	Silicon nitride
Ti	Titanium
TiAlN	Titanium aluminum nitride
TiC	Titanium carbide
TiCN	Titanium carbo-nitride
TiN	Titanium nitride
V	Vanadium
W	Tungsten
W-EDM	Wire-electro discharge machine
Zr	Zirconium

Chapter 1 Introduction to hard turning process

1.1 Introduction

Manufacturing is constantly changing nowadays due to certain key factors like resource limitation, competition in the global market and increase in expectation of customers. The importance of health and environmental factors related to the use of metal cutting fluids are growing. Simultaneously, the demand for dry and near dry machining using wear resistant tool materials are also increasing. Enhancement of surface quality, tight tolerance and high accuracy in manufacturing are few of the key drivers to the progress of cutting technology. Byrne et al. (1995) observed that these factors have direct impact on cutting tool material, its geometry, cutting parameters and work piece material.

Machining is one of the most important manufacturing processes in any industry. Machining in broad term encompasses several manufacturing processes like turning, milling, drilling, finishing, grinding, lapping, honing and so on. Machining processes are widely adopted because of high dimensional tolerances and surface quality that can be attained. Processes like metal cutting, metal forming, metal joining and metal casting are the pillars of any manufacturing industries. One of the most important manufacturing processes for any industry is the metal cutting operation. The main principle of a metal cutting process is the removal of metal through shearing action due to the relative motion between the work piece and a sharp cutting tool.

One of the traditional machining processes for obtaining cylindrical, conical or tapered parts is turning. Turning is a machining process of generating external surfaces of revolutions on a rotating work piece employing a traversing cutting tool. It has a long back history as early as 1300 BC when Egyptians developed the lathe. In the starting age, manpower was utilized in lathe machines to rotate the work piece and to move the cutting tool. Further, people started using mechanical power for work piece rotation. In this era, fully automated lathe is used. In this process a single point turning tool of relatively harder material compared to work piece and having a sharp cutting edge is fed against the rotating work piece. The cutting action takes place due to the fracture of work piece material at shear zone so as to remove unwanted part for producing desired geometry.

1.2 Hard turning

Hard tuning is done for material having hardness greater than 45 HRC using a variety of slanted cutting inserts namely cubic boron nitride (CBN), polycrystalline cubic boron nitride (PCBN), ceramics and coated carbide. Although, for achieving better surface finish at high feed, grinding is a good option, however, hard turning can also produce good surface finish at significantly higher material removal rate (MRR). Although, the process is performed at small feed and depth of cut, however, the machining time for hard turning is 60% lesser than the conventional turning. Manufacturers all over the world do hard turning as low cost solution to preserve the price of their manufactured goods competitive in the market. Worldwide, an enormous pressure is there on the manufacturer due to the demand for better quality of the machined part at lower price. According to the market demand, everyone looks for the cost effective manufacturing process with higher product quality.

In the automotive industries, generally very hard materials are required. Currently, the predominant method for finishing these parts like gears, shafts, bearings and pinions is grinding because of its features like easy to operate and control. However, the grinding process has some serious drawback like it takes longer time to finish due to its fixed shape of bonded wheel. Also, it has an issue with the cost increment due to the use of coolant. Shaped wheel is used as a solution to the first problem, however, it is very expensive. Furthermore, the use of coolant has its own environmental hazards associated with its use and disposal. These issues gave rise to the efforts to develop a cost effective and environmentally safe process to finish hardened parts to the similar level as of grinding. Nowadays, due to the improvements in machine tool rigidity and due to the development of PCBN cutting tools, hard turning is gaining ground as a cost-effective alternative to grinding. For continuous cuts, the high tool-tip-temperature during dry turning anneals (or, softens) the pre-cut area of work piece lowering its hardness value which makes the material easier to shear. This explains the advantages of increasing cutting speed during hard turning. Cutting without coolant provides obvious cost benefits as well.

1.2.1 Environmental concerns during machining

Nowadays, environmental concerns are very important factor for any industry. Hence, every industry calls for the reduction of cutting fluid in metal cutting practices. In recent time, effective consumption of cutting tool in machining is an important focus for researchers. The performance

of cutting tool depends on process parameters and cutting environment. A cutting fluid is used to boost the tool life and to improve surface quality. Although, there are some benefits of cutting fluids in machining process, however, it contains environmentally harmful or potentially damaging chemical constituents which can be inhaled by the operators causing respiratory irritation, asthma, pneumonia, dermatitis and several types of cancers in oesophagus, skin, lung, pancreas, colon etc. Dry machining has the benefits of non-pollution of the atmosphere and water. It also has benefits in reduction of the disposal and cleaning cost without any danger to human health. Due to this, dry machining has become popular with regards to the non-pollution of the environment with low production cost.

1.2.2 Complications in hard turning

For better cutting during hard turning, some requirements like insert's quality, work piece hardness, coolant condition etc. should be fulfilled (Sivaraman and Prakash, 2017). The recent trend in manufacturing technology put tremendous pressure on manufacturing industries for higher productivity with lesser cost as well as lower machining time. Hence, the manufacturing industries are trying to reduce the machining cost to improve the quality of the machined parts and to machine hard and brittle materials easily. Hard turning with high speed reduces the machining time leading to improved machining efficiency. While machining ferrous and hard materials such as steel, cast iron and super alloys, the softening temperature and the chemical stability of the tool material restrict the cutting speed. The need for enhancement of productivity of manufacturing processes imposes the acceleration of the design and evolution of improved cutting tools to achieve superior tribological attainment and wear-resistance. Improved high speed machining is the main concern of mechanical engineering over last few decades. Therefore, the development of newer cutting tools with respect to material and design to improve the quality of the products is going on.

1.2.3 Cutting tool materials

Cemented carbide is the most widely used insert material. Machining operations which requires complex cutting tools like reamers, drills, broaches, taps and milling cutters etc. use high speed steel (HSS). HSS is used for 40% of total tool material and rest 60% considers other materials. Powder metallurgy is the process behind making of cemented carbides using certain particular type of carbides like tantalum carbide, titanium carbide, tungsten carbide and niobium

carbide. The percentage of hard particles lies somewhere between 60 to 90%. The international organization for standardization (ISO) uses the symbol M (yellow color, alloyed tungsten carbide grades) for machining nickel based super alloy, steel and ductile cast iron, P (blue colour, highly alloyed tungsten carbide grades) for machining steel and K (red colour, straight tungsten carbide) for machining grey cast iron, nonmetallic material and nonferrous alloys. A number is assigned to each grade in the group to denote its position from maximum hardness to maximum toughness. The rating for M grade is from 10 to 40, for K grade 1 to 40 and for P grade 1 to 50.

Cobalt enrichment is one of the fields of development in carbide inserts. Higher concentration of cobalt binder improves toughness of outer layer while maintaining core material hard. Collectively cemented carbides, ceramic plus metals are called as 'cermet' comprising hard particles based on titanium carbonatite, titanium carbide and titanium nitride rather than tungsten carbide (WC). Cermet has higher resistance to abrasive wear, higher chemical stability and hot hardness, and minimal tendency for oxidation wear than cemented carbide. However, it has lesser toughness and strength than cemented carbide. Vast range of cermet's application takes care a certain range of cutting speed and feed.

Ceramic tool materials are used in milling and turning of super alloys, cast iron and finishing of hard materials. Ceramic tool materials can be further classified on the basis of matrix materials i.e. Al_2O_3 and Si_3N_4. Ceramics have the properties like inertness to chemicals, high hardness and high resistance to wear. Ceramics minimize wear by chemical erosion and adhesion. High strength is one of the characteristics of these materials that avoid plastic deformation during machining.

PCBN and CBN are harder than ceramics or cemented carbides and have exceptionally high hot hardness. CBN is widely used for machining of ferrous materials when cutting temperature is relatively high. The main chemical and physical properties of CBN are stability at elevated temperature, chemical inertness and hot hardness. At 750 °C temperature, the hardness of CBN is still equivalent to the of tungsten carbide and oxide ceramics at normal temperature. According to several studies, polycrystalline diamond (PCD) is considered as the hardest material and has higher resistance to abrasive wear as compared to any other insert materials. However, the main problem with PCD inserts is its high affinity to ferrous materials. PCD tool inserts are very helpful in the cutting of highly abrasive aluminum alloy having low tensile strength, high silicon content nonferrous and nonmetallic material, copper, zinc and the alloys of these metals.

Although in actual practice, no material possesses all the required properties of an insert. The material properties of bulk material and its requirement at the surface are completely different.

The insert's surface must possess the property of low thermal conductivity, high hardness, low frictional coefficient and must be inert chemically. Bulk material must have high thermal conductivity so that it can take away the heat penetrated in the insert. The bulk material should be sufficiently strong and tough enough so that it resists chipping or breakage of insert due to impact forces. Besides that, uncoated inserts are unable to sustain high temperature generated during dry machining. Coating is a layer that is generally 5 µm thick and it prevents the tool from getting worn out while increasing tool life. Hence, inserts are coated to satisfy different requirements.

1.2.4 Cutting tool coatings

The demand for economic and environmental friendly manufacturing processes in the field of sustainable manufacturing is increasing rapidly. Hence, commercialization in the field of coating of tool materials is also increased. It is considered as one of the best solution to address the environmental issues faced in wet machining. Figure 1.1 shows the growth of production in German machine industry, where, during 3rd millennium's first decade there has been a remarkable growth in surface treatment industry. The surface treatment industries made an approximate 110% growth as compared to base year of 2000, with major contribution in thin film coating technologies mostly from Europe (72%) and USA (54%). High demand for coatings in Indian market, specifically in the metal working industries, is also forcing the manufacturers to supply high end efficient tools. As analyzed by International Monetary Fund (IMF), the Indian sub-continent is among one of the top four countries in the world in terms of their Gross Domestic Product (GDP) after USA, China and Japan (Adwani, 2012). Coating technologies for cutting tools have undergone rapid development in past few years as shown in Fig. 1.2. In 1980, only TiN coating was used and until 1988 only CrN and TiCN coatings were used. 14 standard coatings were available in 2000. Nowadays, many tool materials are coated with differently structured soft/hard layers of coating to increase gains in tool life and to increase its productivity by applying higher cutting speeds.

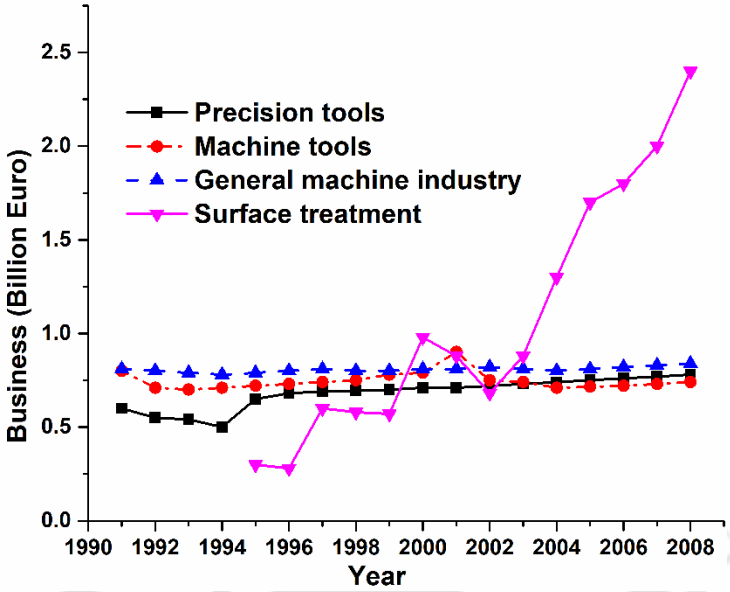

Fig. 1.1 Growth of production in the German machine industry (Cselle et al., 2009)

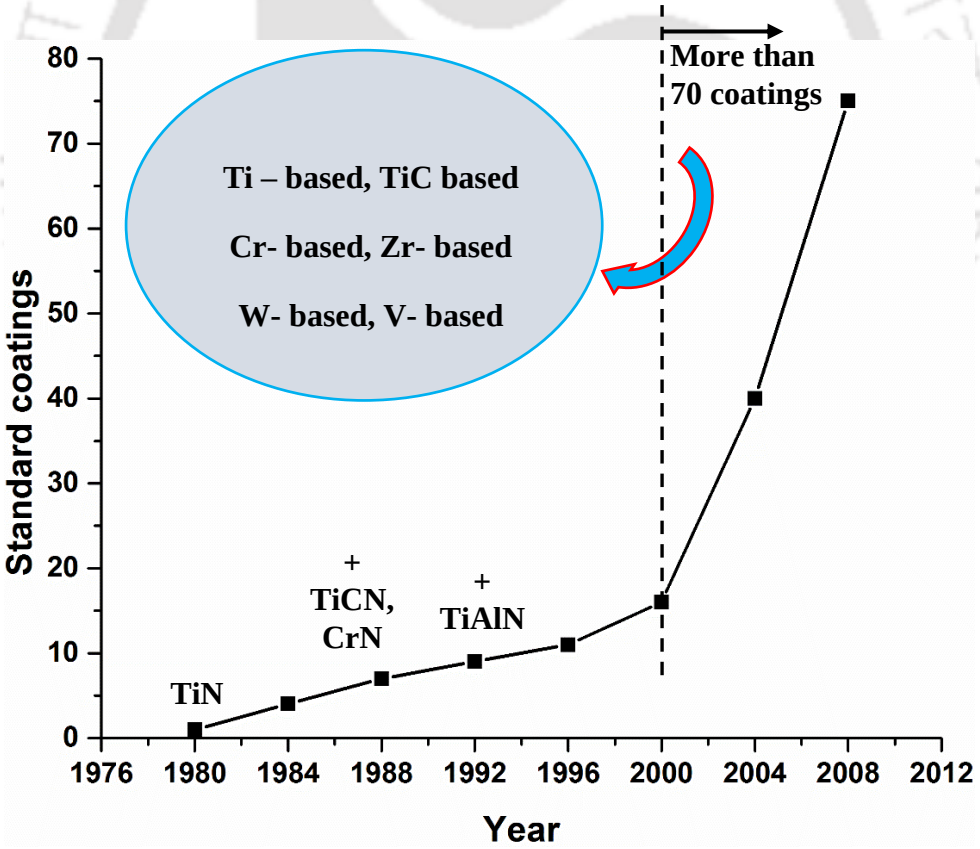

Fig. 1.2 Standard coatings developed in last three decades (Cselle et al., 2009)

Presently, there are 70 different types of coatings with different chemical compositions are available in the market. Two different coating techniques such as chemical vapour deposition

(CVD) and physical vapour deposition (PVD) are largely used in manufacturing sector for applying coating on carbide tools. Coating can alter the performance of cutting process by increasing resistance to few particular types of tool wear, changing heat generation, friction or heat flow which is basically the reason behind such rapid development of coating technology and the popularity of coated tools in metal cutting industries. Coatings are quite harder, provides high abrasion resistance to the cutting edge and its high temperature resistance enables to transfer maximum amount of generated heat to the chips. As coating reduces the frictional coefficient, the chip thickness ratio decreases. Therefore, a reduction in the cutting force is observed. Materials used in coating have extremely low solubility in iron at the machining temperature and therefore protects the tool from heat affected wears such as diffusion, chemical and oxidation wear. One more advantage of using coatings is that it acts as a lubricant preventing the chips to stick to the inserts and therefore reduces friction. Along with coating's beneficial effects on contact and tribological phenomena, the structure and other properties of coating should be decided considering specific tool-work piece combinations and the conditions under which machining process is taking place.

1.2.5 Coating techniques

Coating techniques can be classified into two categories namely, Chemical Vapor Deposition (CVD) and Physical Vapor Deposition (PVD). CVD process involves transportation of reactants to the reaction chamber where, they are activated thermally either by thermal methods or by means of laser or plasma, in the vicinity of the substrate, which deposits the reactants in the form of solid on the substrate surface. The substrate surface is generally pre-heated to about 900°C prior to deposition. In case of deposition on carbide substrates, CVD induces tensile residual stress. This is due to the difference in coefficient of thermal expansion of the substrate material and the coating. In order to enhance the toughness, a new technique of CVD is implemented called as MT-CVD (Medium Temperature CVD), where deposition temperature ranges from 700 to 900°C. This leads to the development of cobalt enriched layer near the substrate surface thus providing better toughness. MT-CVD with shorter coating cycles is also helpful in reducing residual stress and development of a tougher tool cutting edge.

PVD relies on the process of condensation of material vapors on the substrate thereby, generating a coating on the substrate. Process such as ion plating, evaporation and sputtering comes under this category. In order to generate the material vapor of the coating, the substrate is heated

up to evaporation temperature. This is usually done by resistive heating, electron beam heating, laser heating etc. This cloud of generated vapor is then condensed onto the substrate to achieve coating. Coating by sputtering is a technique that uses a target coating material which is bombarded with ions resulting in ejection of target material which is deposited on the substrate. In the process of ion plating, the substrate is set to negative potential and ionized target material is made to deposit on the substrate. PVD uses less than half of the temperature required by CVD. This lower processing temperature results in less thermal cracking of fine grains, low coefficient of friction and a smooth and bright coating. Coating of sharp edges and chip breakers are also possible with PVD. For coating of cutting tool materials generally PVD techniques such as ion plating, electron beam evaporation, cathodic arc evaporation, closed field unbalanced magnetron sputtering, and high power impulse magnetron sputtering (HiPIMS) are used. HiPIMS is a pulsed PVD technique that produces highly ionized target material. For sputtering application into the target material, this high energy power pulses (generally in the range of MW) creates a highly energetic plasma which provides high power density of the sputtering process. Application of HiPIMS for the sputtering process in case of tool coating results in improved coating structure as compared to conventional methods. The coatings generated by HiPIMS shows an increase in hardness to Young's modulus ratio which indicates higher toughness of the coatings. HiPIMS also produces denser and more thermally stable coatings as compared to the conventional ones.

1.3 White layer formation

One of the important feature of hard turning is the formation of white layer which needs special attention. Three mechanisms are mainly responsible for white layer formation as discussed below.

- The plastic flow mechanism produces a homogeneous structure or very fine grain structure.
- The formation of white layer due to quick heating and cooling mechanism during hard turning.
- Surface reaction such as, carburizing, nitriding, and ploughing is another probable reason for the formation of white layer.

Cooling rate also plays a major role in the white layer formation. Because of austenite having higher density than ferrite, the transformation temperature will reduce with specific cutting

pressure. The generation of heat caused by high strain rate reduces the necessary stress for deformation. The hardness and the transformation temperature are significantly affected by the quench rate in case of low carbon steel. Grain refinement which is generated due to severe plastic deformation at moderate cutting speed results in white layer formation by hard turning of steels (in this case AISI 52100) using hard coated inserts. Whereas, at higher cutting speeds, the white layer formation is due to the phase transformation. Four aspects that need to be considered during analysis of white layer formation while grinding are chemical composition, surface structure characteristics, microstructure and micro-hardness. White layer formed during grinding is more strained than in turning. A turned white layer is etching resistant while the ground one is not. Also. the turned white layer has more retained austenite than ground one. White layer at all cutting speeds in turning has very fine grains compared to bulk material.

Schwach and Guo (2005) experimentally studied surface integrity and fatigue life of machined component. They found that with increased tool wear, tensile residual stress and white layer depth increase. Also, compressive residual stress increases deep into the subsurface at higher tool wear. Favorable surface integrity and improved fatigue life were seen with decreased feed rate and increased cutting tool sharpness. With higher feed and negative tool rake angle, white layer thickness during turning increase.

1.4 Simulation of hard turning

The two basic methods of metal cutting using a single point tool are orthogonal or 2D, and oblique or 3D. Orthogonal cutting occurs when the cutting face of the tool is at right angle (90˚) to the path or the line of action of the tool. Study of chip formation and its morphology provides sufficient information on the cutting process. It depends mainly on the cutting conditions and the properties of the work piece material (Trent and Wright, 2000). Many physical parameters, such as, cutting force, tool wear, temperature, coefficient of friction between tool-work piece interface, machining power, surface finish are affected by the chip morphology and chip formation process. Nowadays, finite element method (FEM) is widely used for simulation and analysis of material removal processes, supported by highly developed computers and software packages. Along with minimizing the need for high cost and time consuming experimental setups, it also predicts the difficult to measure variables such as stress, strain and machining temperature.

It shows how adequately the selection of the input parameters reflects the deformation process involving chip formation. The currently used FEM based software includes

ABAQUS®/Explicit, Advantage®, Deform® 2D/3D etc. Deform® 3D has specifically a module for the modeling of metal cutting simulation under machining category providing advanced algorithms like Adaptive Lagrangian Meshing which focuses on both residual stress and temperature. However, ABAQUS® /Explicit uses mainly Lagrangian method for the simulation purpose and fits the best to our use. The simulation results provide information about different parameters accounting for the behavioral changes in the machining process.

In typical turning of hardened surfaces, the chip load area is rather small due to the smaller depth of cut and low feed. As a result, net cutting force and energy consumption may not be larger while cutting hardened steel than cutting soft steels. When a soft steel bar is turned with a cutting tool and is fed along the axial direction of the work piece, the principle cutting force (tangential) is the largest among the three force components. However, in case of hard turning, the depth of cut is small and the nose radius is large, so chip formation takes place near the nose radius and hone or chamfer of the cutting tool. As a result, the radial force can increase more and more and becomes the largest force component as the material hardness increases.

Chapter 2 Literature survey

2.1 Introduction

In the present age of economic growth, the need of industries is to produce high quality machined parts and components. With the help of proper selection of machining process and cutting parameters, the required aim can be achieved. In this field, hard turning is one of the suitable machining processes. Hard turning is a machining process which has its own consequences to be considered. It requires an adamant and cost effective machine tool which produces better surface finish or, at least, comparable to that of grinding. There are many factors like cutting parameters, tool geometry and tool wear which affects process performance. There are some important process responses such as cutting forces, surface finish, white layer generation and residual stress, which have been taken up by the researchers across the globe, to characterize the process. In the present chapter, a detailed picture of the state of the art in hard turning is discussed. In machining process cutting forces play an important role in order to predict power consumption and process efficiency. It also helps in studying tool wear and cutting temperature.

2.1.1 Forces, tool life and surface roughness

Figure 2.1 shows some important factors which are associated with machining performance (Jawahir, 1988). In this section, literature available on different aspects of performance measures namely, tool life, surface roughness and cutting forces under dry machining condition with most frequently used coated carbide tools is presented. Cutting forces can provide better understanding of the machining process as they directly relate to the cutting condition and tool condition during machining. Normally, when the depth of cut is lesser than the nose radius of the tool in finish hard turning operation, radial component of the tool force is more dominant than others. With variable horn radius, the value of tangential force becomes more than radial force thus increasing cutting efficiency. At low cutting speed, higher cutting force is encountered due to low cutting temperature and built-up edge formation. Higher speed results in higher cutting temperature thus reduced force due to softening of the workpiece. It is observed that radial force is highly sensitive to the work piece hardness, negative rake angle and tool wear evolution. It is observed that cutting force is mostly influenced by depth of cut than by feed or speed. The force modelling shows that cutting force increases with increasing feed, depth of cut and nose radius. In machining, the cost

effectiveness of the process is important factor, hence, a basic understanding about cutting conditions and process variables are required.

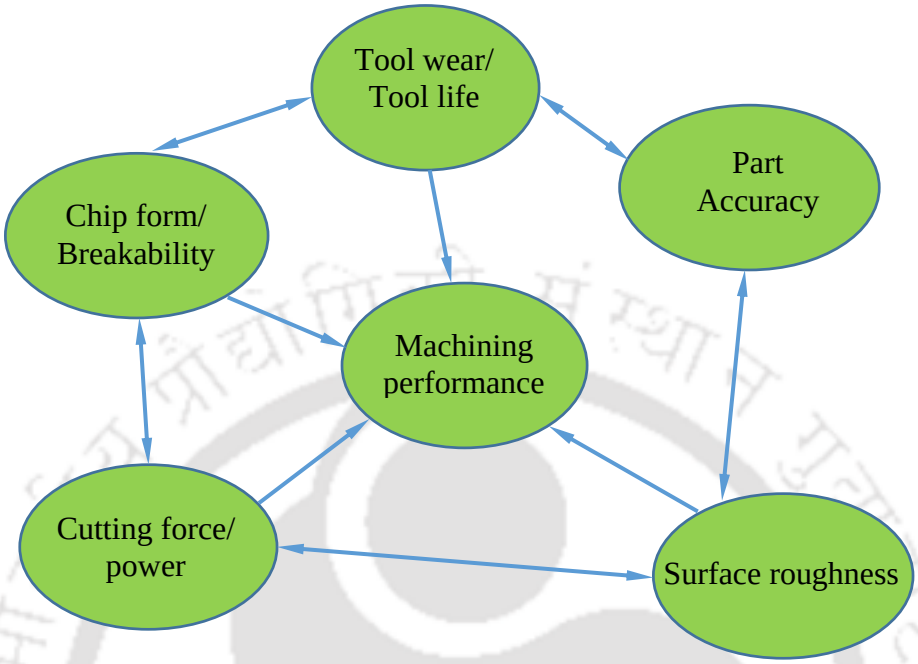

Fig. 2.1 Representation of the factors influencing machining performance (Jawahir, 1988)

Panda et. al (2018) studied flank wear during hard turning of AISI 52100 steel by using both multi-coated carbide and mixed ceramic insert at different cutting parameters. They found that the value of flank wear for both the tools are within acceptable limit of 0.3 mm. Kumar et. al (2018) observed the performance of both uncoated and Al_2O_3 coated carbide inserts for hard turning of AISI D2 steel having hardness 55 HRC. They found that the uncoated tool completely failed during machining. Kumar et. al (2018) analyzed machining performance while turning Inconel 825 alloy with TiAlN, AlCrN, TiAlN/AlCrN coated carbide insert and its comparison with uncoated carbide insert. They found that the performance of TiAlN/AlCrN coated insert is better in terms of forces, surface roughness and the tool wear.

Sahoo and Sahoo (2012) studied surface roughness, chip morphology, cutting force and flank wear during hard turning of AISI 4340 steel with uncoated as well as two different multilayer coated carbide tools ($TiN/Al_2O_3/TiN/TiCN$ and $TiN/TiCN/ZrCN/Al_2O_3$). They found that the tool life of multilayer $TiN/Al_2O_3/TiN/TiCN$ coated carbide tools was more as compared to $TiN/TiCN/ZrCN/Al_2O_3$ coated carbide and uncoated inserts. Also, the cutting temperature in case of multilayer coated carbide inserts was relatively lower. Further, they developed a regression model which can predict surface roughness of cold worked high chromium tool steel (22 HRC) with coated carbide tools during turning operation. From ANOVA, they concluded that surface

roughness is mostly affected by feed followed by cutting speed and depth of cut (Sahoo and Sahoo, 2012).

Fang et al. (2011) compared and analyzed the effect of both sharp and round edged tools in orthogonal cutting. From their analysis it was inferred that cutting force variation is more stable in case of sharp tool than the round edge tool. Li et al. 2012 studied the progression of tool failure during milling of Ti-6Al-4V at high speed with multilayer CVD coated carbide tool. An increase in cutting force and cutting temperature was observed as tool wear progresses (Li et al., 2012).

Suresh et al. (2012) experimentally concluded that hard turning gives more advantages over grinding which includes higher productivity owing to higher MRR, minimum cost for processing, enhancement in material properties, etc. They carried out experimental investigation using multilayer TiN/TiCN/Al_2O_3 CVD-coated cemented carbide tools while turning hardened AISI 4340 steel (48 HRC). Machining force were minimized by adjusting process parameters and an optimal machining condition was obtained while keeping lower value of feed and depth of cut at higher cutting speed. To reduce the cutting force, higher cutting speed was selected. The cutting power and insert wear increase almost linearly with the increase in feed and cutting speed. Surface roughness can be minimized by providing lower feed rate at higher cutting speed. Also, they claimed that at higher cutting speed, the temperature at the contact zone increases considerably and consequently, tool wear progresses rapidly in case of hard turning. After analyzing the effect of cutting parameters and cutting time, Suresh et al. 2012 concluded that surface roughness and force can be minimized by optimizing depth of cut, feed and machining time while maintaining higher cutting speed.

Asilturk and Akkus (2011) did optimization of machining parameters, using Taguchi method to reduce surface roughness during turning process of hardened AISI 4140 steel with TiC and Al_2O_3 coated carbide inserts. They summarized that the factors affecting surface roughness are feed rate, cutting speed and depth of cut (Asiltürk and Akkuş, 2011).

Aneiro et al. (2008) studied how the response parameters like insert temperature, cutting forces, tool wear and surface roughness are affected by input factors while using two different inserts namely Al_2O_3/TiN/TiCN coated carbide and PCBN. It was found that coated carbide tool is most suitable for medium hardened steel for achieving maximum productivity. They summarized that depth of cut is the most significant factor affecting cutting force and temperature. The coated carbide has very long tool life with very low flank wear. Although the life of coated carbide tool was approximately half of PCBN for same machining parameters, however, hard

machining is more economical for coated carbide insert owing to its lower cost (one-tenth price) as compared to costly PCBN.

Different researchers (Tuffy et al. 2004; Mubarak et al. 2008; Sargade et al. 2011) analyzed how the characteristics of TiN coatings deposited on tungsten carbide tools is being influenced when coating thickness is varied between 1.8–6.8 μm during machining of carbon steels. The best turning performance was found in case of TiN coating with thickness of 3.5 μm on carbide inserts. They came up with the conclusion that the reason behind the coating failure in thicker coating is because of higher level of compressive stresses due to the chipping off of the cutting-edge in coating material.

Cakir et al. (2009) investigated how different coating layers and various cutting parameters affect output responses such as work piece surface roughness. For this analysis, they used multi-layer CVD coated Al_2O_3/TiN/TiCN and single-layered PVD coated TiAlN while turning AISI P20 tool steel having hardness 52–55 HRC. They found feed as most influencing parameter for surface roughness followed by cutting speed. However, depth of cut was found as insignificant factor. Also, while using CVD-coated inserts at higher cutting speed, the surface roughness is further increased. However, the variation in surface roughness in case of PVD–coated inserts was almost negligible at higher cutting speed. Owing to the dissimilar behavior of two different coated inserts against cutting speed, the author suggested the need of further analysis regarding tool life (Cakir et al., 2009).

Better surface finish was observed with PVD-coated single-layer TiAlN inserts by some group of researchers (Ezugwu and Okeke, 2002; Ramesh et al., 2009; Ibrahim et al., 2009) while machining titanium and nickel based alloys. Few researchers also observed that tool life is improved in case of multi-layer CVD coatings (Unesco. et al., 1986; Ezugwu and Okeke 2002; Ibrahim. et al., 2009). However, in another analysis by some group of researchers (Moreno et al., 2010; Dobrzanski and Golombek, 2005), it was found that thin layer of TiAlN/TiN or TiN/(Ti,Al,Si)N/TiN coated tools having coating thickness less than 4 μm performs almost same or far better than cemented carbide inserts having thick layer (greater than 10 μm) of TiCN/Al_2O_3/TiN coating.

The behaviour of carbide multi-layer TiCN/Al_2O_3/TiN coated tools was analyzed by Lima et al. (2005) in order to analyse the applicability of these tools during cutting of hardened steel having high hardness values. During turning of hardened AISI 4340 steel having different hardness values viz. 23, 35, 42 and 50 HRC, cutting forces, tool life and wear mechanism were evaluated.

From their analysis it was found that even at lower value of MRR, the coated carbide tools were not able to machine the work piece with hardness as high as 50 HRC. Also, experimentally it was revealed that the relation between work piece hardness and machining force was not linear. The magnitude of cutting force was maximum and that of thrust force was less than cutting force. Therefore, feed force being the least in magnitude. The principal mechanism of wear as observed was abrasion wear, often followed by abrupt fracture after a considerable cutting time (Lima et al., 2005).

The surface roughness model was developed by Sahin and Motorcu (2005) for turning with TiN coated carbide inserts. The first and second-order models were developed based on experimental data of response surface methodology (RSM). According to their analysis it was found that the main governing factors for surface roughness was feed followed by cutting speed. At the same time, they observed that the effect of depth of cut was not significant. During machining with coated carbide tools, the influence of feed, cutting velocity and side cutting edge angle (SCEA), on machining force and surface roughness was analyzed by Noordin et al. (2004). Their study revealed that it is the feed that affected the tangential force and surface roughness mostly. Apart from that they also noticed the influence of SCEA and the interaction effect of feed and SCEA on the surface roughness which was secondary. They also observed the contribution of SCEA, the interaction effect of feed and SCEA, and the cutting speed in determining the magnitude of tangential force.

Aouici et al. (2012) investigated the effect of feed, cutting speed, work piece hardness and depth of cut on surface roughness and cutting force during hard turning. AISI H11 steel was hardened to 40, 45 and 50 HRC and further turned using CBN inserts. Further, a regression model for surface roughness was developed using the RSM technique. Their experimental results indicated that the most important parameters that affected cutting force were depth of cut and work piece hardness. However, surface roughness was greatly influenced by feed and work piece hardness.

Dogra et al. (2012) analyzed tool wear as well as the machined surface properties using both carbide and CBN tool. The carbide tool was found to be more economical than expensive CBN tool. Experimentally they found that in case of CBN tool, the tool life is more. However, for carbide tool the total machining time of all the four cutting edges was found to be close to the machining time of single cutting edge of CBN tool. Similarly, they observed that the surface integrity (white layer formation, microhardness and surface roughness) achieved with carbide tools was

comparable with that of CBN tools. They observed abrasion and adhesion wear mechanisms at low and medium cutting speed and chipping and breakage of tool edge at higher cutting speed for coated carbide tool. However, abrasion at low and medium cutting speed and adhesion wear at high cutting speed were observed using CBN tool. They also claimed that the cost of machining per cutting edge with carbide tool is approximately one-eighth of CBN tool. Thus, at any cutting speed less than 140 m/min and within the domain of the selected feed and depth of cut, carbide tool could become an economical alternative to costly CBN tool for finish turning of hardened steel (Dogra et al., 2012).

It is hereby confirmed from the literature review that adequate studies were performed to evaluate relative performance of different coatings. The post machining surface roughness was the main interest during hard turning with PVD–coated single layer TiAlN and CVD–coated multi-layer TiCN/Al_2O_3/TiN carbide inserts. The study of tool wear was not focused which is also have considerable share in determining machining performance viz. the quality of the product, tolerance etc. However, few analyses were made with a view to evaluate the tool wear progression considering nickel and titanium alloys as work piece material.

Various analysis was carried out to optimize output responses essentially surface integrity and forces involved in machining. Although, tool life is a very important factor, however, it was not considered during optimization of process parameters. Hence, it is justified to develop a reliable model for machining of hardened steel to optimize the performance of coated carbide tools. With the recent advancement in the modern technology of metal cutting processes, the manufacturing of goods at higher cutting speed and feed has become possible, however, at the same time, the machining processes are accompanied with undesirable tool wear. Effective tool wear monitoring system helps to optimize the use of tools and it reduces damages to the machine tool, downtime and scrapped components to a great extent. Though there are vast amount of literature available in the field of reliable tool monitoring system, however, hardly any of these systems were found successful for industrial application owing to the complex nature of measurement techniques (Dimla, 2000).

Direct measurement techniques are complex in nature which involve optical or chemical analysis of tool particles being carried away by the chip. The indirect measurement techniques include acoustic emission (AE), cutting force, vibration, etc. For tool wear detection and breakage, AE signals and cutting forces are found to be promising techniques. In order to correlate the AE signals (Kakade et al., 1994; Yan et al., 1995) or temperature (Lin, 1995; Dhar et al., 2006; Korkut

et al., 2011) at the cutting edges with tool wear many attempts were made. Although, AE is not an appropriate indicator of tool wear, however, it has been found to be very effective in detecting tool fracture.

Pal et al. (2011) concluded that tool wear detection must be precise as machining with a dull tool influences the machining performance and at the same time economy of the machining process is greatly influenced by replacing the tool before its actual tool life. Also, they developed a neural network-based sensor fusion model for tool wear monitoring in turning to minimize production cost. Also, an optimum cutting condition was obtained by progressive tool wear information (Pal et al., 2011). From experimentation, a relationship between flank wear area and cutting forces has been established by Sikdar and Chen (2002) for turning operation and it was found that with increased flank wear area, all three components of force increase. Choudhury and kishore (2000) developed a regression model from experimental results to predict flank wear of an uncoated tool as a function of various parameters viz. force ratio (feed force to cutting force), cutting speed, feed, depth of cut and diameter of the work piece (AISI 4340 steel). However, this model is not applicable in case of turning with a coated carbide tool for the same work piece (Choudhury and Kishore, 2000). Oraby and Hayhurst (1991) developed mathematical models to describe wear versus time and wear versus force relationships for various phases of tool wear. The flank wear was found to have more effect on the magnitude of the feed and radial force. Also, radial force is most sensitive to nose wear. However, the wear–time model failed to estimate the wear level at a very high tool wear rate (Oraby and Hayhurst, 1991). The experimental relationship between wear and cutting power was described by Cuppini et al. (1990). However, their model did not consider important parameters like work piece properties, cutting speed, feed and depth of cut which is supposed to have considerable effect on tool wear. The relationship between tool wear and surface finish was established by Siller et al. (2009) which is used during face milling of hardened alloys for tool and work piece condition monitoring.

Zhou et al. (2003) observed that in hard turning the value of radial/passive force is highest among all force components due to very small depth of cut and nose radius. Chinchanikar and Choudhary (2013) investigated the nature of forces during hard turning with coated carbide tool. Higher value of cutting force is observed for harder work piece with CVD coated tools. However, in case of harder workpiece, reduction in cutting forces occurred especially at higher feed and depth of cut due to thermal softening of the work piece (Chinchanikar and Choudhury, 2013).

Suresh et al. (2012) observed that at a constant feed, the machining force decreases with increased speed and with further increase in feed, the force increases.

2.1.2 White layer

White layer being most important feature of hard turning needs special attention. Research is going on regrading formation of white layer for different machining process. Aramcharoen et al. (2008) analyzed the formation of white layer during hard turning of H13 tool steel (57 HRC) with two different types of coated carbide inserts i.e. CrTiAlN and CrTiAlN/MoST. They found that at lower speed, the value of white layer thickness is 2.0 and 1.7 µm for uncoated and CrTiAlN coated carbide inserts, respectively. Also, for CrTiAlN/MoST coated carbide insert, an intermittent thickness of white layer as compared to above came out at lower speed. At higher cutting speed keeping other parameters constant, no white layer is detected (Aramcharoen et al., 2008). Chou and Evans (1999) analyzed white layer depth during turning of AISI 52100. They found that white layer depth initially increases with cutting speed and at a critical cutting speed the formation of white layer is reduced or saturated.

Bosheh and Mativenga (2006) analyzed the formation of white layer at different cutting speeds. They also observed the effect of white layer on the work piece hardness. They concluded that the depth of white layer decreases at higher cutting speed. The decrement in the surface temperature at higher cutting speed is the main reason for this trend (Bosheh and Mativenga, 2006). Ramesh et al. (2005) observed the formation of white layer during hard turning of AISI 52100 hard steel. They found that at low to medium cutting speed, the generation of white layer is due to the grain refinement which leads to plastic deformation. However, at high cutting speed, thermally driven phase transformation is the main reason for the formation of white layer (Ramesh et al., 2005).

Shi et al. (2006) analyzed that the white layer thickness for machining of AISI 5200 hard steel with ceramics as well as CBN cutting inserts for both dry and wet conditions at different cutting speed and feed. Also, the nose radius and rake angle are varied during experimentation. They found that white layer thickness increases with increased cutting speed, feed and nose radius. Also, white layer thickness decreases for wet condition (Shi et al., 2006). Bartarya and Choudhury (2016) observed that the white layer produced on work piece subsurface during hard turning of H13 steel with CBN tool, was harder than the bulk material (Bartarya and Choudhury, 2016).

2.1.3 Force modeling

Lotfi et al. (2018) conducted 3D FEM simulation of tool wear during ultrasonic assisted rotary turning of AISI 4140 steel and the results are compared with conventional turning process. Johnson-Cook material's model is used for defining material properties. They investigated heat generation, surface roughness and cutting force for vibratory-rotary motion. They found that this method is very useful and the calculated value of tool wear and heat generation are low (Lotfi et al., 2018). Pervaiz et. al. (2018) performed 2D orthogonal FEM based simulation for machining Ti6Al4V for predicting forces, temperature and Von–Misses stress. They used two different material models like power law (PL) and Johnson Cook (J–C) material model. They found that PL model provided realistic saw tooth segmented chip formation with associated cyclic tangential and thrust cutting forces.

Akbar et al. (2010) validated experimental results with the simulated one for forces and chip thickness while turning AISI/SAE 4140 steel using carbide inserts. For simulation, they used a 2D orthogonal model and fully coupled themo-mechanical FEM model. They studied heat partition between tool and chip. They concluded that heat partition plays a great role in determining stresses, chip morphology, chip-tool interface temperature and tool-chip contact length (Akbaret al., 2010).

A 2D orthogonal cutting model using FEM for the prediction of chip morphology was developed by Priyadarshini et al. (2012) while machining AISI 4340, AISI 1045 and Ti6Al4V workpieces and the effect of friction, mesh and material models are analyzed. Seven different friction models were studied for the analysis of chip morphology and cutting forces. CPE4RT element was used as kinematic contact algorithm. A small gap was provided for the formation of chip, however, no fracture criterion was used. An intermediate layer was provided to set the direction of cutting. This layer specified the damage model. Arbitrary Lagrangian Eulerian (ALE) was used to prevent excessive displacement. For segmented chip, coupled analysis showed good correlation with the forces. Different vaules of Johnson–Cook parameters are applied from literature which showed different results. However, at higher cutting speed all frictional models showed similar results.

Xie et al. (2005) used ABAQUS® FEM code with CPE4RT element to predict tool wear. They used three steps during simulation; in first two steps, the tool was considered as rigid and in third step they considered it as deformable. Movahhedy et al. (2000) compared between different FEM formulations i.e. ALE, Lagrangian and Eulerian model using Deform–2D software package. According to them, no node separation criterion is required for ALE formulation.

Takabi et al. (2007) discussed the benefits of ALE model than Lagrangian and Eulerian models for orthogonal simulation using ABAQUS software package for turning 42CrMo4. They used coulomb's friction model and Johnson–Cook materials model and employed coupled dynamic method for analysis. ALE formulation was found to be better than Eulerian and Lagrangian formulations. Shi and Liu (2004) compared different material models i.e. Johnson–Cook, Litonski-Batra, Bodner–Partom, and power law models using ABAQUS 6.2 for orthogonal turning of HY-100 steel. They found that Litonski–Batra model predicts some forces better than other three material models. The chip morphology and residual stresses vary in all four models. The prediction of chip thickness and shear angle are found to be closer to experimental results for all four models (Shi and Liu, 2004).

Miguélez et al. (2006) studied both FEM and analytical modelling for orthogonal cutting. They also studied both Lagrangian and ALE approaches. They found that no element deletion criterion is required for ALE formulation. They concluded that analytical models are time saving (Miguélez et al., 2006). Mabrouki and Rigal (2006) studied thermo–mechanical analysis for the prediction of chip morphology in hard turning. They studied varying thermal contact conductance and fractional friction energy conversion to heat. In this study they showed that material is removed by adiabatic shearing due to localized deformation. The chip is mostly affected due to heat evacuation (Mabrouki and Rigal, 2006).

Ozel (2006) used different friction models in FEM formulation to analyze hard machining. A FEM based software package, Deform®–2D was used for the simulation while machining LCFCS material with P20 grade carbide tool. Lagrangian method with implicit integration technique was used during simulation. He found that the chip–tool interface friction models have significant effect on the chip morphology as well as on forces and stress distribution (Özel, 2006).

Özel and Zeren (2005) did dynamic-explicit- Arbitrary Lagrangian Eulerian (ALE) formulation based for FEM analysis of high speed machining of AISI 1045, 4340 steels and Ti6Al4V with round edge cutting tools. From simulation, they found a very high deformation zone near tool nose area. They predicted very high and localized temperature at the tool–chip interface due to the application of proper friction model (Özel and Zeren, 2005). Pantale et al. (2004), observed unsteady chip formation with the help of 2D and 3D FEM models. They used damage law for the analysis considering cutting tool as rigid body.

2.2 Gaps in the literature

After carefully analyzing the literate survey, the following gaps in literature are observed as discussed below.

- Very less number of published literature is available for hard turning with coating thickness higher than 4 – 5 µm.
- Very less number of published literature is available for turning of hard material having hardness more than 50 HRC. Particularly, literature about hard turning on AISI 52100 steel with hardness 55 HRC is limited with coated carbide tools.
- The performance of carbide insert with HSN^2 (2nd generation of TiAlxN super nitride) coating for machining of hard material has also been less explored.
- Coating thickness is also an issue in the field of hard machining.
- Very less number of literature is available on the characterization of coating.
- Insufficient literature in the field of formation of white layer and the reason behind its formation during hard machining with fresh tip of cutting insert is noticed.

2.3 Motivation for the present thesis

On the basis of previous literature, it is found that low cost machining of hard material is a very challenging job for the industries. The main issue during machining of hard material is the selection of cutting tool insert. Generally, CBN and PCBN are used for the cutting of hard material. However, due to their higher price, limits their usage in industry. In the field of hard machining, finding the usability of cheaper coated carbide inserts for machining of harder material (more than 50 HRC) motivated the present work. Also, white layer formation during hard turning is an important study which also motivated the present work.

2.4 Objectives of the thesis

Cutting tool plays a very important role in the field of hard turning process. However, the main issue in the selection of cutting tool is the cost and the capability of the cutting tool for machining hard materials. The motivation behind the use of the coated carbide insert for machining hard material having hardness more than 55 HRC, is due to the lack of information through experimental investigation regarding its performance. Also, very less information is available

regarding coating thickness. Considering above gap in literature, the following objectives have been attempted in the present thesis as discussed below:

- Selection of coating material on the basis of their properties (thermal and oxidation stability, hardness) and determination of coating thickness based on preliminary experimental study on hardened steel (AISI 52100, hardness 55 HRC).
- Selection of different cutting parameters along with their experimental range during preliminary experimental investigation while using newly developed coated carbide inserts (HSN^2). Analysis of cutting force and surface roughness for the selected cutting parameters. Also, analysis of tool wear at different cutting conditions.
- Statistical design of experiments within the selected range of process parameters and multi-objective optimization study for the selection of significant cutting parameters and their optimum values for machining hardened steel using coated carbide inserts. Detailed study regarding the analysis of effect of process parameters on output responses.
- Analysis of white layer thickness on machined surface at different cutting speeds using different optical and scanning electron microscope and its further validation using XRD analyses. Determination of retained austenite and phase change of the machined surface before and after machining using XRD analysis. Also, examination regarding the change in hardness of the sample with white layer thickness generated at different cutting conditions.
- Simulation of hard turning process for cutting force analysis during machining AISI 4340 steel having hardness 52 HRC with Al_2O_3 coated carbide insert using a FEM based software package ABAQUS®.

2.5 Organization of the thesis

The thesis is organized into seven chapters with references. A brief introduction to the hard turning process is discussed in **Chapter 1.** In the introduction part, each and every aspect of hard turning is discussed like cutting forces, surface roughness, tool wear and white layer formation during machining.

The literature survey concerning different aspects of hard turning like cutting forces, surface roughness, tool wear and white layer formation are discussed at different sections in **Chapter 2**. Literature review focuses on dry cutting performance to get limiting cutting condition of coated

carbide inserts during high speed machining. Also, gap in literature and objectives of the thesis is discussed.

In **Chapter 3**, preliminary experimental investigation regarding performance analysis of a new type of coating material i.e. HSN^2 on carbide insert during hard turning of AISI 52100 hard steel having 55 HRC hardness is carried out. Also, the range of thickness of the coating is optimized experimentally. Further, few characterization study regarding properties of the coating such as thermal and oxidation stability, hardness of the coating are conducted.

In **Chapter 4** central composite rotatable design (CCRD) of design of experiments (DOE) technique has been used to plan the experiments. Optimization of the process parameters of hard turning process is conducted to achieve optimized value of process parameter at which the cutting will be ideal for this combination of tool and workpiece. Also, ANOVA study is carried out to find out most effective process parameters and their percentage contribution.

In **Chapter 5**, white layer analysis of the machined surface is carried out. In this chapter a relationship is established between cutting speed and white layer thickness and is verified with XRD analysis. Also, the effect of white layer on work piece hardness is observed.

In **Chapter 6**, simulation of hard turning and further validation with experimental results have been carried out. A system of dry hard turning is modelled with FEM based software package ABAQUS® subjected to given loads and boundary conditions. The model created is an idealization of real physical system for yielding accurate solution. The main objectives of the simulation study are to optimize the material removal process by increasing tool life and by producing better surface integrity. It is difficult to obtain output responses at the deformation zone through practical experiments. In the present work, cutting force is predicted for orthogonal cutting of AISI 4340 steel with Al_2O_3 coated tungsten-based cemented carbide inserts at different cutting speeds for constant feed and depth of cut. Further, the predicted values of the cutting forces are validated with the experimental results. To study the plastic deformation that occurs into the workpiece, Johnson–cook material's model is used.

Discussion about the conclusions and findings of the present work with future scope are presented in **Chapter 7**. The references are added at the end.

Chapter 3 Preliminary experimental investigation

3.1 Introduction

Hard turning has been securing its acceptance in many industries throughout last two decades. The strong affinity towards hard turning as it can possibly replace grinding operation. Hard turning is a better solution than grinding process in various industries like ball bearings, transmission shafts, axles, engine components, and flap gears, etc. where hardened steels are extensively used. Generally, hard turning is carried out on work piece material with a hardness greater than 45 HRC (Mia and Dhar, 2017). Hard turning is advantageous over grinding operations because it can be carried out in a dry condition, greater flexibility in producing better surface finish on either continuous or interrupted surface (Bartarya and Choudhury, 2012; Khan et al., 2017). Several researchers analyzed cutting forces as well as surface finish throughout hard turning. It was noticed from literature that during finish-hard turning operation, the tool nose radius is more than the value of depth of cut (a_p) and the radial direction of force dominates on the other forces (Mondal et al., 2016). Bagaber and Yusoff (2017) analyzed the possibility of minimum power consumption in the turning process of SS 316 steel at lower cutting speed with uncoated carbide tool (Bagaber and Yusoff, 2017). However, few researchers reported that because of built up edge formation and generation of low temperature at reduced cutting speed there is a rise in main cutting force (F_c). With the increase in cutting speed, there is a diminution in the cutting force because of work piece material softening due to the generation of elevated cutting temperature (Ebrahimi and Moshksar, 2009). Generally, PCBN, CBN and ceramics are used for hardened steel machining (Dogra et al., 2012; Ferreira et al., 2016). However, this is not a cost effective way of turning hardened steel due to their higher price. During machining, two important purposes are mostly considered are to achieve high dimensional accuracy and high surface finish at a lesser cost. Also, it is required to target the machining operation in a dry condition or at least near dry condition in order to keep off environmental issues due to the usage of cutting fluids.

Due to the recent technological advancement, there is a huge pressure on manufacturing industries to reduce the machining cost, to improve machined parts quality and to machine hard and brittle materials easily. While machining at high-speed, machining time reduces significantly which leads to the improved machining efficiency. While machining ferrous and harder materials for example steels, cast iron, and super alloys, the cutting speed during turning is restricted by the

thermal softening and chemical stability of the tool material. To enhance the productivity of the manufacturing process, there is a need for accelerated design and development of a better cutting tool which can provide more resistance to wear due to its improved tribological attainment. Improved high-speed machining is the main concern of today's manufacturing industries over the last few decades. Hence, there is a need for the design and development of new tool materials to enhance manufacturing productivity.

Nowadays, hard coatings like TiCN, TiN, TiAlN, etc. are extensively used in cutting tools to reduce wear due to their good tribological characteristics and high oxidation temperature (Kulkarni and Sargade, 2015; Mohanty et al., 2016). These coatings have been applied in industry for improving mechanical properties and life of the cutting tool. There is an adhesion between the substrate and the layer of the coatings which is a very important property of the coating materials since various kind of thermal, cyclic and mechanical loads are applied during machining (Vannan et al., 2017).

The mechanism of wear for coated carbide inserts with TiN and uncoated cermet's inserts are studied by Ghani et al. (2004) at different, depth of cut, feed (*f*) and cutting speed (V_c) combinations for machining of AISI H13 tool steel. Sharma et al. (2015) investigated the consequence of convention and nano fluid lubrications in the presence of carbon nano tube during machining of AISI D2 steel. Sharma et al. (2015) found that because of carbon nano tube, the surface quality of the work piece improves. The time taken for coated (TiN) carbide tools to initiate breaking is more as compared uncoated cermet tools. The cermet tools show uniform and gradual flank wear (V_B) as compared to the carbide inserts with TiN coating. Noordin et al. (2007) did performance investigation of TiCN coating on cermets (KT 315) and carbide (KC 9110) tools on martensitic stainless steel work piece which is tempered (hardness 43–54 HRC). They further observed that the tool life of coated cermet is better than coated carbide tool.

Sayuti et al. (2014) observed that SiO_2 nano-lubrication is useful for machining of hard AISI 4140 work piece, which improves the quality of tool and work piece surface. Lima et al. (2005) analyzed the performance of PCBN tool on AISI 4340 (50 HRC) and multilayer coated carbide tool on the same material having 42 HRC. They found that better surface finish and lower cutting force can be obtained by PCBN tool (Lima et al., 2005). The performance of low-cost TiN coated tool in comparison to the expensive CBN tool was evaluated by Ko et al. (1999). They suggested that, machining of harder materials is possible at less cost with tool coated with TiN. Chinchanikar and Choudhary (2013) studied the functioning of single-layer TiAlN coated tools using PVD

technique and also CVD applied multilayered coated (MT-TiCN/Al_2O_3/TiN) carbide tools on AISI 4340 steel on work pieces having hardness 35 and 45 HRC, respectively. They found that multi-layer coatings give better result while comparing single layer coated tool (Chinchanikar and Choudhury, 2013). Pal and Deevi (2003) used three types of coated carbide tools and they found that carbide tool with (Ti, Al) N coating gives more effective results at high cutting speeds in dry condition while machining abrasive alloys due to its hardness in the range of 28-32 GPa, high oxidation resistance, low thermal conductivity, low value of residual stress (5 GPa), and high hot hardness of that coating (Pal and Deevi, 2003). Roy et al. (2009) investigated the performance of both uncoated and TiC, TiN, and Al_2O_3 coated carbide tools for during dry machining of aluminum, ferrous materials and Al-Si alloys. They reported that the tungsten based coated tools are suitable for dry machining of ferrous materials, however, not suitable for aluminum and its alloys due to build-up edge formation.

In the current study, carbide tool inserts are PVD coated using newly developed 2nd generation TiAlxN super nitride i.e. HSN^2 coating. After that, the behavior of HSN^2 coating material is characterized by micro hardness testing, oxidation stability in the air by thermogravimetric analysis (TGA) and thermal stability at elevated temperature by differential scanning calorimetry (DSC). Preliminary experiments are executed for the feasibility study of the HSN^2 coating for machining AISI 52100 steel having hardness 55 HRC. Later, the effect of cutting speed, feed rate and depth of cut which affect the machinability characteristics e.g. forces, tool wear (TW) and roughness (*Ra*) of the sample surface with HSN^2 coated inserts are carried out.

3.2 Experimental investigation

In the present study, experiments are performed on a high-speed precision lathe (HMT NH-26). The lathe spindle is driven by an 11 kW and three phase induction motor. Total 23 different rotation speeds between forty to two-thousand-forty rpm and twenty-seven different feeds (0.04 to 2.24 mm/rev) are available with the lathe machine. Cutting conditions are chosen on the ground of machine potentiality, preliminary experiments, literature survey and insert manufacturer's guidelines.

3.3 Work piece material

Experiments are carried out on hardened EN–31 (AISI 52100) steel bar having 400 mm length and 80 mm diameter with an average hardness value of 55 HRC over the entire surface. The hardness of the work piece is maintained uniformly throughout its cross-section during hardening and tempering with a maximum variation of ±1 HRC. Figure 3.1 depicts the photograph of the experimental set up with attached work piece, tool insert and dynamometer.

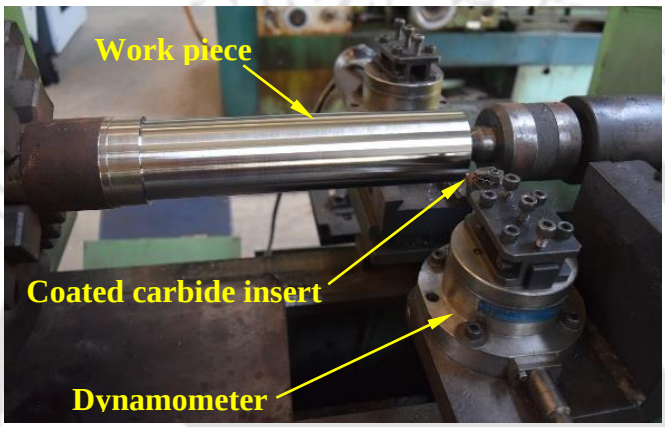

Fig. 3.1 Hard turning experimental set up

3.4 PVD coating of tool insert

Experiments are carried out with cemented carbide inserts (ISO class KU10) coated with HSN^2 (2^{nd} generation TiAlxN super nitride). The insert is PVD coated with an average thickness of 12 µm. The ISO designation of the tool holder and insert geometry are MCLNR 2020 K12-BB and CNMG 120408MBB, respectively. Clearance angle of the insert is 0˚.

By reducing machining time, the machining efficiency during hard turning can be improved while going for high-speed machining. However, the chemical stability and thermal softening of the insert at elevated temperature plays a role while limiting the cutting speed. While cutting very hard materials like cast iron, steel alloy etc. the machining efficiency depends on the material of the cutting insert. Therefore, tool material plays a vital role in machining efficiency. Hence, in the present study, the carbide tool inserts are coated with a new coating material i.e. HSN^2 using PVD technique. The carbide inserts are polished with different finishing techniques before their loading into the PVD set up. Initially, the inserts are cleaned inside an ultrasonic bath followed by micro blasting steam (MBS). Figure 3.2(a) shows the ultrasonic bath for cleaning tool insert. After

finishing, the inserts are loaded into an insert fixture (Fig. 3.2(b)) which is placed inside the PVD setup (Fig. 3.2(c)). CemeCon coating systems with DC sputter technology is used for HSN^2 coating on tool insert. PVD CC800®/9 ML setup (Fig. 3.2(c)) is used for this purpose.

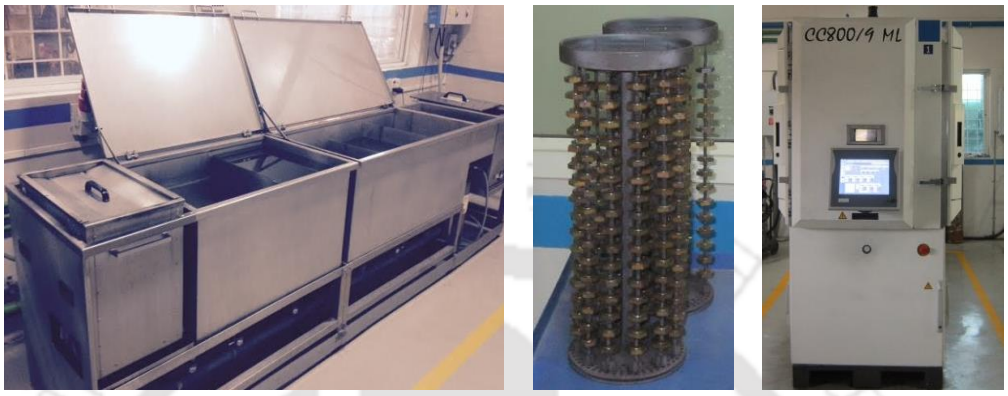

(a) (b) (c)

Fig. 3.2 (a) Ultrasonic bath, (b) fixture for tool insert and (c) PVD CC800®/9 ML set up

3.4.1 Characterization of the coating

After PVD coating of the carbide tool inserts, it is required to characterize the coating materials to confirm its property with the composition of HSN^2. For this purpose, EDX spectroscopy is performed to determine the elemental compositions of the both uncoated and HSN^2 coated tungsten carbide inserts as shown in Figs. 3.3(b) and 3.3(a), respectively.

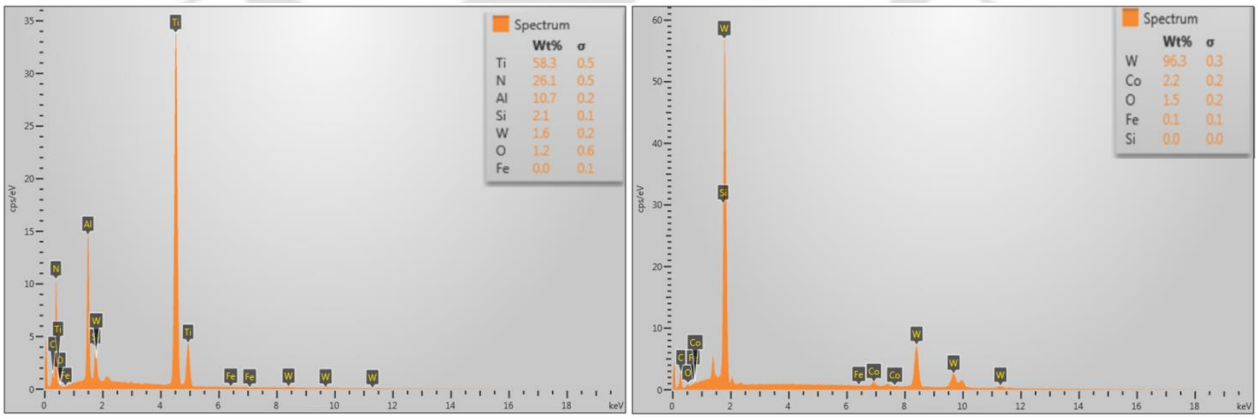

(a) (b)

Fig. 3.3 EDX elemental analysis of (a) HSN^2 coated and (b) uncoated carbide inserts

The major identified elements along with their weight percentages are provided in the caption of Fig. 3.3 for both the inserts. The most significant add-on elements i.e. Ti, N, Al, and Si

are observed during EDX analysis of HSN^2 coated carbide insert (Fig. 3.3 (a)) which matches with the composition mentioned in the literature (Famex Coating India Pvt. Ltd.; Aluspeed, 2012). The mechanical properties of the coating are studied using Vickers micro hardness testing machine to determine micro hardness. Vickers's hardness number (HV) is defined by the load applied on unit surface area of indentation. The average micro hardness of the coating material is measured as 3800 HV with a load of 2 kgf.

3.4.2 Physical-chemical properties of coating

Oxidation confrontation of the coating with respect to the temperature in the air has been studied by using Thermogravimetric–Differential Scanning Calorimetry (TG-DSC). Both of TGA and DSC plots of the HSN^2 coating are shown in Fig. 3.4.

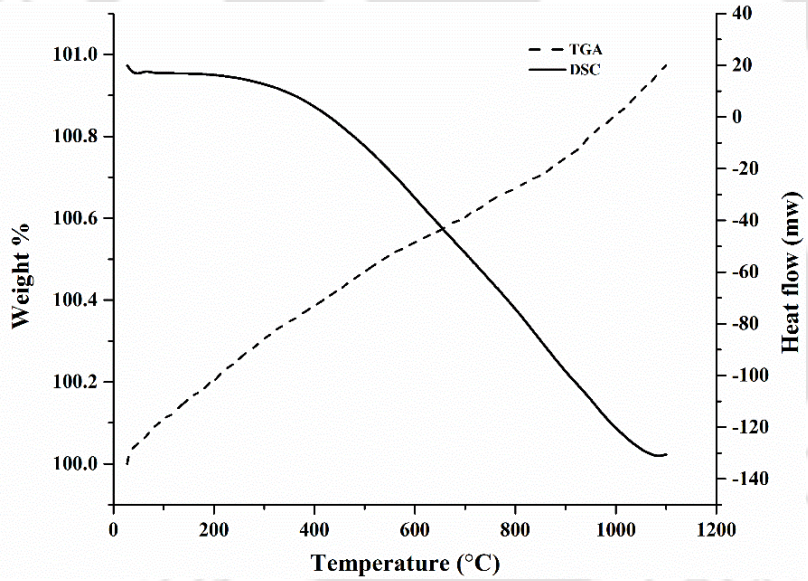

Fig. 3.4 Thermogravimetric analysis (TGA) and differential scanning calorimetry (DSC) plots at different temperature for HSN^2 coating in air

TGA data for HSN^2 coating showed almost no change in weight % (as % wt. varies from 100 to 100.8% which is negligible) up to 1000 °C. A nominal increase in the rate of change in % weight is observed beyond 1000 °C. Hence, from TGA curve it can be concluded that there is a very less amount of weight gain by the sample at high temperature beyond 1000˚C for HSN^2 coating. Therefore, a minor oxidation behavior is observed for the present coating beyond 1000˚C which is below the temperature raised during present hard turning operation. Hence, the coating does not get oxidized during hard turning operation which prevents tool wear at very high

temperature. Further, differential scanning calorimetry (DSC) is conducted to investigate the response of coating material due to heating. In Fig. 3.4, DSC plot shows the heat flow throughout the range of given temperature. However, in the DSC plot of HSN^2 coating, not a single endothermic and exothermic peak is observed which means that the performance of the coating material with respect to the heat flow at elevated temperature is satisfactory. Hence, HSN^2 coating has a very good heat capacity consisting of better-quality thermal behavior, which is beneficial for the frictional surface between tool insert and work piece during hard turning operation.

3.5 Preliminary experiments

Initially, preliminary experiments are carried out at different cutting speeds using 8 µm thick HSN^2 coated insert to find out the sustainability of the insert for machining AISI52100 work piece at high speed. Experimentally it is observed that, although the insert works fine for lower cutting speed range, however, it fails at higher cutting speed range. Hence, for further experiments, the coating thickness of the inserts is increased to 12 µm and experiments are repeated at the same cutting speeds. A comparative study of their performance for both the coated inserts is carried out as shown in Fig. 3.5. For both the coated inserts i.e. 8 and 12 µm coating thickness, surface roughness and flank wear are measured after each experiment as shown in Figs. 3.5(a). Also, during machining all three force components are measured (Fig. 3.5(b)). The observations from Fig. 3.5 lead to the conclusion that the 12 µm thick coated carbide insert provides better overall performance than 8 µm thick coated insert.

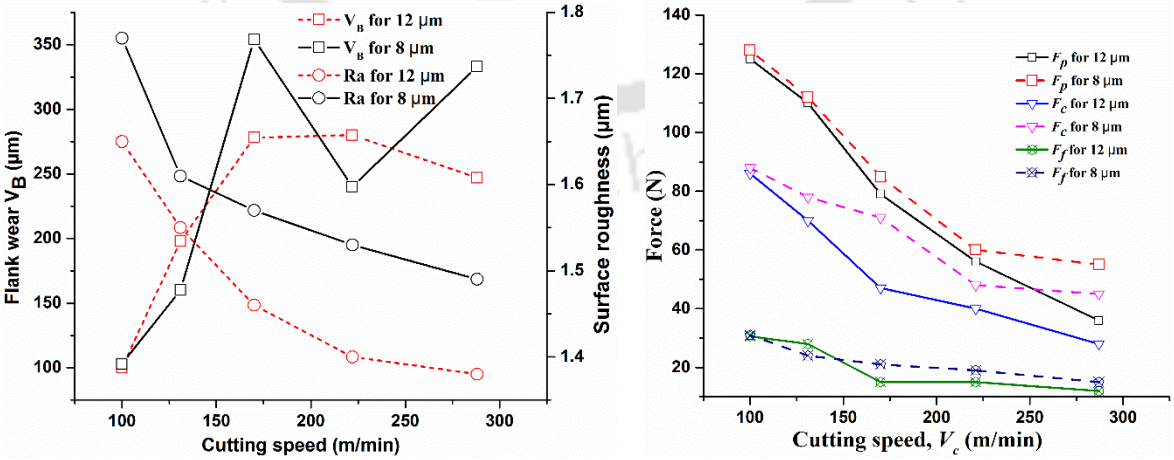

(a) (b)

Fig. 3.5 Effect of cutting speed on (a) flank wear and work piece surface roughness and (b) measured forces comparing two different coating thickness

The observation from Fig. 3.5 (a) shows that both the coatings work fine at low speed. At higher cutting speed, 8 µm coated insert fails as the flank wear reaches beyond 300 µm i.e. failure limit for flank wear (Nouari and Ginting, 2006). Hence, 8 µm thick coated insert does not sustain at higher cutting speeds. However, 12 µm thick coated insert sustains at higher cutting speeds. Higher value of surface roughness is found for 8 µm thick coated insert at all cutting speeds as compared to 12 µm thick coated insert. From Fig. 3.5 (b), it can be concluded that all the three components of the forces measured in case of 8 µm thick coated insert are higher than 12 µm thick coated insert. At 288 m/min cutting speed, the comparison between the microscopic views of two different thickness of coated inserts are shown in Fig. 3.6. It is clear from Fig. 3.6 that the coated insert of 8 µm thickness fails at 288 m/min cutting speed with flank wear of 333 µm (Fig. 3.6(b)). From above discussion, it is observed that 12 µm thick HSN^2 coated insert gives better performance than 8 µm thick coated insert during high-speed machining of AISI 52100 work piece. Hence, in the present study, further experiments are carried out with 12 µm thick coated carbide insert.

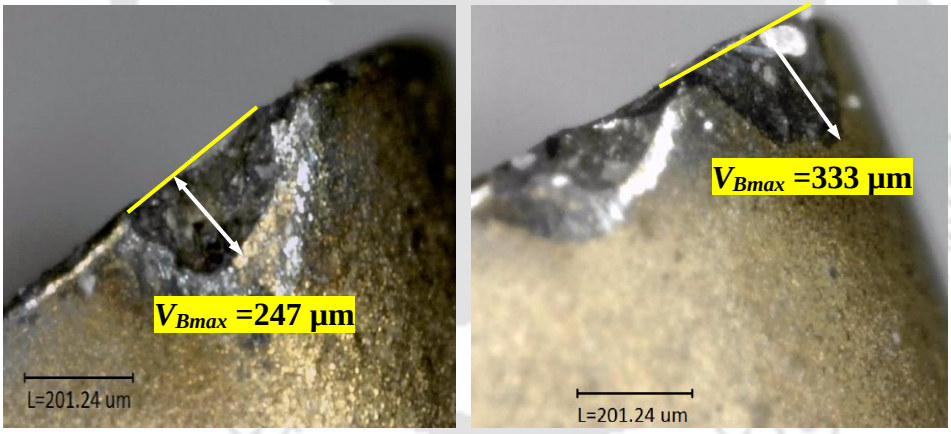

(a) (b)

Fig. 3.6 Comparison between maximum flank wear of two different thickness (a) 12 and (b) 8 µm of coated carbide inserts at 288 m/min cutting speed

3.6 One variable at a time (OVAT) experiments

Experiments are conducted by varying one variable at a time (OVAT) keeping other parameters fixed at a certain value. The cutting speeds (V_c) are varied initially during hard turning experiments which are shown in Table 3.1. The other parameters are kept fixed at feed =0.1 mm/rev, depth of cut =0.08 mm. After that experiments are carried out at different feeds (Table 3.1) keeping cutting speed and depth of cut fixed at 170 m/min and 0.08 mm, respectively.

Similarly, next set of experiments are carried out at different depth of cut keeping cutting speed and feed fixed at 170 m/min and 0.1 mm/rev, respectively. During experiments, three forces (i.e. main cutting force (F_c), radial force (F_p) and feed force (F_f)) on the tool are measured online using a Kistler dynamometer. The Surface roughness of the work piece after each experiment are measured on the work piece surface at five different points along the axial direction and an average is calculated. Further, a microscope is used to measure the flank wear of tool insert after each experiment.

Table 3.1 Process parameters during hard turning

Process parameters	**Range of cutting parameters**				
Cutting speed, $\boldsymbol{V_c}$ (m/min)	100	131	170	222	288
Feed, $\boldsymbol{f}$ (mm/rev)	0.06	0.08	0.1	0.12	0.14
Depth of cut, $\boldsymbol{a_p}$ (mm)	0.04	0.06	0.08	0.1	0.12

3.7 Results and discussion

In this section, the surface roughness, cutting forces and flank wear are analyzed experimentally for hard turning operation of cylindrical shaped hard steel rod. In the current study, different cutting parameter's effect on forces generated during continuous cutting of steel work piece with a single layer of coated carbide insert is analysed.

3.7.1 Forces

Figure 3.7 (a) shows the effect of cutting speed on main cutting force at 0.1 mm/rev feed and 0.08 mm depth of cut. It is found from Fig. 3.7(a) that as cutting speed increases, all three forces decrease. An increase in shear angle is observed with the increase in cutting speed, which results in a reduction in the plane area of chip thickness. This is probably the reason for the decrease in machining force at high cutting speeds. Figure 3.7(b) shows the effect of feed rate on forces which shows an increasing trend at higher feed for a fixed value of 170 m/min cutting speed and 0.08 mm depth of cut. This is because when high feed is employed, the area of interaction between the cutting tool and work piece increases which results in increased machining force. Fig. 3.7(c) shows the influence on machining forces at different depth of cut. The fixed parameters are feed = 0.1 mm/rev and cutting speed = 170 m/min. It indicates higher forces at higher values of depth of cut. This is because as the depth of cut increases, it results in a higher contact length between tool and

work piece. At the same time, chip thickness becomes significant and it results in larger amount of deformed metal and needs larger cutting forces for cutting chip. The experimental results show that all the three forces are mainly influenced by the most significant parameter i.e. depth of cut followed by the cutting speed, feed during hard turning. Also, it is noticed that the magnitude of the cutting force is less than the radial force. Higher radial force is attributed due to the ploughing effect (Lalwani et al., 2008).

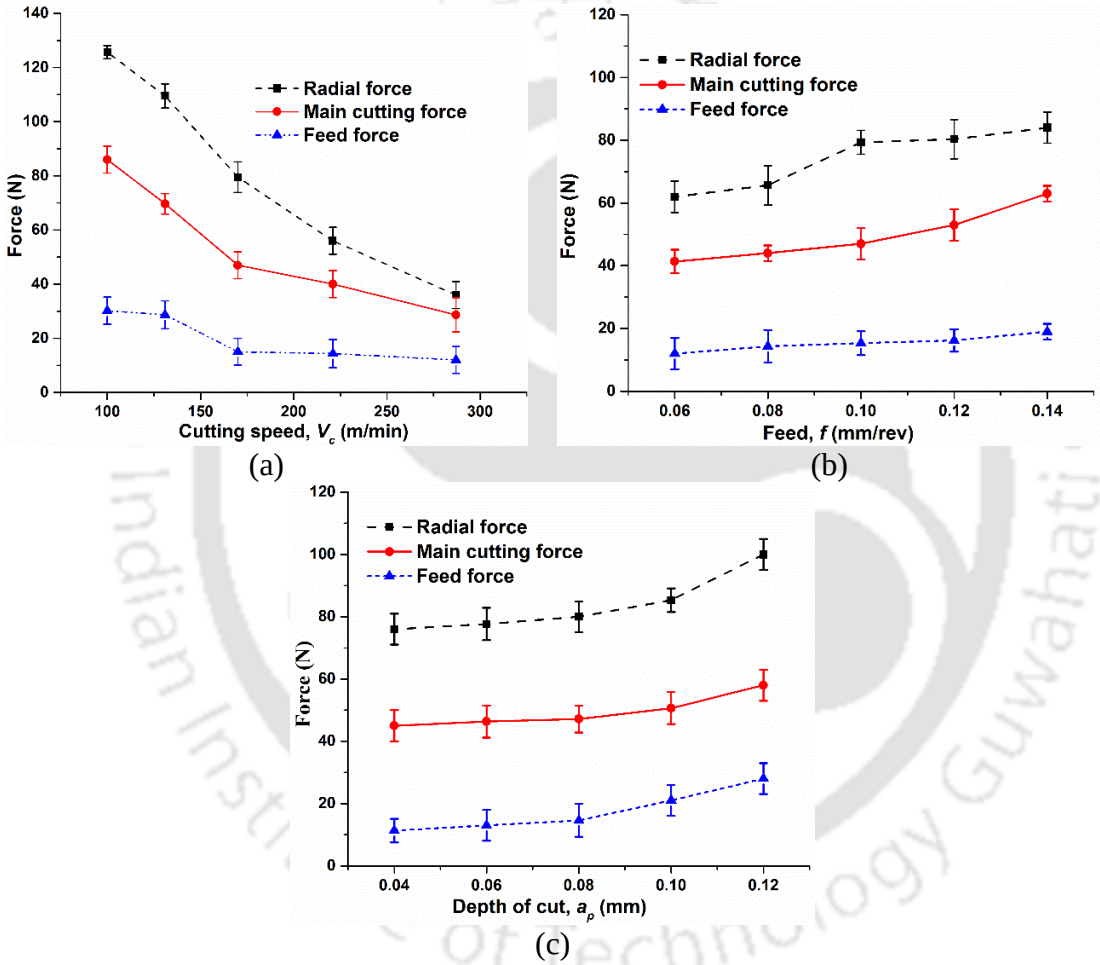

Fig. 3.7 Effect of (a) cutting speed (f=0.1 mm/rev, d=0.08mm), (b) feed (V_c=170 m/min, a_p=0.08 mm) and (c) depth of cut (V_c=170 m/min, f=0.1 mm/rev) on cutting tool forces

3.7.2 Surface roughness

Figures 3.8 (a), (b) and (c) show the surface roughness plots at various cutting conditions. As the other parameters were kept constant, at higher cutting speed the surface roughness decreases sharply. When the feed is increased, the machining force increases. It is observed that the area under tool–chip interface is subjected to an increased temperature with increased cutting speed,

which leads to the work piece material get softened. Hence, surface roughness reduces. However, when feed is increased, the radial force also increases, which directly leads to more vibration and generation of more heat. This, in turn results in higher surface roughness. From Fig. 3.8 (b), it is found that the value of surface roughness is considerably sensible at different feed rates mainly at lower cutting speeds in comparison to its higher value. Due to the reasons mentioned above the surface roughness is detected to be minimal when the cutting speed is higher and the feed rate is lower. It is observed from Fig. 3.8(c) that surface roughness value increases as depth of cut increases. This happens due to increased tool–work contact length which generates more pressure on the tool. Thus the value of surface roughness is increased at a higher feed and depth of cut. Therefore, to achieve enhanced surface finish, the value of depth of cut and feed should be kept lower.

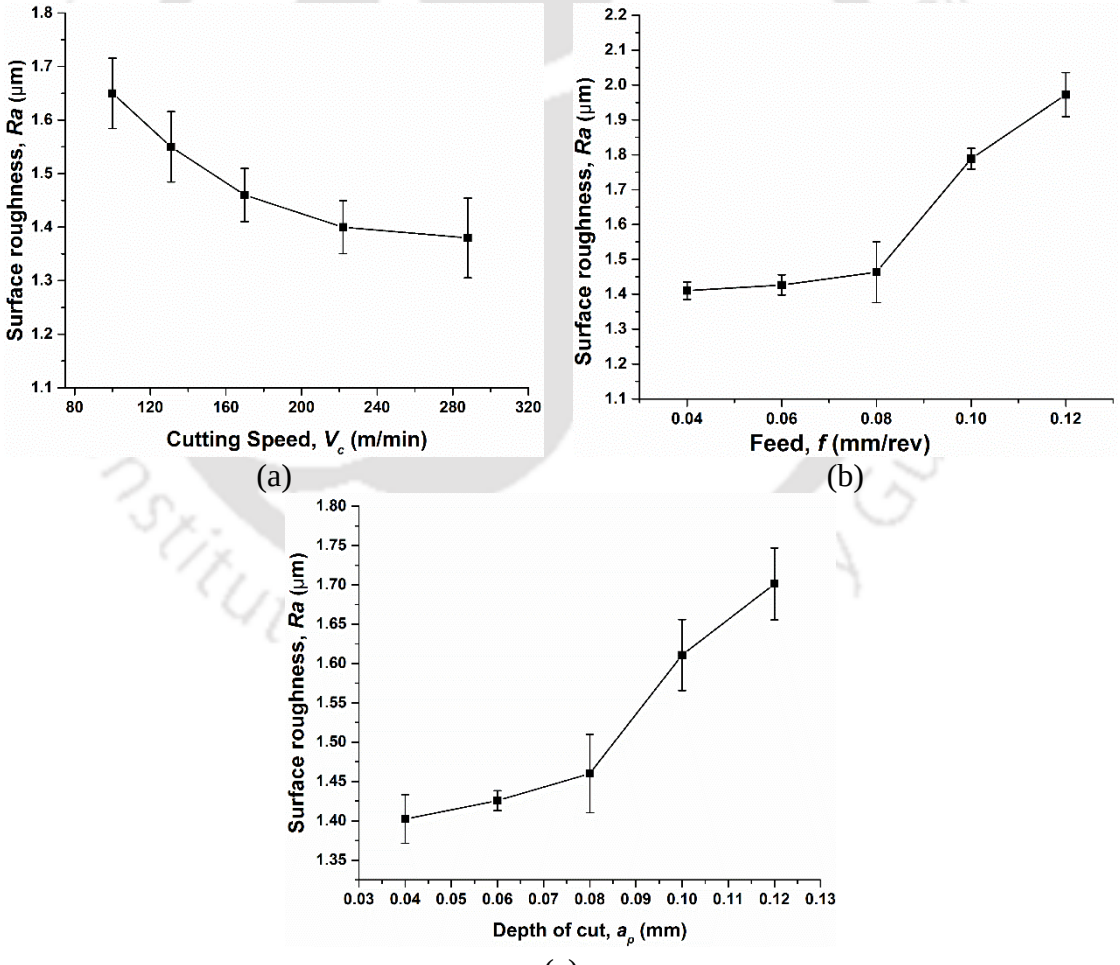

Fig. 3.8 Effect of (a) cutting speed (f=0.1 mm/rev, a_p=0.08mm), (b) feed (V_c=170 m/min, a_p = 0.08 mm), and (c) depth of cut (V_c=170 m/min, f=0.1 mm/rev) on surface roughness (R_a) of the work piece

3.7.3 Maximum flank wear (VB_{max})

The major reasons of the tool wear are due to mechanical, thermal, chemical or any combination of these factors induced during hard turning. The mechanism of tool wear is very complex due to several factors acting together. The tool life is limited by different combinations of wear in flank and crater, nose radius, or edge chippings. The combination of the insert and work material, machining parameters and the use of cutting fluid also greatly affect the tool life.

Figures 3.9, 3.10 and 3.11 show the microscopic view of the maximum flank wear (VB_{max}) of the coated carbide tools after machining at different cutting speed, feed and depth of cut, respectively (Table 3.1). Figures 3.12 (a)–(c) depict the magnitude of the maximum flank wear (VB_{max}) at different cutting speed, feed and depth of cut. Here, it is found that the tool wear increases at higher cutting speed between 100 to 222 m/min. During hard turning, maximum flank wear is mainly caused by the temperature. As the temperature of the cutting edge increases at higher cutting speed, the flank wear also increases. As the tool's temperature rises with the increasing of cutting speed, it causes the inserts to lose hardness and it accelerates tool wear. However, with increased cutting speed from 222 to 288 m/min, a gradual decrease in tool flank wear from 280 µm to 247 µm is observed. This phenomenon can be attributed due to combined effect of chip embrittlement and cutting temperature (Su and Liu, 2012).

The effect of feed on flank wear is shown in Fig. 3.12(b). Also, the flank wear does not follow a definite pattern (Fig. 3.12(b)) with feed due to the combined effect of temperature and chip embrittlement. An increment in feed from 0.06 to 0.08 mm/rev and further 0.1 to 0.12 mm/rev leads to an increment in the cutting temperature and thermal softening of the work piece. Hence, flank wear reduces. The effect of depth of cut on maximum flank wear of tool is shown in Fig. 3.12 (c). With the increase of the depth of cut, the tool work piece contact area also increases. As there is large contact area between the insert and the work piece, friction force dominates on the flank face of the insert. Hence, flank wear increases. However, after 0.8 mm depth of cut, slightly decreased value of the flank wear is observed due to the chip embrittlement. The cutting speed is the most significant process parameter to affect the tool flank wear. From experimental analysis, it is found that for the reduction in tool wear a lower value of both cutting speed and depth of cut is helpful.

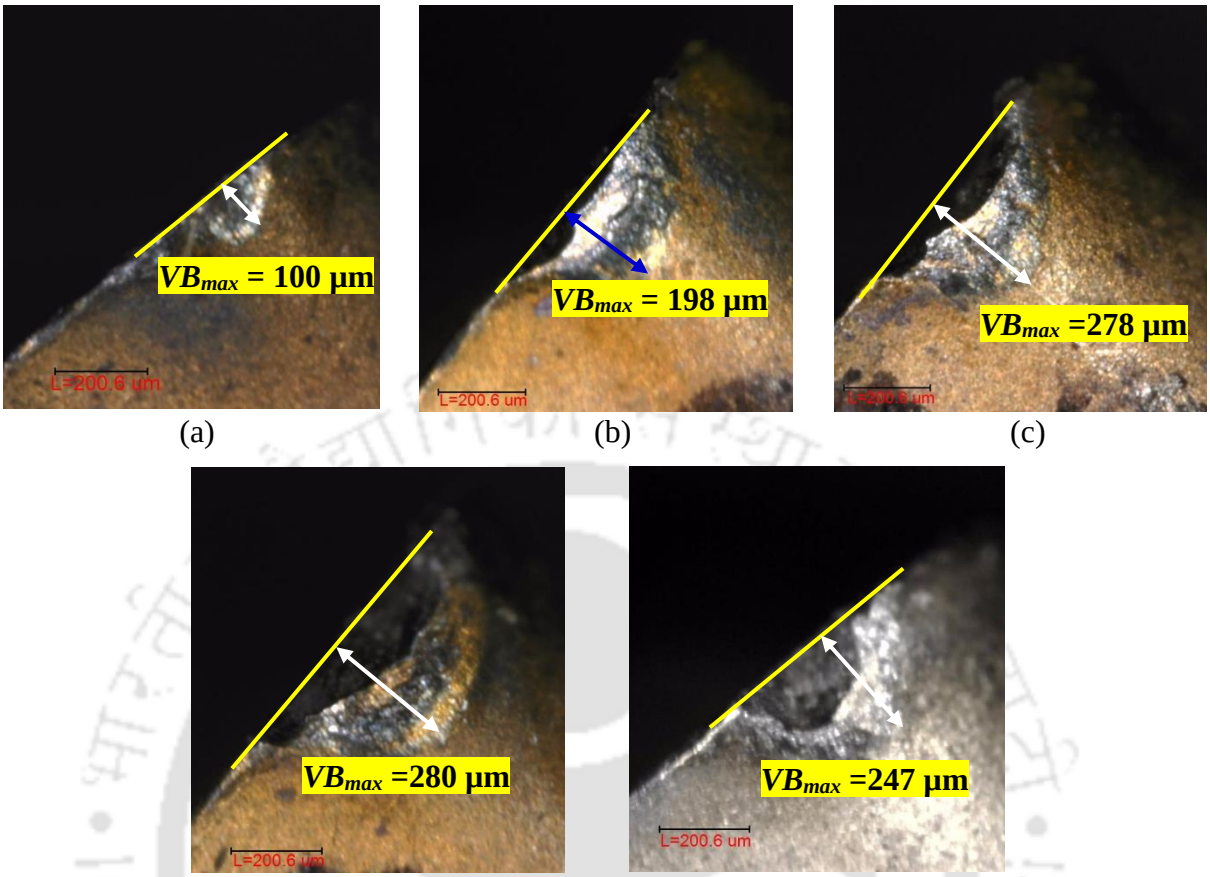

Fig. 3.9 Flank wear of the tool at different cutting speeds; (a) 100 m/min, (b) 130 m/min, (c) 170 m/min, (d) 222 m/min and (e) 288 m/min for f= 0.1 mm/rev and a_p =0.8 mm

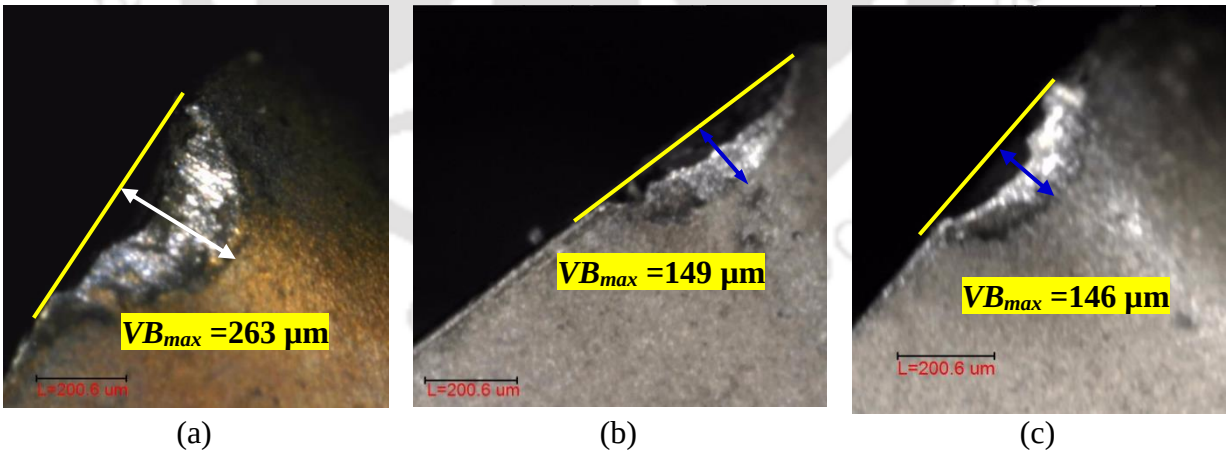

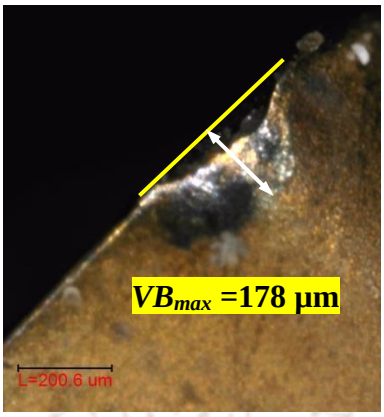

(d)

Fig. 3.10 Flank wear of the tool at different feed; (a) 0.06 mm/rev, (b) 0.08 mm/rev, (c) 0.12 mm/rev and (d) 0.14 mm/rev for V_c =170 m/min and a_p = 0.8 mm

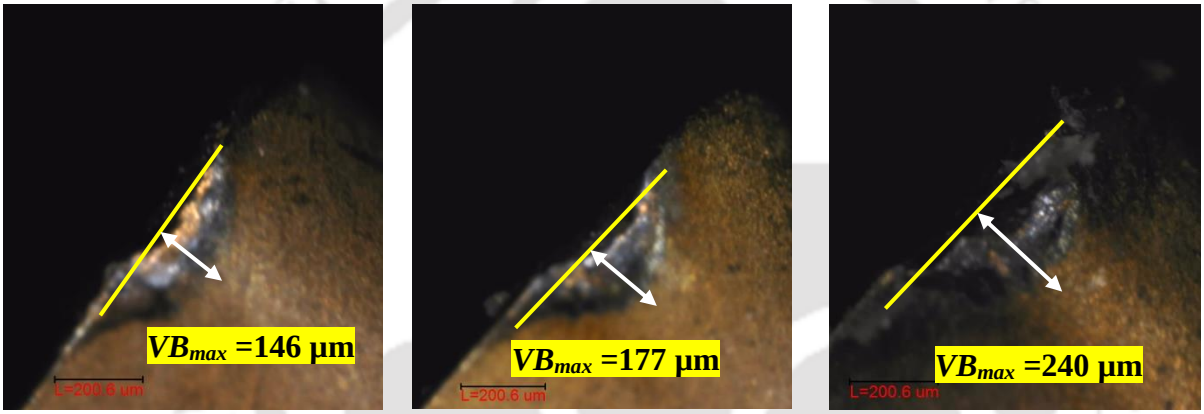

(a) (b) (c)

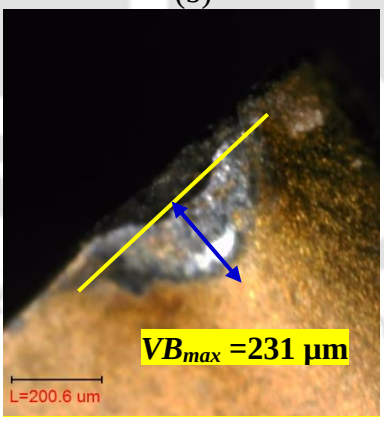

(d)

Fig. 3.11 Flank wear of the tool at different depth of cut; (a) 0.04 mm, (b) 0.06 mm, (c) 0.1 mm and (d) 0.12 mm for V_c=170 m/min and f= 0.1 mm/rev

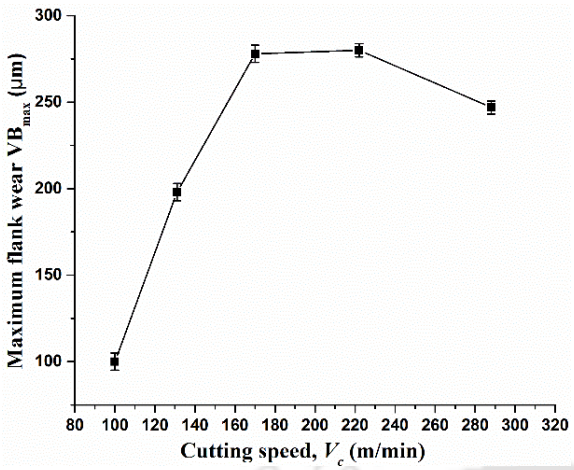

(a)

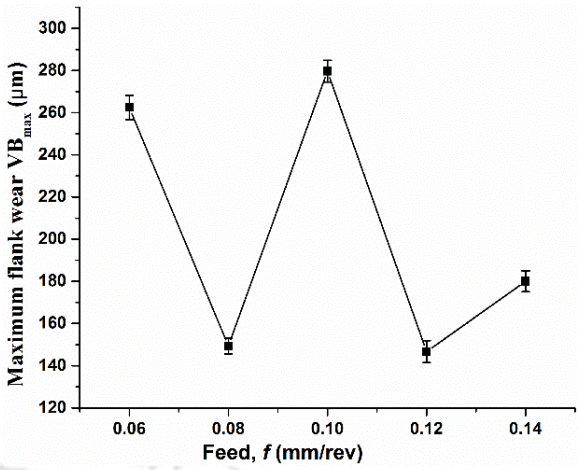

(b)

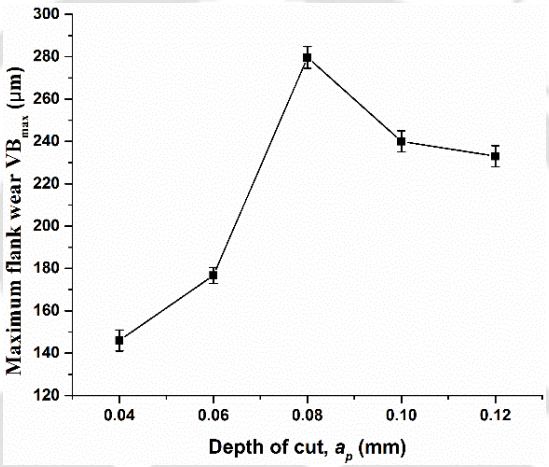

(c)

Figure 3.12 Effect of (a) cutting speed (*f*=0.1 mm/rev, a_p =0.08 mm), (b) feed (V_C=170 m/min, a_p =0.08mm), and (c) depth of cut (V_C=170 m/min, *f*=0.1 mm/rev) on flank wear of the tool

3.8 Chip analysis

Cutting tool material and its properties are very important aspect as the inserts need to withstand very high temperature during machining. The tool should have resistance to abrasive wear as well as should have high toughness so that it can resist edge micro-chipping and breakage. The tool should be chemically stable and should have high thermal conductivity. Cemented carbide is the most widely used cutting tool. During hard turning, an important field that needs to be studied is chip morphology as it is one of the most crucial factors when it comes to nature of the machining process. The parameters on which chip formation and its nature depends are feed (*f*), depth of cut (a_p), cutting speed (V_c), type of the insert and work piece, tool-chip interface friction, rake and clearance angles and so on. Some of these parameters play a less significant role in deciding chip morphology as compared to others (Wang and Liu, 2016). In recent manufacturing trends, the

study of chip formation is extensively increased mainly in hard turning process. It is very important to conduct studies on formation of chip and its morphology to decide the material property of the insert as well as choice of tool geometry. Also, the issues related to the formation of white layer and residual stress concentration are majorly affected due to chip formation. It can be seen from the experimental work by Poulachon and Moisan (2000) and Dolinšek et al. (2004) that feed, cutting velocity and depth of cut adversely affect the chip morphology. Chip formation can be of different types like segmented, serrated and continuous etc. due to the interplay between all or some of the above mentioned process parameters (Afonasov and Lasukov, 2014). The effect of cutting velocity on the formation of chip, and rake angle were their main considerations (Kountanya et al., 2009). Presently, high speed cutting (HSC) is an important technique used for rough machining when it comes to manufacturing of machine components (Bartarya and Choudhury, 2012).

The experiments are conducted at various cutting speed (V_c) as displayed in Table 3.2 keeping parameters like feed (f) and depth of cut (a_p) as constant (0.1 mm/rev and 0.08 mm, respectively). Another set of experiments are conducted in which depth of cut and cutting speed are kept constant as 0.08 mm and 170 m/min, respectively and the feed is varied.

Table 3.2 Process parameters during hard turning

Process parameters	**Range of cutting parameters**				
Cutting speed, V_c (m/min)	100	130	170	222	288
Feed rate, f (mm/rev)	0.06	0.08	0.1	0.12	0.14
Depth of cut, a_p (mm)			0.08		

3.8.1 Geometry of the chip

Optical microscope is used to observe the chip micrographs that produced during experiments. The procedure followed is polishing and moulding of the chips with the help of a BUEHLER polisher. From optical micrograph, thickness of the chip (t_{max} and t_{min}), segment distance (d_{ch}) and angle of inclination ($\varnothing_{seg}$) measurements are carried out. The degree of segmentation (δ) is calculated as (Sutter and List, 2013)

$$\delta = \frac{t_{\max} - t_{\min}}{t_{\max}} \tag{3.1}$$

The schematic diagram of chip generation is shown in Fig. 3.13. The segment inclination angle ($\emptyset_{seg}$), also called as localized shear angle, as well as shear angle ($\emptyset$) are shown in Fig. 3.13. Although it is not possible to measure shear angle directly from the chips that are produced, however, the segment angle of inclination can be measured. The relationship between shear angle ($\emptyset$), pitch of serrated chip (d), length (p) and segmentation angle ($\emptyset_{seg}$) can be obtained utilizing the condition of incompressibility in plastic deformation as (Sutter and List, 2013)

$$a_p \times p = \frac{a_p \times d}{\sin\phi} = d_{ch} \times \left(\frac{t_{\max}}{\cos\phi_{seg}} - d_{ch}\tan\phi_{seg}\right) \tag{3.2}$$

where, a_p is depth of cut and d_{ch} is pitch of segmented chip length. Figure 3.14 shows the optical microscope morphology of the chip generated after hard turning. Assuming the magnitude of a_p and d_{ch} are approximately equal, the estimation of shear angle can be calculated as (Sutter and List, 2013)

$$\phi = \arcsin\left\{\frac{a_p}{\frac{t_{\max}}{\cos\phi_{seg}} - d_{ch}\tan\phi_{seg}}\right\} \tag{3.3}$$

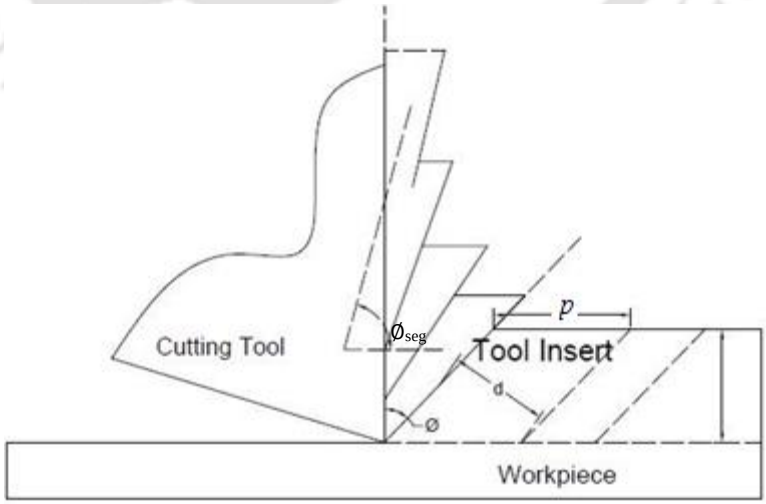

Fig. 3.13 Schematic diagram of chip generation during turning

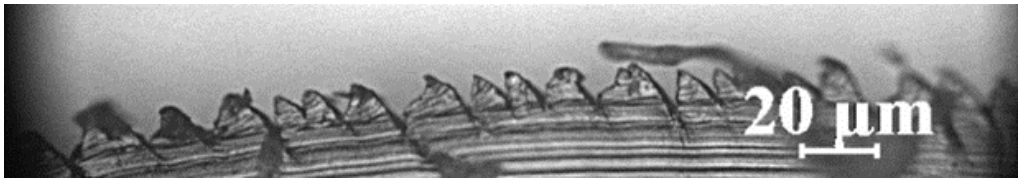

Fig. 3.14 Chip morphology at V_c = 130 m/min, f = 0.1 mm/rev and a_p= 0.08 mm

3.8.2 Results and Discussion

In this section, the average values of maximum (t_{max}) and minimum (t_{min}) chip thickness, length (p) and localized shear angle (∅) are measured experimentally and further chip thickness, shear angle, chip thickness ratio are plotted and analyzed at different experimental conditions. Average value of minimum three readings is considered.

3.8.2.1 Chip thickness

The variation of chip thickness with respect to cutting speed is shown in Fig 3.15(a). As the cutting speed increases, the cutting temperature also increases. At elevated temperature, material softening occurs and machining forces decrease. As a result, the thickness of the chip decreases. The plot of chip thickness Vs. feed is displayed in Fig. 3.15(b) where it is seen that as the feed increases, the chip thickness also increases. This is because as feed increases, the unreformed chip thickness increases. Also, the tangential force is proportional to the unreformed chip thickness. Due to this increased unreformed chip thickness, shear plane area increases which leads to the increase in chip thickness.

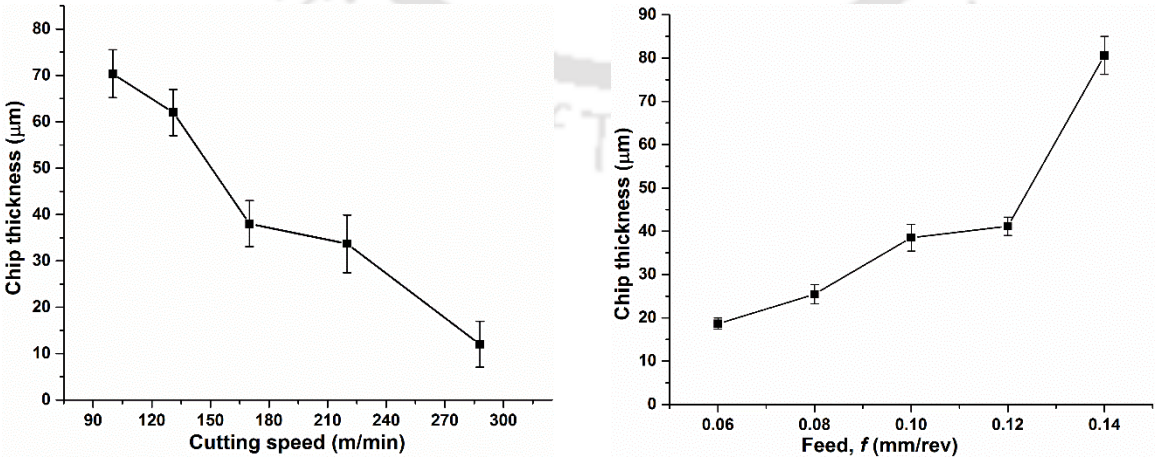

(a) (b)

Fig. 3.15 Variation of chip thickness at different (a) cutting speed and (b) feed

3.8.2.2 Chip reduction ratio

Figures 3.16 (a) and (b) show the variation of chip reduction ratio with cutting speed and feed, respectively. The value of chip reduction ratio near to 1 represents favorable cutting condition at higher cutting speed. Similarly, from Fig. 3.16 (b), it can be seen that at lower feed, the value of chip reduction ratio is near to 1 which means lower feed is good for hard turning for the present tool and work piece combination.

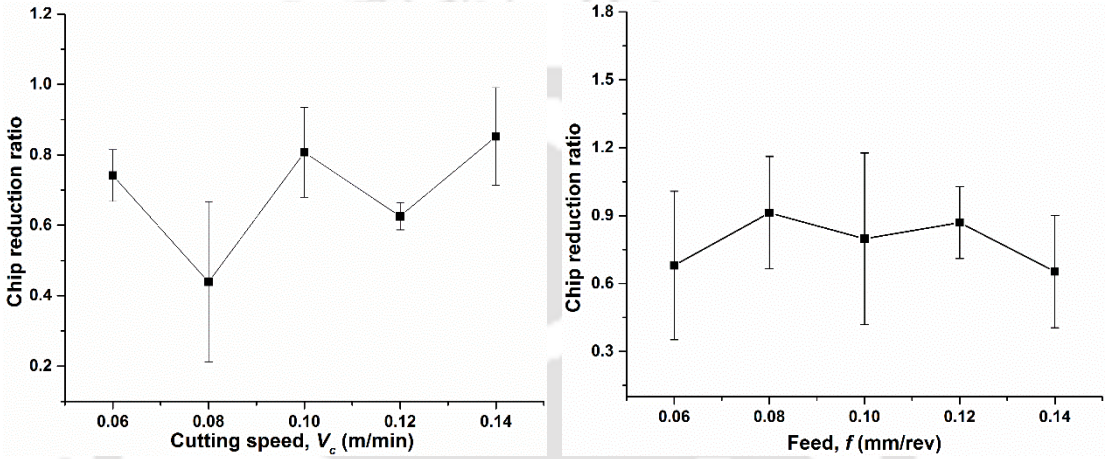

(a) (b)

Fig. 3.16 Variation of chip reduction ratio at different (a) cutting speed and (b) feed rate

3.8.2.3 Shear angle

For understanding the mechanism of chip formation, the study of shear angle is required. At higher cutting speed, the rate of plastic deformation decreases and the value of shear angle increases (Fig. 3.17(a)) permitting the reduction in area or section of shearing. Hence, cutting force decreases. Due to this, shear angle increases at higher cutting speed. From Fig. 3.17(a), it is observed that at higher cutting speed shear angle approaches to its limiting value of 45°. This is expected due to continuous chip formation at higher cutting speed. With increasing feed, shear angle decreases (Fig. 3.17(b)). It is clear that shear angle approaches to 45° at higher speed, hence, lower feed is better for hard turning.

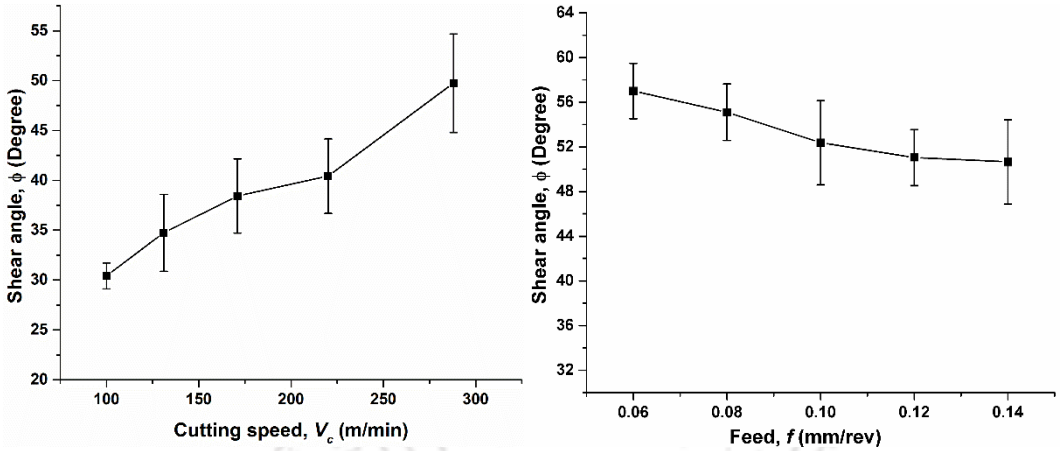

(a) (b)

Fig. 3.17 Variation shear angle at different (a) V_c and (b) f

3.9 Summary

In the present study, high speed machining of AISI 52100 grade steel is carried out using a newly developed coating (HSN^2) on carbide tool insert to observe the effect of process parameters on cutting forces, surface roughness and maximum flank wear. From TGA – DSC analysis, it has been found that the HSN^2 coating has high oxidation stability and better thermal behaviour in a wide temperature range. Experimentally it is found that the carbide insert's thickness with HSN^2 coating of 12 µm performs better than 8 µm. The highest value among all three forces is found with radial force due to ploughing effect. The value of maximum flank wear for all experiments is less than standard acceptable value of 0.4 mm (ISO Standard 3685) for carbide insert. Hence, the HSN^2 coating can be successfully used for turning hardened AISI 52100 steel having hardness 55 HRC. From analysis of chip morphology, it is observed that the value of chip reduction ratio tends to 1 at higher cutting speed and lower feed which shows their favourable range. The value of shear angle at higher cutting speed approaches to 45° indicating smoother chip formation at higher cutting speed.

Chapter 4 Statistical design of experiments

4.1 Introduction

The sustainability of the environment is one of the main aims for any manufacturing process (Zhang and Liu, 2017). One of the most unsustainable process is cooling/lubrication based machining process due to cutting fluid's bad impact on health as well as the environment (Krolczyk et al., 2017). Lubricants for the cooling purpose are mostly used in industries for metal cutting. There are some benefits of these lubricants during machining like enhanced tool life, good surface finish and easy chip transportation (Park et al., 2015; Rabiei et al., 2015; Maruda et al., 2017). Also, lubricants help to reduce friction between tool and work piece (Park et al., 2015; Rabiei et al., 2015; Maruda et al., 2017). Krolczyk et al. (2018) studied work piece surface topography for dry turning as well as using minimum quantity cooling lubricant (MQCL). They found that the surface topography gains better yield with MQCL as compared to dry turning (Krolczyk et al., 2018). The key factor for high-proficiency cutting is effective lubrication (Maruda et al., 2018). Kaynak et al. (2013) also analyzed the tool wear for NiTi alloy for dry machining as well as MQL condition. They found that tool life increases with MQL condition as compared to dry condition (Kaynak et al., 2013). However, the use of these lubricants is associated with problems faced in a working environment even in the disposal of the waste. Because of this, the number of ecology related problems increases. Presently, in an environment of increasingly strict work safety and environmental lawmaking, it produces more economical problems for manufacturing based industries (Klocke and Eisenblätter, 1997). According to one of the German automotive manufacturing industries, the cost of fluids or lubricants which are used during different cutting processes is about 7 to 17 % of the labour cost (Bagaber and Yusoff, 2017). Also, cutting fluid recycling is costly due to the difficulties faced during removal process of these fluids or lubricants (Bagaber and Yusoff, 2017). Due to the safety purpose of the environment in the field of machining, dry hard turning is getting positive impact due to concerned environmental safeguard (Noordin et al., 2007). In recent years, there is a huge demand for extremely tough steel in the manufacturing industries which forms new challenges for the machining process and cutting tools (Chinchanikar and Choudhury, 2014). Heat treatment is mandatory to attain the required hardness of hard turning material and further to generate required shape of the hardened material, high speed machining is carried out by removing extra material in the form of chip (Mia et al., 2017; Mia et al., 2018; Mia and Dhar, 2018). If the work piece hardness lies in between 40 to 65 HRC which is

turned with a harder cutting tool insert, then the process is called hard turning and it is a subtractive process (Mia and Dhar, 2017; Mia et al., 2018). Hard turning with a single and multilayer coated carbide tool is more beneficial than grinding process as it reduces processing cost by increasing productivity. Also, material properties after machining by hard turning are improved. This process facilitates manufacturers to improve efficiency and product quality with reduced machining cost and material handling time. Dry hard turning is opted by many manufacturers because it does not require any lubricants or other cutting fluid and it promotes sustainability (Mia, 2018). Dry cutting is advantageous as it eliminates the cost of cutting fluids and the high cost of fluid disposal system. The necessity to encourage productivity with improved machined surface quality during machining of hard materials have guided manufacturing industries to exploit novel cutting tool materials. Hard coating of cutting tool inserts is being vigorously researched in last few years for different applications. Coatings with greater hardness are actually a lean film which has different range of coating layers with thickness varies between few nanometres to few millimetres. Hard coating increases tool life as much as 10 times because it slows down the insert wear which leads to less frequent tool changes. Hence, the batch size of the components that could be manufactured per tool increases.

There is a never ending need for machining of metals in a more effective and efficient way, especially when it comes to hard materials. For machining very hard components, hard turning is increasingly preferred over grinding process on the shop floor. A comparable or even better surface finish and higher MRR can be achieved by hard turning than grinding operation. Aside from grinding, hard turning has acquired considerable responsiveness for quality machining in terms of finishing of hardened steel (Dogra et al., 2011). Hard turning is accomplished with a special tool because tool's hardness should be more than the work piece's hardness. It becomes a challenging task to pick up the right tool for the right material while consuming less power during machining. Also, the life of the tool should be high. Presently, the demand for extremely hard steels in industries are unendingly growing which creates never ever disputes for machining operations and places higher demand for superior inserts (Chinchanikar and Choudhury, 2014). Kupczyk and Komolka (2015) studied tungsten carbide and cobalt tool inserts for various machining processes like turning, milling, etc. and found the coating material to be very effective in reducing tool wear. Generally, tool material with fine grain structure gives enhanced mechanical properties as compared to coarse one (Kupczyk, 2015). A considerable development has also been observed in

the present days in the field of new cutting tool coating materials which results in the newest developments in the sphere of thin films and coating deposition technologies.

Ferreira et al. (2016) investigated the functioning of the conventional and wiper ceramic tool on AISI H13 steel during hard turning and found that wiper ceramic insert gives better result. Suresh et al. (2012a) experimentally observed the performance of a carbide tool which is multi-layered by CVD technique during hard machining of AISI 4340 steel. They found that, with increased cutting speed (*Vc*), the power required during machining increases. Also, lower feed and higher cutting speed help in reducing work piece surface roughness. Presently, coating materials like TiN, TiCN, TiAlN etc. are frequently used on different types of cutting tool inserts because of their better tribological behaviour and higher oxidation resistance at elevated temperature (Kulkarni and Sargade, 2015; Mohanty et al., 2016). These coatings enhance the mechanical properties and tool life of the inserts. Sahoo and Sahoo (2012) did experimental investigations between coated (both TiN and ZrCN) and uncoated carbide inserts to compare their performance. They reported that the results obtained using carbide inserts with coated surface are better than the one which is uncoated. Also, the performance of carbide insert with TiN coating is better than ZrCN coating. Rosa et al. (2017) performed experiments to find the ability of TiAlN ultra-fine grain coating on carbide insert at different cutting conditions on AISI 420C stainless steel work piece having hardness of 53±2 HRC. They found that the cutting speed is more dominant factor than other parameters for tool life.

Surface quality of work piece as well as tool wear (TW) are the major concerns in the field of hard turning. Both higher hardness and oxidation resistance of the tool insert at a very high temperature are very important requirements for hard and dry machining (Dobrzański et al., 2004; Faga et al., 2007; Ichijo et al., 2007; Rafaja et al., 2007). Ozel et al. (2005) observed that during hard turning, cutting forces depend on cutting condition as well on the geometry of the cutting edges and work piece hardness. They observed that both softening of the work piece surface at elevated temperature and lesser value of cutting edge radius cause lower value of radial and tangential force components. Yigit et al. (2008) optimized the process parameters to minimize TW and surface roughness (*Ra*) during hard machining using a 10.5 µm thick multilayer coated insert. Rocha et al. (2017) optimized the cutting parameters using response surface methodology (RSM) for higher MRR, tool life, force ratio and lower surface roughness value with PCBN wiper tool on AISI H13 steel. Kumar et al. (2017) applied Taguchi approach to optimize different cutting parameters to minimize surface roughness of the work piece, energy consumption during

machining and to maximize MRR. They found that analytical hierarchy process weight (AHPW) method gives best result for higher MRR and lower energy consumption. Gupta et al. (2016) applied particle swarm and bacterial foraging techniques for optimizing input parameters while machining titanium alloy of grade 2 with cubic boron nitride (CBN) inserts using cutting fluids.

From literature survey on hard turning, it is observed that generally ceramic, CBN and PCBN tools are mostly used for cutting extremely hard materials. However, these cutting tool inserts are very costly which increases cost of machining. Hence, coated carbide insert is the best option while considering cost effectiveness of the process with better dynamic performance. Also, coating materials like TiAlN and AlTiN having higher aluminium content has higher strength, thermal stability and oxidation resistance (Kulkarni and Sargade, 2015; Thakur and Gangopadhyay, 2016). The coating material on the carbide inserts is the best selection in this regard as the ceramic, CBN and PCBN tools are comparatively costly and the cost of carbide inserts with coating is about one-tenth of ceramic, CBN and PCBN tools. Though the utilization of coating material on carbide insert is still lacking while machining hard materials whose hardness is greater than 50 HRC because of their less thermal stability and oxidizing nature at elevated temperature.

Based on literature survey discussed above, the present work has been carried out after being motivated from the research gaps as mention below.

- Literature on the use of coated carbide tools in hard turning of material with hardness more than 50 HRC, particularly on AISI 52100 steel with hardness 55 HRC are limited.
- The performance of carbide insert with HSN^2 (2nd generation of TiAlxN super nitride) coating for machining of hard material has also been less explored.

In the present study, PVD coated HSN^2 i.e. 2^{nd} generation TiAlxN super nitride, a newly developed coated carbide insert is used. Turning experiments on AISI 52100 steel of hardness 55 HRC are conducted based on statistical experimental design. Later, the influence of different cutting parameters i.e. cutting speed (V_c), feed (f) and depth of cut (a_p) are analyzed which affect machinability characteristics e.g. main cutting force (F_c), radial force (F_p), feed force (F_f), maximum flank wear (VB_{max}) and work piece surface roughness (R_a). Also, the process parameters are optimized and the confirmation tests are carried out to validate the responses obtained at the optimized process parameters with experimental results. Also, the maximum flank wear (VB_{max}) and total cutting force are compared with the previous literature having different coating materials.

4.2 Experimental investigation

Experiments are conducted in a HMT NH-26 high speed precision lathe. By using a dynamometer (Kistler, model 9272), the forces in three different directions i.e. main cutting force (F_c), radial force (F_p) and feed force (F_f) are measured during turning. Hard turning experimental setup with attached dynamometer and a specially designed tool holder is shown in Fig. 4.1. The surface roughness (*Ra*) of the work piece after machining is measured by using a Pocket Talysurf (Mahr pocket surf, model 44100).

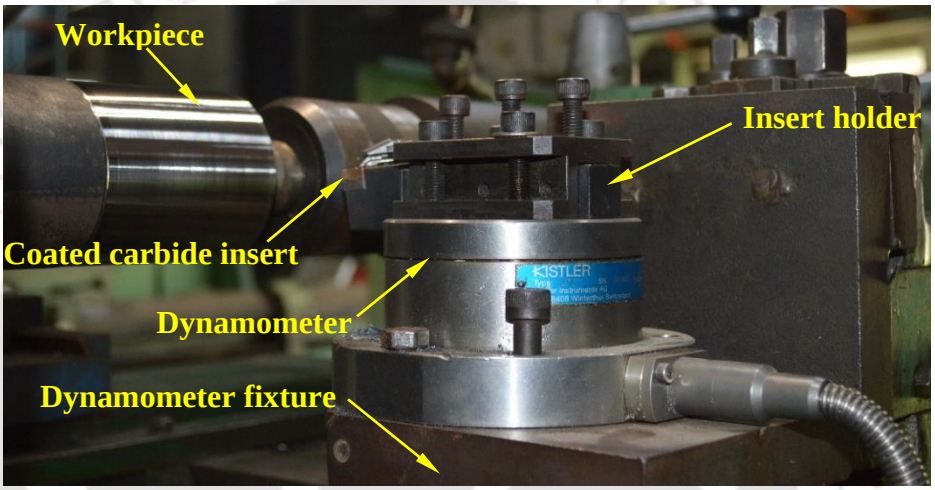

Fig. 4.1 Photograph of hard turning experimental set up

The maximum flank wear (VB_{max}, µm) is measured using Dinolite® digital optical microscope. All values of maximum flank wear (VB_{max}) of insert are measured after machining for a fixed length of work piece (400 mm) at different cutting conditions.

4.2.1 Work piece material, tool and its geometry

In the present study, hard to turn steel alloy i.e. EN-31 (AISI 52100) is selected as the work piece material which is a bar of round shape having 400 mm length and 80 mm diameter. The work piece hardness measured after tempering is 55 ± 2 HRC. AISI 52100 steel is extensively used for manufacturing bearings, CV joints, ball screws, gauges and axles. Energy dispersive X-ray (EDX) spectroscopy of AISI 52100 steel is carried out and the weight percentage of the elemental composition is shown in Table 4.1. Carbide inserts (ISO KU10 class) with HSN^2 coating are used for all the experiments. The average thickness of the coating on carbide insert is 12 µm. The tool

holder and the geometry of the insert are designated by ISO as MCLNR 2020 K12-BB and CNMG 120408MBB, respectively. The insert with 0° clearance angle is used.

Table 4.1 Elemental composition (wt %) of AISI 52100 steel

Fe %	F %	Cr %	Si %	P %	Mg %
95.4	2.8	1.2	0.4	0.1	0.1

4.3 Design of experiments

Statistical design of experiments (DOE) is carried out to find out the consequence related to the appraise of each input value of cutting parameters and their interactions on output responses. A new approach of RSM which is called Central Composite Rotatable Design (CCRD) is introduced in the present study to solve the problem of more number of experiments and also to solve the whole space of cutting parameter. The cutting parameters are selected on the basis of preliminary experiments (Alok and Das, 2018). The range of selected process parameters are given in Table 4.2.

Table 4.2 Cutting parameters with ranges

S. No.	**Parameter**	**Unit**	**Levels**		
			-1	**0**	**1**
1	Cutting speed (V_c)	m/min	140	195	250
2	Feed (f)	mm/rev	0.08	0.1	0.12
3	Depth of cut (a_p)	mm	0.06	0.08	0.1

During DOE, experiments are conducted by varying all the three cutting parameters simultaneously. For the evolution of the consequence of input parameters on output responses during hard turning, a large number of experiments are involved and RSM is applied to predict these values with a given set of conditions. The DOE Table for all 20 experiments with their responses are provided in Table 4.3.

Table 4.3 Experimental table based on CCRD and measured responses

Exp. No.	Process parameters			Responses				
	V_c (m/min)	f (mm/rev)	a_p (mm)	F_f (N)	F_p (N)	F_c (N)	Ra (µm)	*VB_{max} (µm)
1	195	0.1	0.08	31	80	42	1.53	262
2	140	0.12	0.1	50	142	75	2.1	202
3	195	0.1	0.08	28	80	41	1.48	256
4	195	0.1	0.11	35	97	46	1.6	266
5	195	0.1	0.08	30	77	35	1.53	258
6	250	0.12	0.06	20	47	24	1.3	285
7	195	0.1	0.08	32	76	38	1.6	253
8	287	0.1	0.08	11	30	15	0.84	270
9	250	0.08	0.06	16	43	23	1.1	275
10	250	0.12	0.1	23	54	27	1.31	292
11	195	0.1	0.06	28	78	38	1.38	252
12	140	0.12	0.06	48	119	59	1.78	188
13	195	0.1	0.08	31	69	36	1.4	259
14	195	0.1	0.08	29	78	39	1.55	252
15	140	0.08	0.06	40	103	51	1.2	185
16	250	0.08	0.1	21	52	25	1.23	288
17	195	0.13	0.08	37	91	42	1.75	262
18	195	0.06	0.08	29	72	32	1.33	252
19	140	0.08	0.1	49	121	61	1.5	190
20	102	0.1	0.08	57	156	83	1.9	116

*VB_{max} – maximum flank wear, F_f, F_p, F_c – feed, radial and main cutting forces, V_c – cutting speed, f – feed, a_p – depth of cut

4.4 Results and discussion

The responses from the experiments are studied to understand the process under different cutting conditions. Also, the experimental results are further compared with the previous work (Alok and Das, 2018) to understand the effectiveness of the present process. The experimental results are gathered on the basis of DOE in terms of forces, surface roughness and maximum flank wear. Further, the effect of individual process parameters (V_c, f and a_p) on output responses i.e. forces F_f, F_p, F_c, VB_{max} and Ra are analyzed using regression models (Eqs. (4.1–4.5)) within their selected experimental ranges.

4.4.1 ANOVA study

To find out the most effective process parameters affecting responses, analysis of variance (ANOVA) is the most effective tool. The outcomes are examined statistically to survey the

influence of turning parameters on feed, radial and main cutting force, surface roughness and maximum flank wear (VB_{max}). The ANOVA for feed, radial and main cutting force are given in Table 4.4 and the ANOVA for surface roughness and maximum flank wear are given in Table 4.5. Quadratic model is suggested in ANOVA for all the responses except surface roughness. The statistically significant model term indicates that the value of *p* in ANOVA table is less than 0.05 for 95% confidence interval.

Table 4.4 ANOVA for forces F_f, F_p and F_c

	F_f			F_p			F_c		
Source	**F value**	**p-value Prob > F**	**% Contrbn.**	**F value**	**p-value Prob > F**	**% Contrbn.**	**F value**	**p-value Prob > F**	**% Contrbn.**
Model	186.51	< **0.0001***		173.05	< **0.0001***		104.35	< **0.0001***	
Vc	1561.14	< **0.0001***	92.85	1425.11	< **0.0001***	91.35	836.10	< **0.0001***	89.15
f	37.22	**0.0001***	2.21	31.94	**0.0002***	2.04	21.44	**0.0009***	2.28
a_p	43.53	< **0.0001***	2.58	44.99	< **0.0001***	2.88	24.23	**0.0006***	2.57
$V_c f$	0.71	0.4203	0.041	9.33	**0.0122***	0.59	7.56	**0.0205***	0.80
$a_p V_c$	0.71	0.4203	0.041	6.07	**0.0335***	0.38	9.23	**0.0125***	0.98
$a_p f$	6.36	**0.0303***	0.37	0.087	0.7736**	0.005	1.03	0.3351**	0.10
V_c^2	18.23	**0.0016***	1.10	29.40	**0.0003***	1.88	33.67	**0.0002***	3.62
f^2	10.65	**0.0085***	0.62	1.39	0.2663**	0.08	0.57	0.4692**	0.06
a_p^2	2.78	0.1262	0.16	11.71	**0.0065***	0.74	3.98	0.0741**	0.42
Lack of Fit	0.47	0.7863**		0.55	0.7390**		0.59	0.7100**	

*Significant, **Non-significant, R^2 = 0.99 for F_f, 0.99 for F_p, 0.99 for F_c

The percentage contribution (F/ΣF) for each model term in Tables 4.4 and 4.5 gives rough but efficient guide for the percentage contribution of the terms. F_f is significant for feed force model (Table 4.4). Also, from Table 4.4, it is found that *Vc*, *f*, a_p, fa_p and are significant factors. The meaning of the insignificant of lack of fit in Table 4.4 signifies the model fits well with experimental data. From Table 4.4, it is also found that cutting speed is the predominant factor affecting feed force having 92.85% contribution compared to depth of cut (2.58%) and feed (2.21%). The regression equation is an imperial relationship among cutting conditions and responses. The regression equation for feed force in actual values of the factors is stated as

$$F_f = 78.07 - 0.36V_c - 146.83f + 238.53a_p - 0.34V_c f - 0.34a_p V_c - 2812.50a_p f + 4.74\times10^{-4}V_c^2 + 2712.42f^2 + 1386.59a_p^2 \quad (4.1)$$

The R^2 (co-efficient of multiple determination) value of 0.99 for feed force (F_f) shows good fitting of regression model (Eq. (4.1)) with input parameters.

Similarly, Table 4.4 shows the ANOVA for radial force (F_P) and the significant terms are highlighted. From Table 4.4, the model for radial force is found significant. Also, from Table 4.4, it can be seen that the model fits well with the experimental data for radial force as the lack of fit is insignificant. With a contribution of 91.35 %, the cutting speed is the most significant factor as compared to other significant parameters i.e. feed (2.04 %) and depth of cut (2.88 %) for radial force. The regression equation (R^2 = 0.99) for radial force in terms of actual values factors is

$$F_p = 192.13 - 0.75V_c + 329.94f - 507.75a_p - 3.52V_c f - 2.84a_p V_c + 937.50a_p f + 1.70\times10^{-3}V_c^{\,2} + 2782.03f^2 + 8085.33a_p^2 \quad (4.2)$$

The ANOVA for main cutting force is provided in Table 4.4 and the model is significant. Insignificance lack of fit is observed for main cutting force. Cutting speed is the most significant factor for main cutting force accounting 89.15% of the total variability compared to other parameters i.e. feed (2.28%) and depth of cut (2.57%). The regression equation (R^2 = 0.99) in terms of actual values of the factors for main cutting force is given as

$$F_c = 71.78 - 0.42V_c + 641.28f - 104.03a_p - 2.15V_c f - 2.38V_c a_p + 2187.50fa_p + 1.24\times10^{-3}V_c^2 - 1210.79f^2 + 3208.62a_p^2 \quad (4.3)$$

The model for surface roughness is significant as observed from ANOVA (Table 4.5) with V_c, f, a_p, $V_c f$ and $a_p V_c$ as significant terms. Also, insignificant lack of fit is observed for the model (Table 4.5). Cutting speed is the most dominant factor for surface roughness having 60.12 % contribution compared to feed (24.11 %) and depth of cut (6.55 %). The regression equation (R^2 =0.92) for surface roughness, (*Ra)* is given as

$$Ra = -1.86 + 0.01V_c + 30.37f + 17.89a_p - 0.10V_c f - 0.05a_p V_c - 31.25a_p f \quad (4.4)$$

The ANOVA for maximum flank wear (VB_{max}) is given in Table 4.5 and the model is significant. V_c, f, a_p and V_c^2 are significant model terms. Insignificant lack of fit is observed for maximum flank wear. In Table 4.5, V_c is the most dominant factor having 79.78 % contribution as compared to feed (0.41 %) and a_p (0.77 %). The regression equation (R^2 =0.99) for maximum flank wear, (VB_{max}) is given as

$$VB_{\max} = -177.15 + 3.69V_c - 182.99f - 408.08a_p - 0.11V_c f + 0.11a_p V_c + 937.50a_p f - 7.29\times10^{-3}V_c^2 + 1489.49f^2 + 3257.26a_p^2 \quad (4.5)$$

Table 4.5 ANOVA for *Ra* and VB_{max}

Source	***Ra***			***VB_{max}***		
	F value	**p-value Prob > F**	**% Contrbn.**	**F value**	**p-value Prob > F**	**% Contribution**
Model	23.61	< 0.0001*		351.99	< **0.0001***	
V_c	85.16	< **0.0001***	60.12	2501.76	< **0.0001***	79.78
f	34.15	< **0.0001***	24.11	13.11	**0.0047***	0.41
a_p	9.29	**0.0093***	6.55	24.43	**0.0006***	0.77
$V_c f$	10.06	0.0074**	7.10	0.011	0.9198**	0.0003
$a_p V_c$	2.86	**0.1145***	2.01	0.011	0.9198**	0.0003
$a_p f$	0.12	0.7301**	0.09	0.096	0.7631**	0.003
V_c^2				593.72	< **0.0001***	18.93
f^2				0.44	0.5238**	0.01
a_p^2				2.09	0.1791**	0.06
Lack of Fit	2.88	0.1298**		1.31	0.3883**	

*Significant, ** Non-significant, R^2 = 0.92 for *Ra* and 0.99 for VB_{max}

4.4.2 Validation of the present model

Three confirmation tests are conducted at different parameter conditions chosen arbitrarily within experimental range for the validation of the present model developed from regression analysis as shown in Table 4.6. The predicted values are calculated from the regression equations (Eqs. (4.1–4.5)) for each case. For confirmation tests, each experiment is repeated for three times and an average value is considered for final response. Figure 4.2 shows the comparison between predicted responses and actual experimental results with % error for (a) feed force, radial force, main cutting force and maximum flank wear and (b) surface roughness (*Ra*). The maximum error

among all parameters in Fig. 4.2 is observed as 6.7% for feed force which seems to be good match between the predicted and experimental results.

Table 4.6 Experimental conditions for validation tests

Exp. No.	V_c (m/min)	f (mm/rev)	a_p (mm)
1	120	0.08	0.06
2	180	0.08	0.06
3	240	0.08	0.06

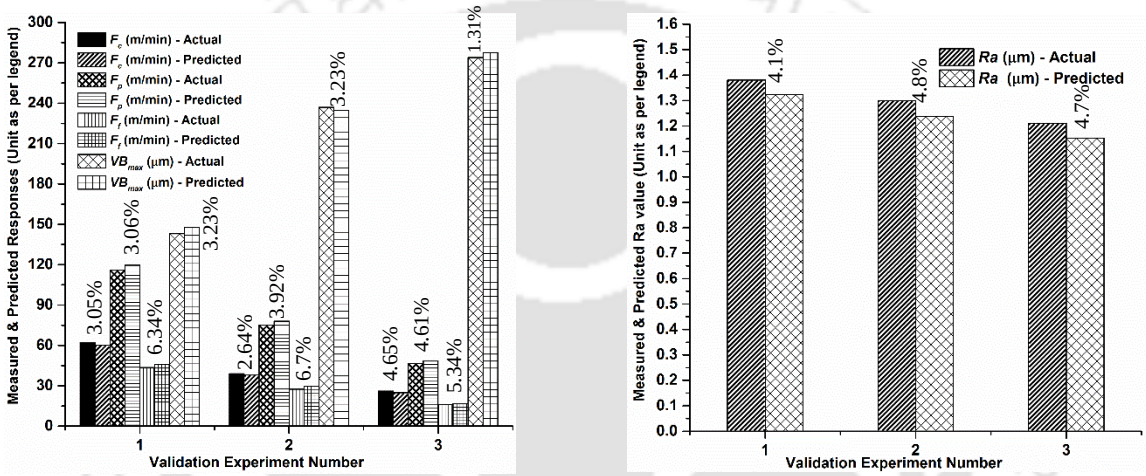

(a) (b)

Fig. 4.2 Validation tests to compare between experimental Vs. predicted responses (with % error) for (a) forces F_f, F_p, F_c and maximum flank wear (VB_{max}) and (b) Ra value

4.4.3 Forces

Figures 4.3 (a), (b) and (c) show the effect of cutting speed at different feed on main cutting, radial and feed force (F_c, F_p and F_f), respectively. As shown in Fig. 4.3, all three forces decrease with increased cutting speed for a given feed. The forces decrease due to the increment in shear angle with the increased cutting speed which leads to reduced chip thickness. Hence, the value of all three forces decreases. At lower cutting speed, rubbing phenomena occurs between tool insert and work piece surface. Due to this, the cutting tool experiences high pressure which induces diffusion. Hence, the shear force is not sufficient enough to generate the chip. Therefore, lower value of strain rate is generated. This is the probable reason for the increment in forces at lower cutting speed. Similar phenomena were reported by Suresh et al. (2012).

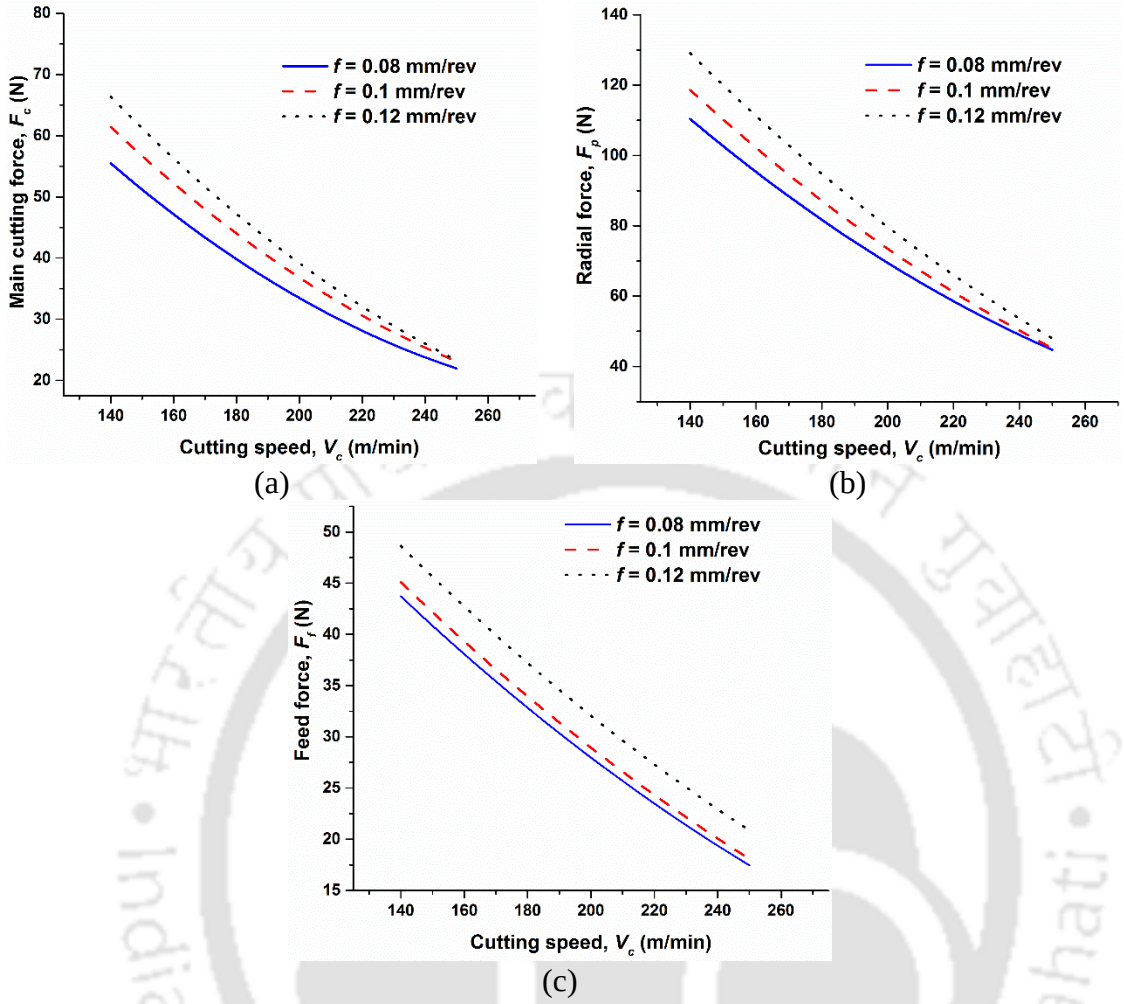

Fig. 4.3 Effect of cutting speed at different feed on (a) main cutting force (F_c), (b) radial force (F_p) and (c) feed force F_f

The nature of all three forces (i.e. F_c, F_p and F_f) with feed is shown in Figs. 4.4 (a), (c) and (e), respectively. Also, the 3D surface plots showing the combined effect of feed and cutting speed on F_c, F_p and F_f are shown in Figs. 4.4(b), (d) and (f), respectively. From Fig. 4.4, it is observed that forces F_c, F_p and F_f increase nonlinearly with increased feed for a certain value of cutting speed. The area of contact between insert and work piece increases as feed increases. As the contact area increases, the frictional force between work piece and tool insert also increases which leads to increased forces in all three directions (i.e. F_f, F_p and F_c).

Figures 4.5 (a), (c) and (e) describe the nature of all three forces with depth of cut and it is noted that these forces increase nonlinearly with increased depth of cut for a certain value of feed. This is because with the increase in depth of cut, the working area between tool and work piece increases. Because of this increased working area, material removal rate increases and it enhances pressure on the cutting edge of the insert (Suresh et al., 2012). Hence, all the three forces increase.

It is also observed from all experiments that F_p is greater than F_c. This happens due to the ploughing effect (Lalwani et al., 2008).

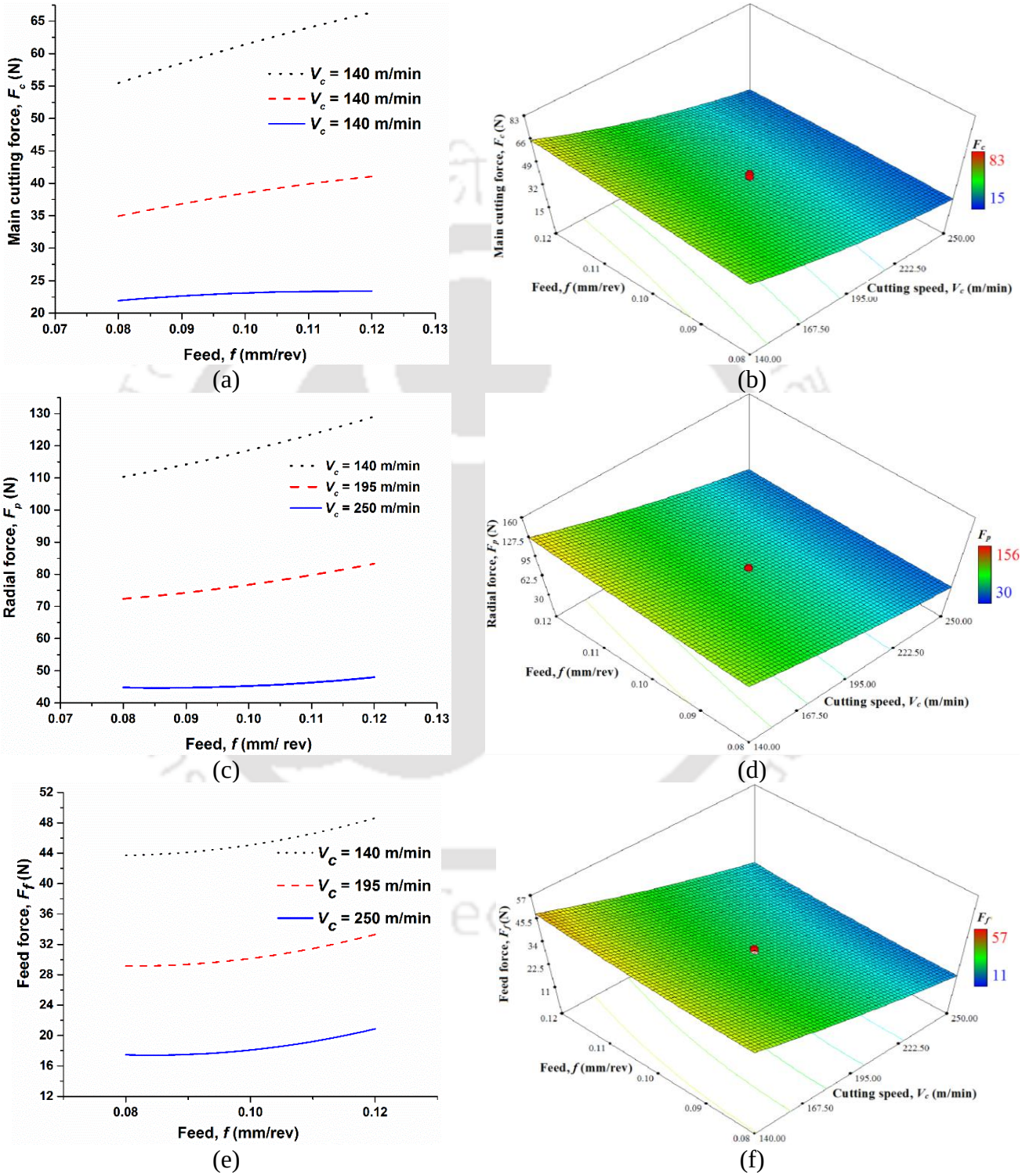

Fig. 4.4 Effect of feed on (a) F_c, (c) F_p and (e) F_f at different cutting speeds; 3D surface plots showing combined effect of feed and cutting speed on (b) F_c, (d) F_p and (f) F_f

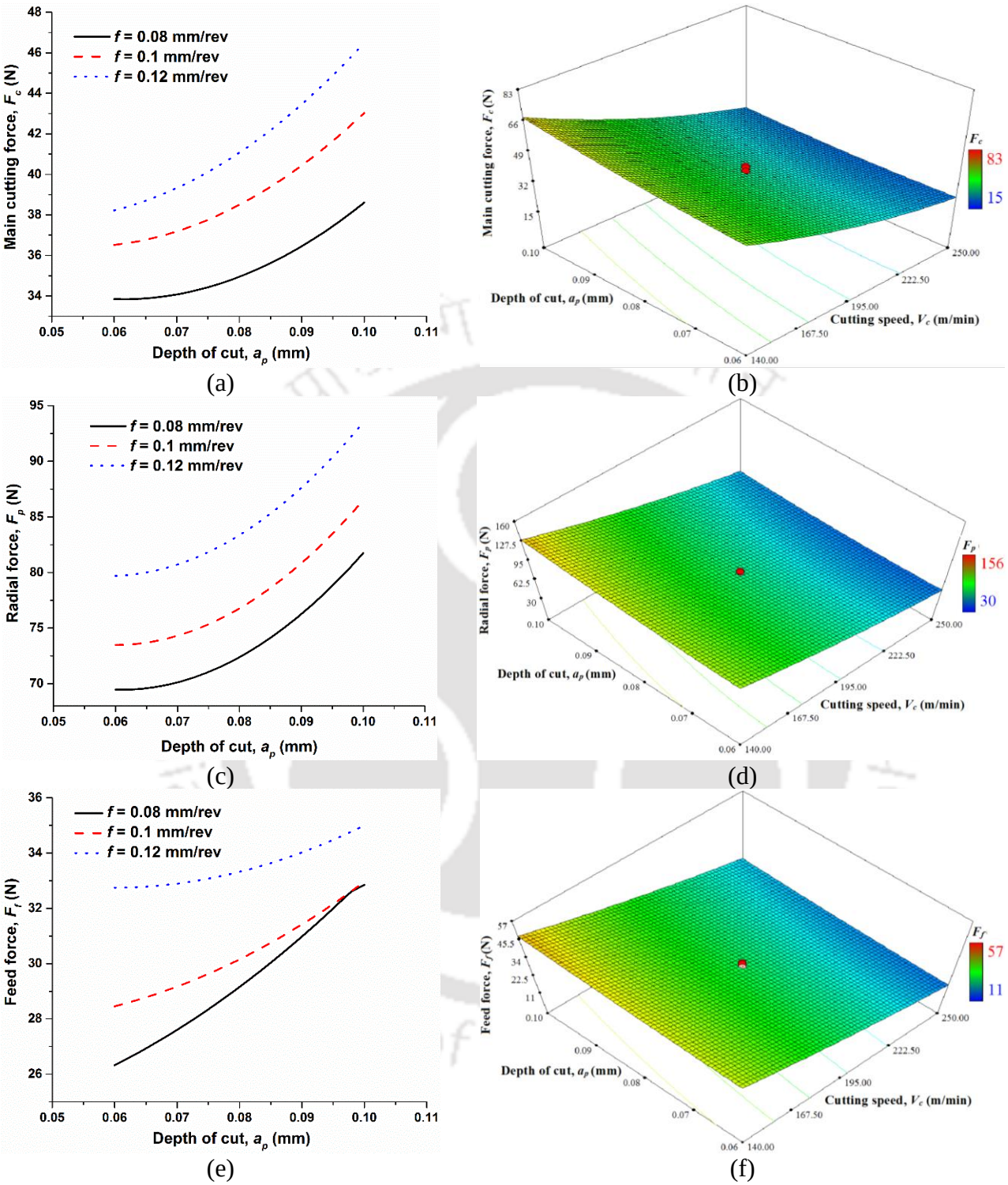

Fig. 4.5 Effect of depth of cut on (a) main cutting force (F_c), (c) radial force (F_p) and (e) feed force F_f) at different feed; 3D surface plots as combined effect of depth of cut and cutting speed on (b) F_c (d) F_p and (f) F_f

Further, the total cutting force (F_m) is calculated as

$$F_m = \sqrt{F_c^2 + F_p^2 + F_f^2} \tag{4.6}$$

Figures 4.6 (a), (b) and (c) show the effect of cutting speed, feed, and depth of cut, respectively on total cutting force (F_m) at different cutting conditions. The nature of plots for total cutting force in Fig. 4.6, shows similar trend as individual forces (F_c, F_p, F_f) as discussed above. Similar trend of total cutting force at different experimental conditions is also observed by Suresh et al. (2012).

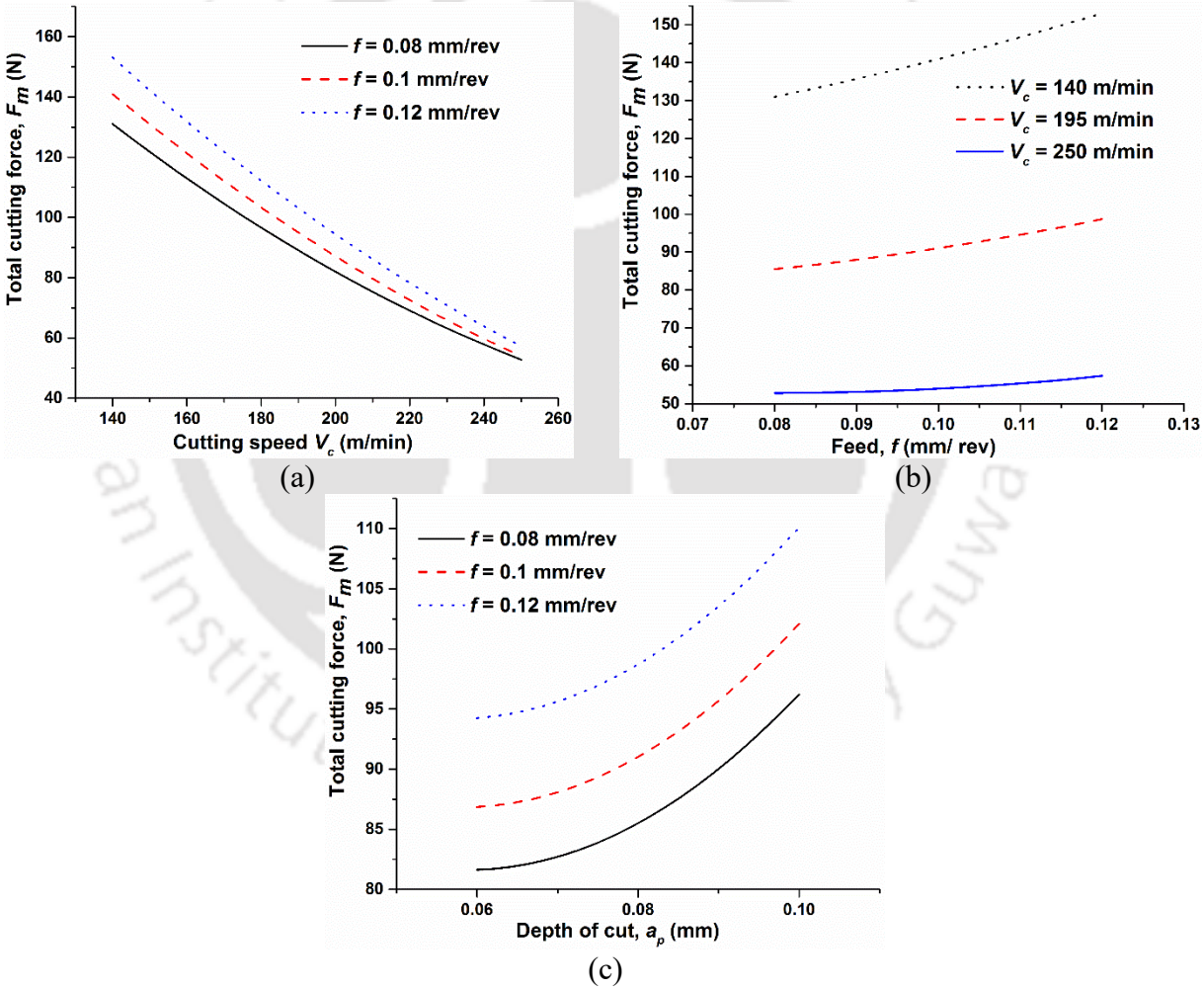

Fig. 4.6 Effect of (a) cutting speed, (b) feed and (c) depth of cut on total cutting force (F_m)

Their measured value of total cutting force using multilayer TiN/MT–TiCN/Al_2O_3 coated carbide insert is 451.09 N at cutting speed = 140 m/min, feed = 0.1 and depth of cut = 0.8 mm while machining AISI 4340 steel having hardness of 48 HRC. Their reported value of total cutting force

(451.09 N) is very high as compared to the present study (F_m =168.19N) using HSN^2 coated insert for almost same experimental condition (V_c = 140 m/min, f = 0.12 and depth of cut = 0.1 mm) which signifies the higher efficiency of the present coating material.

4.4.4 Surface roughness

The surface roughness values of the work piece at different cutting speed, feed and depth of cut are shown in Figs. 4.7 (a), (b) and (d), respectively. Also, the combined effect of feed & cutting speed, and depth of cut & cutting speed are shown in Figs. 4.7 (c) and (e), respectively. All surface roughness plots in Fig. 4.7 show linear trend at different cutting conditions. From Fig. 4.7 (a), it is observed that the work piece surface roughness sharply reduces with increased cutting speed. At higher cutting speed, the temperature in the cutting region increases. Due to which, the work piece material thermally softens in the cutting zone leading to lower value surface roughness. For a specific depth of cut, the observation shows that there is an increase in work piece surface roughness with increased feed (Fig. 4.7 (b)). During machining, increase in feed contributes to higher thrust force which generates vibration to the tool and more heat is generated leading to increased work piece surface roughness. Also, with the increase in feed, the heat generation increases due to high volumetric material removal. Plastic deformation in the work piece increases as the heat generation increases. It also promotes high surface roughness (Suresh et al., 2012). From Fig. 4.7, it can be seen that the favorable condition for achieving better surface roughness is lower feed and higher cutting speed. From Fig. 4.7 (d), it is evident that there is an increase in work piece surface roughness corresponds to increased depth of cut. The length of interaction between the tip of tool insert and work piece increases during machining due to increased depth of cut, leading to increased pressure on the tool tip. Hence, surface roughness increases.

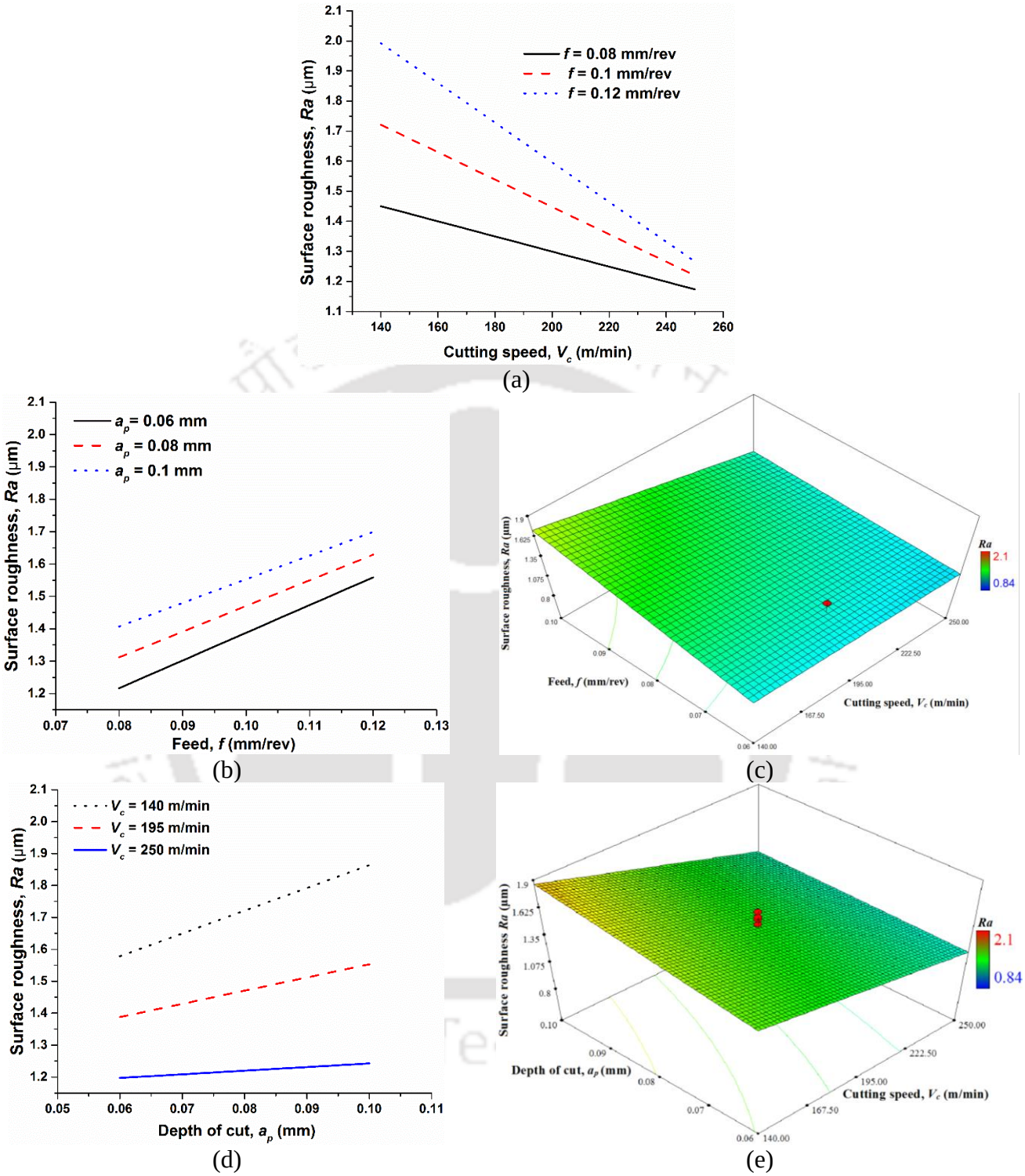

Fig. 4.7 Effect of (a) cutting speed, (b) feed and (d) depth of cut on work piece surface roughness; 3D surface plots showing combined effect of (c) feed and cutting speed and (e) depth of cut and cutting speed on work piece surface roughness

4.4.5 Maximum flank wear (VB_{max})

Different types of tool wear are shown in Fig. 4.8(a). Also, different zones of flank wear are shown in Fig. 4.8 (b) (Trejo et al., 2010). The maximum flank wear (VB_{max}) as shown in Fig. 4.8 (b) is measured using a digital microscope after machining work piece of 400 mm length at different cutting conditions. The maximum flank wear values are verified with tool failure criteria, ISO Standard 3685 as given in Table 4.7 (Mia et al., 2016).

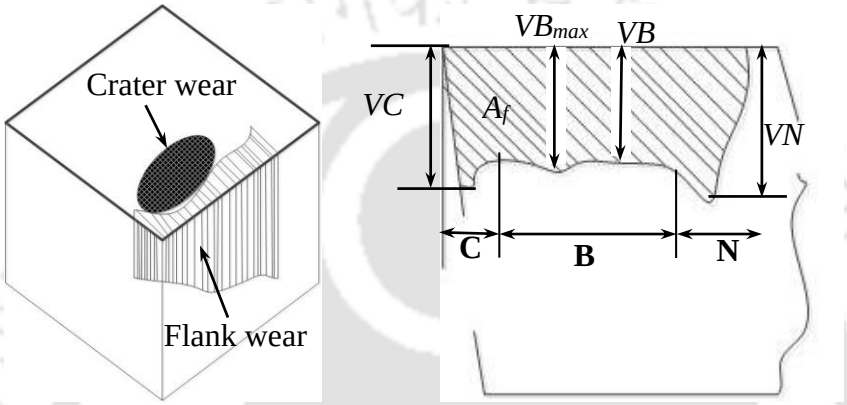

Fig. 4.8 (a) Crater and flank wear, (b) flank-wear area (A_f), width of flank wear (VB) and VB_{max} in zone B, notch wear (VN) in zone N and nose wear (VC) in zone C (Trejo et al., 2010)

Table 4.7 Tool failure criteria as per ISO standard 3685 (Mia et al., 2016)

Average flank wear	≥ 0.3
Maximum flank wear	≥ 0.4
Notch wear	≥ 0.3
Notching at the depth of cut line	≥ 0.6

The effect of depth of cut, feed and depth of cut on maximum flank wear (VB_{max}) are shown in Figs. 4.9 (a), (b) and (d), respectively. Also, the 3D surface plots of the combined effect of feed & cutting speed and depth of cut & cutting speed are shown in Figs. 4.9 (c) and (e), respectively. From the Fig. 4.9, it is noticed that maximum flank wear increases with the increase in cutting speed, feed and depth of cut. As cutting speed increases, it leads to increased temperature of the contact zone. The temperature increase in the cutting zone, often leads to the thermal instability of the material (Ciftci, 2006; Isik, 2007; Quiza et al., 2008). Also, at elevated cutting speed, abrasion effect dominates because of tool–chip friction at the rake surface which probably increases the tool wear (Fig. 4.9 (a)). Figure 4.9 (b) demonstrates the effect of feed on maximum flank wear. It is

found that initially at lower feed, flank wear decreases due to chip embrittlement. After that flank wear increases due to increased temperature at higher feed which leads to lower tool life.

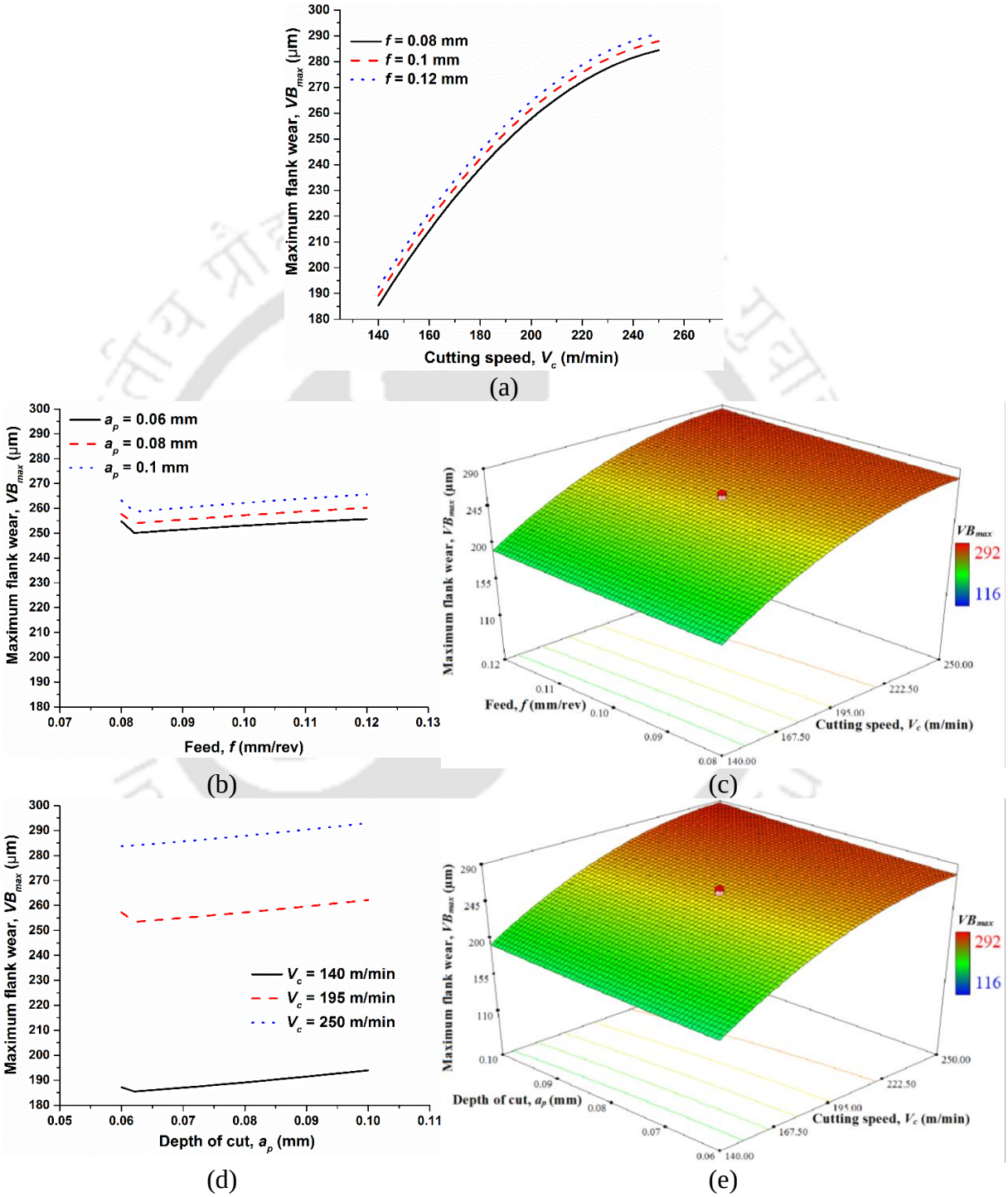

Fig. 4.9 Effect of (a) cutting speed, (b) feed and (d) depth of cut on maximum flank wear; 3D surface plots of combined effect of (c) feed and cutting speed and (e) depth of cut and cutting speed on *VBmax*

Similar observation is noticed by Su and Liu (2012) while machining AerMet steels. Similarly, maximum flank wear decreases initially with increased depth of cut (Fig. 4.9 (d)) because of chip embrittlement. However, at higher depth of cut, the interaction length between tool and work piece increases which leads to increased pressure on the tool. Hence, at higher pressure, maximum flank wear increases. Kumar et al. (2018) reported maximum value of flank wear while machining Inconel 825 alloy with AlCrN coated carbide insert. They found that the highest value of flank wear is 0.278 mm at cutting speed = 75 m/min, feed = 0.25 mm/rev and depth of cut = 0.15 mm. Much lower value of maximum flank wear (116 µm) is observed in the present study using HSN^2 coated carbide insert for almost similar machining condition (cutting speed = 102 m/min, feed = 0.1 mm/rev and depth of cut = 0.08 mm). Hence, HSN^2 coated insert is very effective for machining hard material in terms of tool wear at high cutting speed range as compared to the previous work (Kumar et al., 2018).

4.5 Multi-objective optimization of process parameters

In the present study, desirability function approach by Derringer and Suich (1980) is used for multi-objective optimization of the cutting parameters. Table 4.8 shows the list of constraints applied during optimization. Among all input factors, cutting speed is considered within the range of process parameters.

Table 4.8 Constraints for optimization

Parameters and responses	**Goal**	**Lower**	**Upper**
Cutting speed	In range	140	250
Feed	Minimize	0.08	0.12
Depth of cut	Minimize	0.06	0.1
Cutting force	Minimize	15	83
Radial force	Minimize	30	156
Axial force	Minimize	11	57
Surface roughness	Minimize	0.84	2.1
Flank wear	Minimize	116	292

The other parameters i.e. depth of cut and feed are minimized as their effect are found always positive for all output responses. Moreover, the regression equations (Eqs. (4.1-4.5)) for all three forces, maximum flank wear and surface roughness are considered as the objective functions and are minimized. Desirability study is performed for all three forces, surface roughness and

maximum flank wear. The optimum values of the process parameters are decided based on highest desirability value. The solution having desirability value close to 1 is considered as the best solution. The results of the optimization study are shown in Table 4.9. The solution 1 having combination of lowest possible predicted values of main cutting force, radial force, feed force, surface roughness and maximum flank wear with highest desirability value (0.823) is selected in the present study. The optimized process parameter values are cutting speed = 195 m/min, feed = 0.08 mm/rev and depth of cut = 0.06 mm.

Table 4.9 Optimization of the process parameters

Sol.	**Process parameters**			**Responses**					
No.	V_c (m/min)	f (mm/rev)	a_p (mm)	F_f (N)	F_p (N)	F_c (N)	Ra (μm)	VB_{max} (μm)	Desirability
1	**194.77**	**0.08**	**0.06**	**26.38**	**69.60**	**33.90**	**1.21**	**251.21**	**0.823**
2	189.64	0.08	0.06	27.58	72.42	35.26	1.22	246.67	0.822
3	213.74	0.08	0.06	22.14	59.95	29.46	1.189	264.64	0.820
4	249.88	0.08	0.06	15.01	44.96	23.46	1.138	275.72	0.819
5	222.20	0.08	0.06	20.37	56.05	27.77	1.177	268.94	0.818

4.6 Confirmation tests

A confirmation test as shown in Table 4.10 is carried out at optimized process parameter condition to validate the regression models (Eqs. (4.1-4.5)) developed from the experimental analysis.

Table 4.10 Confirmation tests

Main cutting force	Predicted	33.90
	Actual	32.50
	% error	4.3
Radial force	Predicted	69.60
	Actual	72
	% error	3.33
Feed force	Predicted	26.10
	Actual	28
	% error	6.8
Surface roughness	Predicted	1.22
	Actual	1.29
	% error	6.2
Flank wear	Predicted	250.61
	Actual	252
	% error	0.05

The experiments are repeated for three times and an average value is considered to calculate the responses. The predicted values of the responses are calculated from regression equations (Eqs. (4.1–4.5)) and the actual value of the responses are measured from confirmation tests. Also, the percentage error between predicted and actual responses is calculated and a maximum error of 6.8% is observed for feed force. For all other responses, the % error are even negligible which clearly confirms the outstanding reproducibility of regression equations (Eqs. (4.1–4.5)).

4.7 Summary

From ANOVA, the cutting speed is the found to be most significant factor having 89.13% contribution followed by depth of cut (2.57%) and feed (2.28 %) while considering main cutting force as the response parameter. Similarly, for radial force, cutting speed is the most effective factor (91.33 % contribution) following depth of cut (2.88 %) and feed (2.04 %). Also, for feed force, cutting speed is the most significant factor (92.83% contribution) followed by depth of cut (2.58%) and feed (2.21%). For surface roughness, the most significant factor is cutting speed with 51.55% contribution followed by feed and depth of cut with 20.64% and 5.61% contribution, respectively. For maximum flank wear, the cutting speed has substantial effect (79.78%) followed by depth of cut (0.77 %) and feed (0.41 %). From conformation tests, it is observed that at optimized cutting condition, the predicted results from regression models are very close to the experimental results.

Chapter 5 White layer analysis

5.1 Introduction

In last few decades, many industries accepted hard turning as a leading manufacturing process. Dry hard turning at high speed has many advantages compared to traditional machining like high efficiency, environment friendliness, cost effectiveness, high production rate etc. (Alok and Das, 2018; Alok and Das, 2019; Musavi et al., 2018). Hence, it is very useful for machining hardened material. Hard material having hardness value over 45 HRC is called hard turning (Rashid and Goel, 2016).

Throughout last decade, the material removal by hard turning in various industries is observed highly growing due to fast development in cutting inserts like cubic and poly-cubic boron nitride, ceramic and coated carbide inserts. In past, many investigators studied the behaviour of surface integrity of machined surface which mainly covers (a) surface topography features like surface quality (Grzesik and Zak, 2014), (b) mechanical properties like residual stress and hardness (Ali and Pan, 2015; Farrokhi et al., 2015) and (c) metallurgical study like surface microstructure and phase transformation study of state (Tang et al., 2014). Structural changes on material surface is introduced by metal cutting or any material removal process. This happens mainly due to rapid changes in thermal properties of material leading to metallurgical alteration as well as possible chemical reactions. Huge changes in the material structure can be seen in the machined surface compared to the base material. Due to these reasons, a substantial change in surface integrity, which includes white layer formation, surface finish alteration and residual stress development etc. are observed (Chou and Evans, 1999; Bosheh and Mativenga, 2006). The origin of 'white layer' comes from the fact that when viewed through a microscope (either optical or scanning electron microscope), the machined surface appears white. Therefore, white layer is seen in the form of a basic phase transformation which occurs to the machined surface layers that are very hard and it is observed in ferrous materials which appears white when viewed through microscope under different conditions. Even though the regular way of referring to such layer is 'white layer', many other terms are also used like non-etching layer, white phase, white etching layer, etc. The generation of white layer is due to various factors like mechanical, chemical or thermal process owing to machining.

Some of the manufacturing process like, grinding, electrical discharge machining, turning, and surface treatments process are changed their microstructure, mechanical properties and surface

quality of the bulk material during machining. Normally, this type of changes which is confined to a few micrometres are referred as white and dark layer (Umbrello and Filice, 2009). From last decade, hard machining is eliminating many processes like finishing, heat treatment and grinding while saving production time (Umbrello and Rotella, 2012). Sometime, hard turning is also referred as finish hard turning as it has got advantages over grinding process by providing good surface finish properties at high MRR.

Bartarya and Choudhury (2012) studied white layer after machining of H13 steel with CBN tool. They found that in the region of white layer, the hardness at the subsurface is harder than the bulk material. Rech and Moisan (2003) studied the effect of friction energy which is produced in significant amount during hard machining on white layers. The high amount of heat is responsible in two ways for the formation of white layer i.e. either by tool-work piece interaction due to high tool wear or due to machining at a very high cutting speed. They observed that the martensite in base material is changed to austenite in white layer during hard machining. It has been observed that most of the heat is produced at high speed and it is taken away by the swiftly moving chips (Yallese et al., 2009). Hence, the work piece and tool temperature are substantially reduced. The thickness of white layer is also started reducing as the cutting speed is increased beyond a certain limit. Poulachon et al. (2005) analyzed white layer with the help of metallographic technique and found that an increase in tool flank wear, increases machined surface temperature which in turn results in increased white layer thickness. Also, a thicker white layer was observed on finer microstructure steel than those with a coarse grain structure. It was also noticed that as the white layer thickness and time were increased, the amount of carbon contained in the white layer was also increased (Poulachon et al., 2005). Aramcharoen and Mativenga (2008) studied white layer and subsurface hardening effects in hard turning of H13 steel using coated carbide insert. They observed that the use of coating in the tool helped in reducing both tool and work piece temperature due to low coefficient of friction between tool with both work piece and chip. They found that the coated tools are less prone to work hardening. Negligible thickness of white layer is produced during high speed machining using coated carbide insert.

5.1.1 Formation of white layer

The development of white layers has been found in various manufacturing processes. Generally, the existence of white layers is divided into three fields. Firstly, white layer is found on the surface of the components like roller bearings, piston heads and rail heads immediately after

component's removal from their manufacturing process. Also, white layer which are disadvantageous in many ways to the final performance of the product is very common in the processes like reaming, grinding, drilling, turning, milling and pin-on-disk experiments, etc. (Shaw and Vyas, 1994; Kruth et al., 1995). Therefore, removal of white layers will lead to the reduction in manufacturing cost. Also, it reduces the cycle time for post processing of finishing operations.

White layers are associated with in many operations such as grinding since long time. In case of grinding, work piece surfaces are most likely get damaged. This is due to more relative flow of heat into the surface of the work piece in case of grinding as compared to normal cutting operation because of bad thermal conductivity of the grinding wheel which contains aluminium oxide. Also, negative rake angle of the active abrasive particles in the grinding wheel produces a ploughing effect as compared to normal cutting operation. Thus, the probability of damage due to thermal processes is more in case of grinding when compared to metal cutting. Un-tempered martensite and white layers are produced in abusive grinding conditions. When grinding processes are compared between gentle and abusive grinding environments, it is found that the endurance strength of the machined surface gets limited to 40% for abusive grinding (Griffiths, 2001).

Zhang et al. (2018) analyzed the generation of white and dark layers during hard turning of AISI 52100 bearing steel with PCBN cutting tool and correlated white layers with the results obtained from XRD and TEM. The investigation of surface finish was done by Mativenga and Hon (2003) on tool steel with various types of coatings on inserts using PVD in high speed milling operation. It was inferred from their studies that the majority of the coated tools generate good surface finish for almost all cutting speeds at which they were tested. However, in case of combined titanium-aluminium-nitride (TiAlN) and tungsten carbide coating, an exception was seen. At some notable speed, surface quality of the work piece surface after machining was measured nearly four times than that of other coatings. The authors studied white layer for these two tool materials. As the formation of white layer was affected by tool material, they concluded that the material interactions are mainly responsible for the destruction of surface integrity (Mativenga and Hon, 2003).

From literature survey, it is found that the wear in the cutting tool inserts dominates other factors of white layer formation. Due to phase transformation, white layer is generated and it happens when the interface temperature reaches austenitic temperature or even at lesser temperature. This white layer formation also accompanies with high strain rate. During high speed machining, there is a steady increase in the flank wear over time. However, the formation of white

layer is reduced as the temperature dissipation takes place at the interface between tool and work piece since the chip carries away most of the heat generated in primary shear zone. The cutting parameters and cutting tools have high influence over fatigue strength of the material that has been hard turned. From literature survey it is noticed that there is insufficient literature available in the field of white layer formation. Also, the reasons for its formation during hard machining using fresh tip of cutting tool inserts are not available. In addition, most of the earlier researchers have considered white layer formation using a cutting tool insert which is already worn out i.e. purposefully they have created wear on the tool before machining. These phenomena might have led to an inference that white layer thickness decreases at high cutting speeds. Most of these tests were carried out over a small range of cutting speeds. No previous literature is available on study of white layer formation during machining of AISI 52100 steel using HSN^2 coated carbide insert.

The motivation behind the present work is to explore the changes in the white layer thickness for a wide range of cutting speeds. Also, the thickness of the white layer at different cutting speeds is correlated with (i) micro-hardness, (ii) temperature of the machined surface and also, chip temperature and (iii) phase transformation information of materials measured from XRD.

5.2 Details of experiments

HMT NH-26 lathe machine is used for conducting experiments. All experiments are conducted at different cutting speeds (V_c) for a fixed feed (f) and depth of cut (a_p). Table 5.1 shows the experimental conditions.

Table 5.1 Process parameters and their range for experimentation

	Cutting parameters		
	V_c (m/min)	**f (mm/rev)**	**a_p (mm)**
Range of cutting parameters	100 131 171 220 288	0.01	0.08

5.2.1 Work piece material, tool and its geometry

In the present study, hard alloy steel, EN–31 (AISI 52100) is selected, which is round in shape, having length and diameter as 200 and 80 mm, respectively. After tempering, the required

hardness of the work piece is obtained as 55 ± 2 HRC. EN–31 steel is used at large scale for manufacturing of bearings, gauges, ball screws, CV joints, etc. ISO designated KU10 class carbide inserts with HSN^2 coating (PVD coated) having fresh cutting edge and 0° clearance angle are used for every experiments. The average coating thickness of 12 µm is used on the carbide insert. MCLNR 2020 K12-BB and CNMG 120408MBB are the geometry of the tool holder and insert, respectively which is ISO designated. The elemental composition (wt. %) of AISI 52100 steel work piece is carried out using energy dispersive X-ray (EDX) spectroscopy as shown in Fig. 5.1.

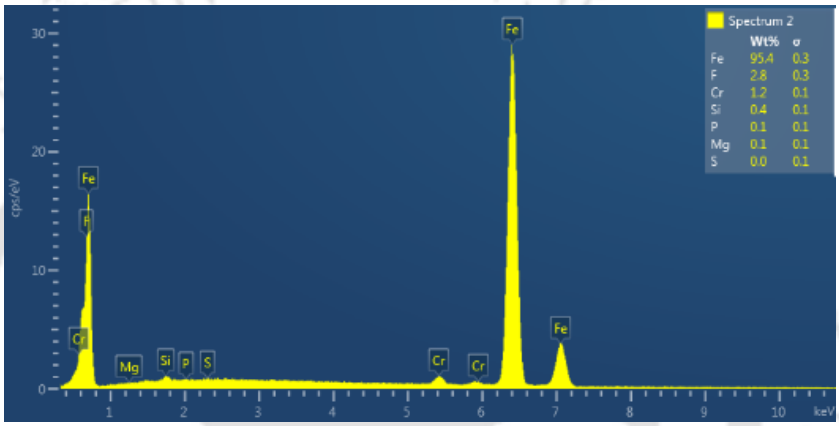

Fig. 5.1 EDX analysis of AISI 52100 steel work piece before machining

5.3 Sample preparation for white layer characterization

The sample is prepared from the test bar having diameter 80 mm and length 200 mm as shown in Fig. 5.1. From this bar, a disc of 4 mm thickness is cut using wire electro discharge machine (W–EDM). Later, the final sample of dimension 5×5×4 mm is prepared from this disk using W–EDM for further characterization. After that the sample is polished by standard metallurgical procedure. The samples are polished using alumina abrasive powder having average grain size of 0.6 µm. After that the samples are etched with 2% nital solution before characterization. Figure 5.2 shows the systematic diagram for sample preparation followed for the measurement of white layer thickness.

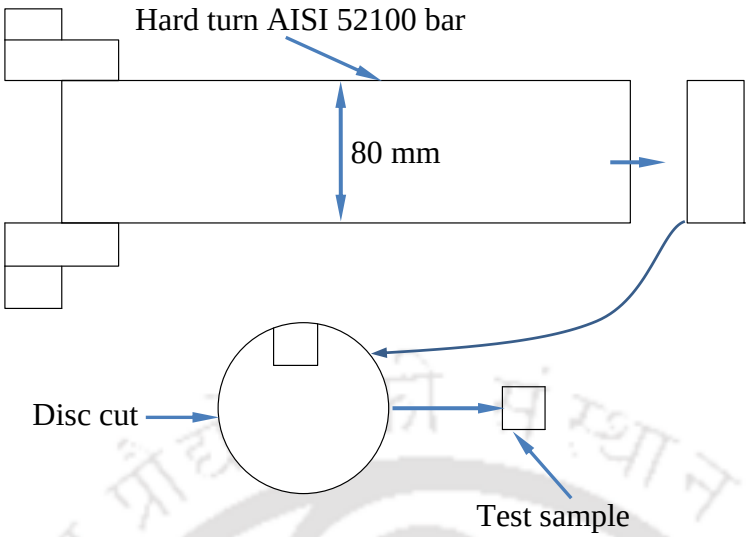

Fig. 5.2 Schematic diagram showing preparation of sample from hard turned bar

5.4 Results and discussion

Many researchers found that cutting speed is the main reason for the rise in temperature at the interface of tool and work piece. Also, the temperature mainly influences the formation of white layer. Hence, experiments are conducted to find out the suitable cutting conditions by changing cutting speed for a fixed feed and depth of cut. Further experimental analysis helps in deriving the relationship between cutting speed with both white layer formation and micro hardness distribution. The experimental results are discussed below.

5.4.1 Workpiece and chip temperature

Analysis of temperature plays a vital role to understand the principle of white layer generation. By using infrared (IR) camera, the temperature of machined surface and generated chips are measured during hard turning. Figure 5.3 shows the temperature plot with time at cutting speed = 100 m/min. From Fig. 5.3, it is seen that at some time the temperature increases suddenly to a very high value. Sudden increment in temperature in Fig. 5.3 is due to the chip interface temperature which has a very high value. The temperature of the machined surface is almost constant throughout cutting time period and its value is 285 °C.

The temperature behavior of chip as well as machined surface are shown in Fig. 5.4 at different cutting speeds. The chip temperature increases from 550°C to 800°C from cutting speed 100 to 288 m/min. The temperature of the machined surface is slightly reduced from 285°C to

261°C for the same cutting speed. Hence, a relationship can be drawn between machined surface temperature with cutting speed which is inversely proportional and between chip temperature with cutting speed is directly proportional. A possible reason for reduced machined surface temperature with cutting speed may be due to faster removal of chip at higher cutting speed which leads to less contact time between chip and work piece machined surface. Hence, less heat is conducted to the work piece and most of the heat is carried away via chip. However, the chip temperature increases with cutting speed as seen in Fig. 5.4 for the entire cutting period due to tool wear. Increment in contact between tool-chip interface at higher cutting speed is the main reason for increased tool wear which leads to higher friction at the tool-chip interface. Hence, chip temperature increases with increased cutting speed.

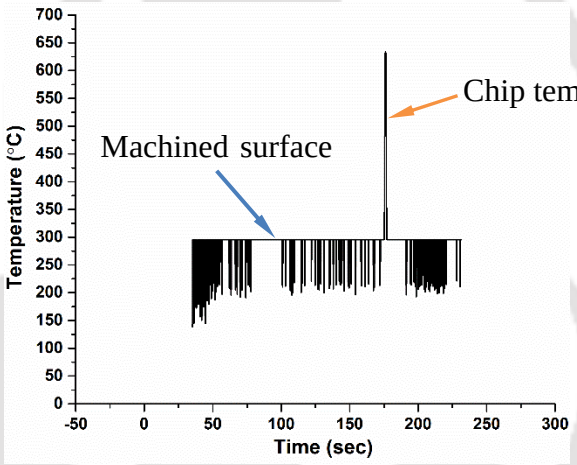

Fig. 5.3 Temp. plot of machined surface along with chip with time at 100 m/min cutting speed

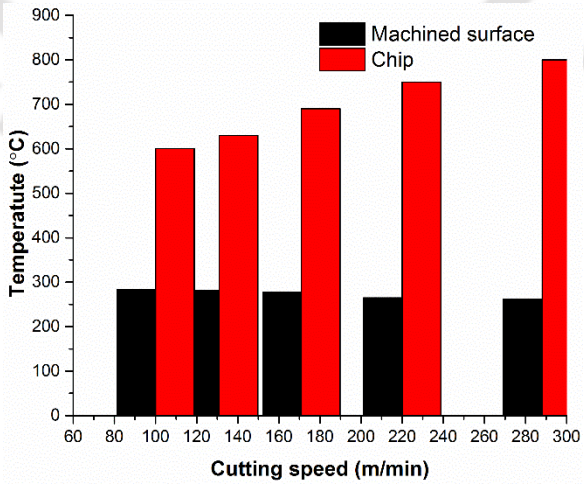

Fig. 5.4 Temperature plot of machined surface along with chip at different cutting speeds

5.4.2 Depth of white layer

Machined surface morphologies at different cutting speed are analyzed by both optical as well as field emission scanning electron microscopy (FESEM) as shown in Fig. 5.5.

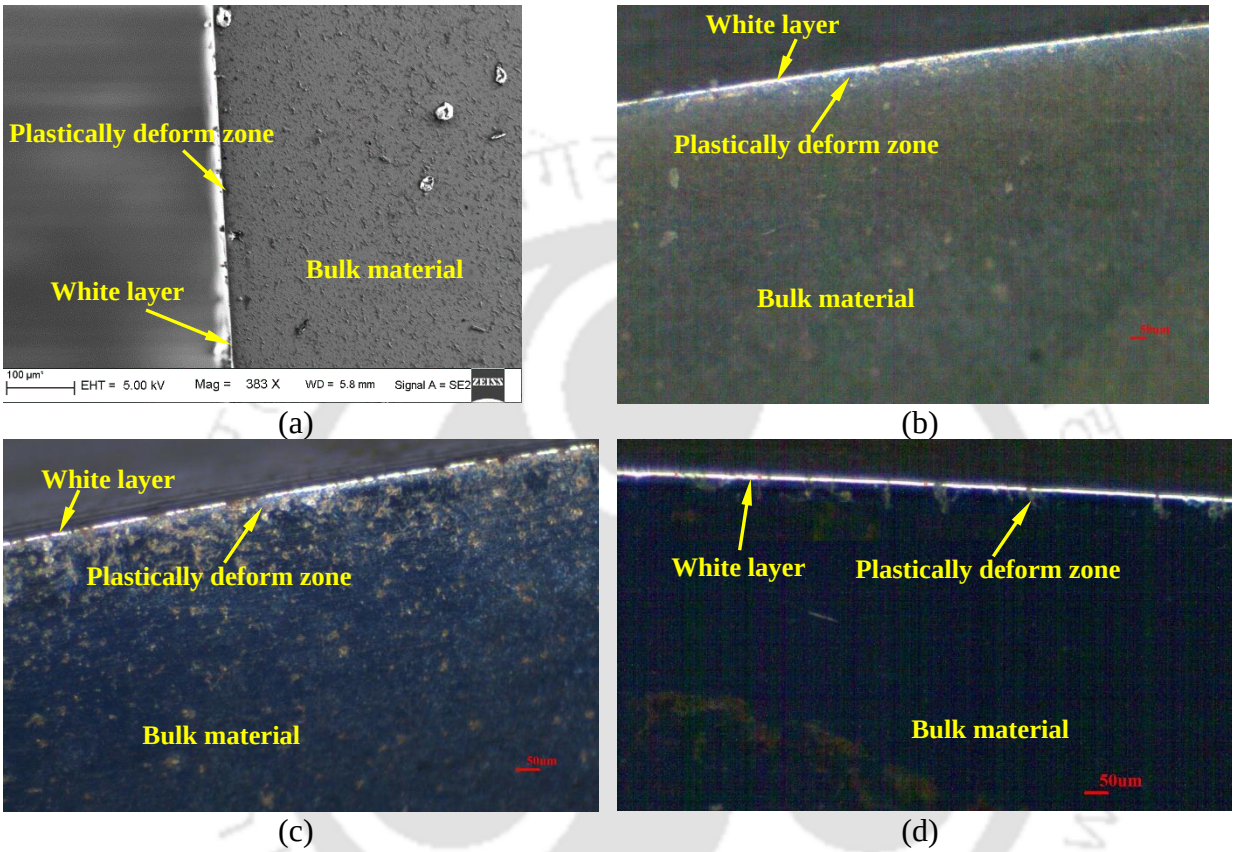

Fig. 5.5 (a) FESEM micrograph at 100 m/min cutting speed, and optical images of white layer at (b) 100, (c) 171 and (d) 288 m/min cutting speeds

The FESEM image of the machined surface (as well as sub-surface) at cutting speed =100 m/min, feed= 0.1 mm/rev and depth of cut =0.08 mm using HSN^2 coated carbide tool is shown in Fig. 5.5 (a). The first layer in the heat affected zone in Fig 5.5 (a) is represented as white layer having thickness of 6.5 µm. A plastically deformed zone just below the white layer is also observed as shown in Fig. 5.5 (a). The optical image micrograph of the machined surface at the same experimental condition is shown in Fig. 5.5 (b) where the white layer is prominently visible along with plastically deformed zone. The machined surface morphologies at 171 and 288 m/min cutting speeds are shown in Figs. 5.5(c) and (d), respectively where thickness of the white layers is also measured. Overall, from Fig. 5.5, it is observed that with increased cutting speed, the white layer thickness decreases and its trend is shown in Fig. 5.6. Highest thickness of the white layer is

observed for lowest cutting speed of 100 m/min and its value decreases with increased cutting speed (Fig. 5.6). The similar trend is also observed by Bosheh and Mativenga (2006).

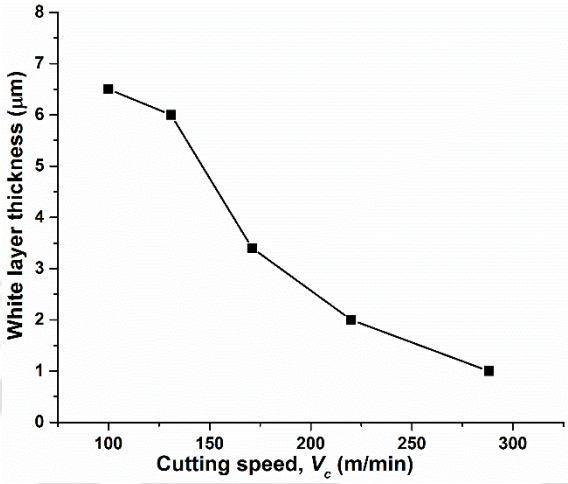

Fig. 5.6 White layer thickness variation plot at different cutting speeds

Many reasons can be attributed to the present trend between depth of white layer with cutting speed. The first reason is that at lower cutting speed, the temperature of the machined surface is higher as compared to higher cutting speed as observed in Fig. 5.6. The influence of thermal conditions is found out to be very crucial in the present case as the machined surface is subjected to rapid heating and further cooling by surroundings as compared to unheated bulk mass. This leads to phase transformation near machined surface which in turn results in a formation of a layer called modified layer or white layer. The high temperature generated at a cutting speed of 100 m/min also increases number of chemical reactions with the surroundings as compared to higher cutting speed. The second reason is reduced plastic deformation at higher cutting speed which further reduces cutting forces as the material is now being subjected to lesser stresses.

5.4.3 XRD analysis of white layer

X-ray diffraction (XRD) analysis of un-machined as well as machined surfaces are conducted to analyze the white layer in terms of metallurgical compositions as shown in Fig. 5.7. In Fig. 5.7, the XRD peaks of different phases of both base material and machined surfaces are compared at (a) 100, (b) 131, (c) 171, (d) 220 and (e) 288 m/min cutting speeds. In XRD peaks (Fig. 5.7), the peaks correspond to body center cubic (BCC) structure indicates α ferrite phase whereas peaks correspond to face center cubic (FCC) structure indicates retained austenite phase.

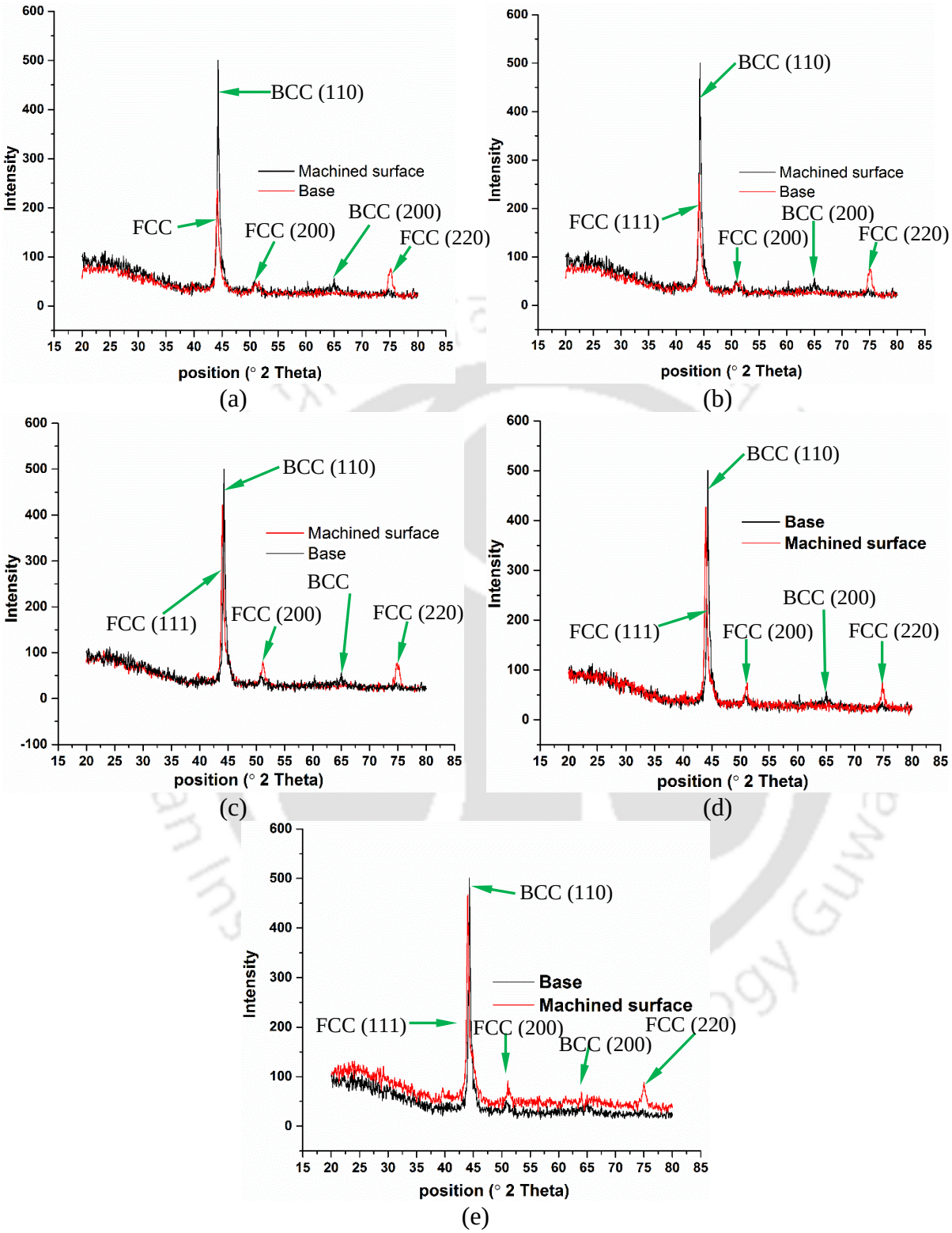

Fig. 5.7 Comparison of diffractograms between base material and machined surfaces at (a) 100, (b) 131, (c) 171, (d) 220 and (e) 288 m/min cutting speeds

From Fig. 5.7, it can be observed that the spectrum obtained from XRD analysis for machined surfaces contains comparatively smaller peaks and broader width as compared to the

base materials for all cutting speeds. From this phenomena, it can be inferred that the white layer crystallinity is meager in case of machined surface as compared to bulk material. Also, inside white layer, refinement of grains occurs as reported by Du et al. (2014). The comparison between base material and machined surface in terms of full width half maxima (FWHM) and retained austenite content (wt. %) are shown in Table 5.2 at different cutting speeds. In Table 5.2, higher value of FWHM is observed for machined surface as compared to the un-machined surface. Increased value of FWHM signifies poorer crystallinity, more grain refinement and higher dislocation density which occurs in the sample. Five peaks are obtained from XRD analysis for base material as well as machined surface as shown in Fig. 5.7. According to PDF2-2004 cards (i.e. XRD software), peaks at 43.67 deg refers to (111) miller index and similarly at 50.67 deg refers to (200) and 74.68 deg refers to (220) miller indices which corresponds to FCC microstructure. Also, the peaks at 44.35 deg and 64.52 deg refer to α–ferrite (BCC) phase at (110) and (200) miller indices, respectively. It is observed from XRD peaks that after machining, the XRD peak at 44.35 deg is shifted to 43.67 deg, which corresponds to retained austenite miller index of (111). Similar, phenomena are also observed by Zhang et al. (2016) and Umbrella and Rotella (2012) from their XRD analysis of hard turned samples.

Table 5.2 Comparison between base material and machined surfaces at different cutting speeds in terms of FWHM and retained austenite content (wt. %)

Sample	**FWHM at 2 theta**	**Retained austenite content (wt. %)**
Base material (without machining)	0.30 (44.4)	5.2
Machined surface at different cutting speed (m/min)		
100	0.52 (43.8)	28.5
131	0.50 (43.8)	24.1
171	0.37 (43.8)	10.4
220	0.34 (43.8)	7.4
288	0.32 (43.8)	6.1

From Table 5.2, it can be seen that more amount of retained austenite is present in the machined surface as compared to the base material (5.2 %). The highest value of retained austenite (28.5 %) is observed at lowest cutting speed (100 m/min) and its value decreases with increased cutting speeds. The minimum % of retained austenite (6.1 %) is observed at highest cutting speed of 288 m/min. The increased retained austenite (28.5 %) at lower cutting speed means it contains

more percentage of carbon which increases work piece hardness. The hardness value of the machined surface is measured and discussed in the next section. Also, it is observed that at lower cutting speeds the white layer thickness is more (Fig. 5.6) due to higher content of retained austenite in the machined surface. Hence, it can be concluded that the austenization occurs (i.e. phase changes from α–ferrite (BCC) to austenite (FCC)) during white layer formation for machined surface even if there is a usage of fresh tip of cutting tool.

5.4.4 Microhardness

During hard machining, the machined surface reaches to a very high temperature and it cools down in air which makes this surface very brittle and hard in the form of white layer. At different cutting speeds depending on different values of the generated temperature and subsequent cooling phenomena, different thickness of the white layer is generated. Hence, in this section the microhardness analysis of the machined surface consisting white layer and deformed zone are carried out at different cutting speeds as shown in Fig. 5.8.

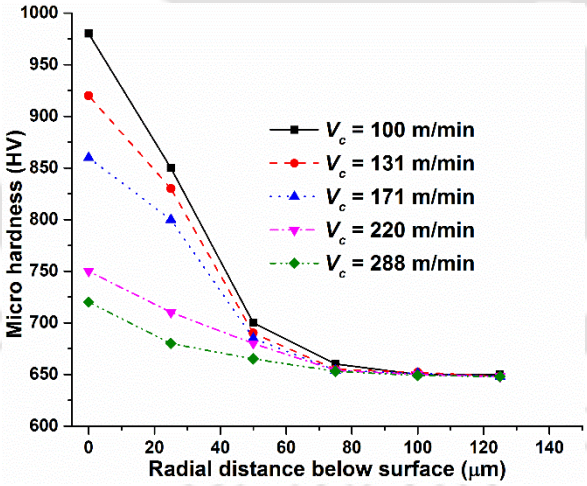

Fig. 5.8 Microhardness plot along radially(at a cross–section) below machined surface at different cutting speeds

In Fig. 5.8, the highest value of the hardness is observed in the white layer on machined surface for any cutting speed. A drop in hardness is observed in the region below white layer which is plastically deformed. At lowest cutting speeds of 100 m/min, the maximum value of hardness measured at the machined surface is nearly 1.5 times higher than that of the bulk material. However, it is observed that with increased cutting speeds, the hardness of the machined surface

decreases. Thermal influences are the main reason for increased hardness in the machined surface. While machining, the temperature of the surface is found to increase to a higher level and subsequently it rapidly cooles down. Due to heating and subsequent cooling, a hard layer is formed during hard turning. Due to carburizing effect, carbon percentage also increases, which leads to increased machined surface hardness. The reduction in surface temperature as discussed in Section 5.4.1 (Fig. 5.4) with increased cutting speed is attributed to the reduced machined surface hardness.

5.5 Summary

From experimental analysis, it is found that white layer thickness during hard machining can be controlled by careful selecting suitable cutting parameters. The machined surface temperature plays significant role for higher thickness of white layer. From XRD analysis of machined surface, it is observed that the retained austenite accumulates at the machined surface during formation of white layer. Maximum hardness value is observed at the top machined surface (i.e. white layer), further its value decreases radially across the cross section at the subsurface at plastically deformed zone and further reaches to the original hardness value at bulk material. The machined surface with white layer is harder than the base material.

भारतीय प्रौद्योगिकी संस्थान गुवाहाटी
Indian Institute of Technology Guwahati

Chapter 6 Simulation of orthogonal hard turning operation

6.1 Introduction

Machining is considered to be the best way for manufacturing and producing of many items. Most of the industries manufacture parts through machining process. Machining is preferred for its high dimensional accuracy and high productivity (Sadat et al., 1991). It contains many material removal processes like turning, milling, drilling, grinding, boring, chamfering, polishing and so on. Each process has its own cutting tool and machining setup. The suitable machining process among these lists is chosen according to the need. Hard turning, a process of single-point cutting of materials with hardness above 45 HRC, has emerged since modern ceramics were first made available for continuous roughing and CBN tools for continuous finishing (Bensouilah et al., 2016). Finish hard machining has been a beneficial practice for machining industries due to its high productivity. AISI 4340 steel alloy of medium carbon steel is known for its hardness and endurance limit and is used for wide varieties of applications. AISI 4340 serves as a viable substitute for AISI 4140 steel due to its high tensile and yield strength (http://www.astmsteel.com/product/4340-steel-aisi/).

Nowadays, Finite Element Method (FEM) is widely used for simulation and analysis of material removal processes, supported by highly developed computers and software packages. Along with minimizing the need for high cost and time consuming experimental setup, it predicts also the difficult to measure variables such as stress, strain and machining temperature. It shows how adequately the selection of the input parameters reflect in the deformation process involving chip formation. The currently used software include ABAQUS/Explicit, Advantage, Deform 2D/3D etc. Deform 3D has specifically a module for the modelling of metal cutting simulation under machining category providing advanced algorithms like Adaptive Lagrangian Meshing focusing on both residual stresses and temperatures. But ABAQUS/Explicit uses mainly Lagrangian method for the simulation purpose and fits the best to our use. The simulation provides information about the different parameters accounting for the behavioural changes in the machining process. Finite element method (FEM) is capable of providing both qualitative and quantitative aspect of the machining process and can also correctly predict the difficult-to-measure variables associated with hard turning process such as shear strains, deformation etc. Numerous

FE codes such as ABAQUS®, DEFORM, Ansys/LS-DYNA have come up that are currently being used by researchers for hard turning simulation.

6.2 Materials and method

All hard turning experiments are performed on AISI 4340 steel using a NH26 Lathe machine with Al_2O_3 coated (5µm coating thickness) carbide insert. The diameter and the length of the work pieces are 80 mm and 200 mm, respectively. Kistler cutting force dynamometer (model 9272) is used to measure the cutting forces. Hard turning operation is carried out at different cutting speed and feed while depth of cut is fixed throughout the experiment. Table 6.1 shows the cutting parameters for the experiments.

Table 6.1 Hard turning process parameters

Process parameters	**Range of cutting parameters**				
Cutting speed, V_c (m/min)	100	131	170	222	288
Feed, f (mm/rev)	0.06	0.08	0.10	0.12	0.14
Depth of cut, a_p (mm)			0.08		

6.2.1 2D FEM formulation of orthogonal cutting

ABAQUS® 6.13 explicit package employing coupled temperature-displacement module is used in the present study to simulate 2D orthogonal hard turning operation. Figure 6.1 shows the 2D computation domain of the process with dimensions.

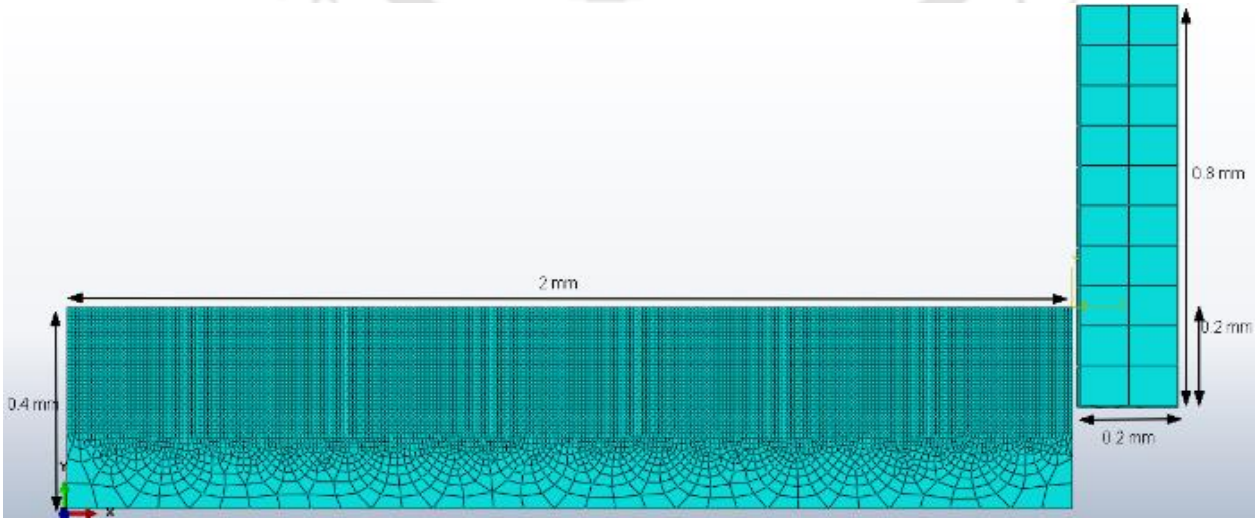

Fig. 6.1 2D computational domain of hard turning with mesh configuration and dimensions

The geometric model consists of two numbers of 2D deformable solid bodies. The workpiece is considered as a rectangular block. The cutting tool is having zero degree rake and clearance angles considered during simulation. Workpiece length and height are considered as 2 and 0.4 mm, respectively. Both tool and workpiece geometry are maintained same as per model by Akbar et al. (2010). The thickness of coating on carbide insert is 5 µm.

6.2.2 Boundary conditions

The cutting tool is given velocity in the negative X direction and it is constrained in the Y direction while the workpiece is kept fixed and constrained in the base in all directions. The dimension of the workpiece is kept such that it will attain a steady state condition while machining. Figure 6.2 shows the boundary conditions.

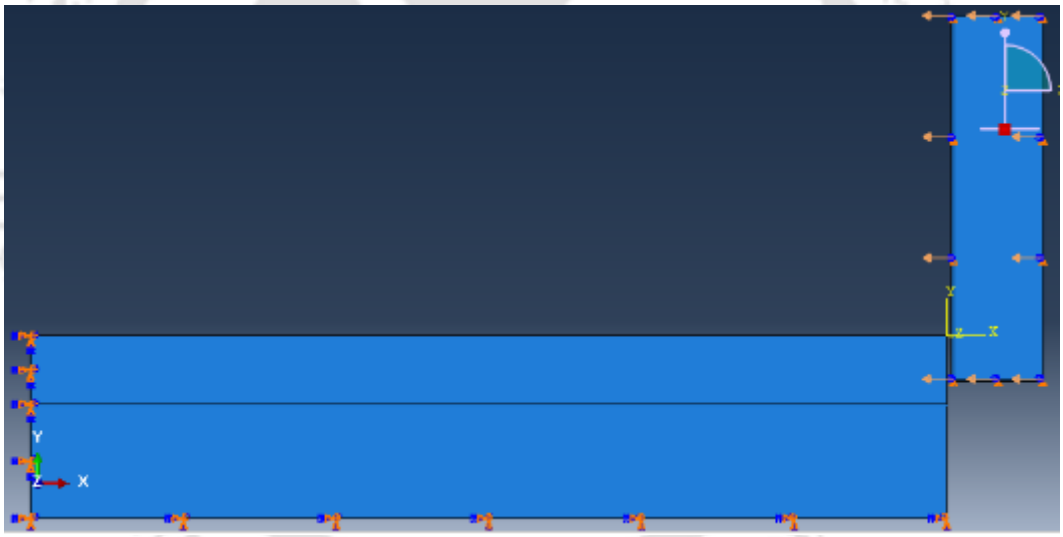

Fig. 6.2 Boundary conditions on cutting tool and workpiece

6.2.3 Element formulation

4-noded bilinear plane strain thermally coupled quadrilateral, bilinear displacement and temperature element (CPE4RT) with reduced integration scheme and hourglass control is used for both workpiece and cutting tool. Workpiece consists of 10010 elements and 10332 nodes while the tool consists of 168 elements and 200 nodes. In coupled thermo-displacement elements, the stress analysis is coupled with heat transfer. These elements have both temperature and displacement degrees of freedom. Elements can use linear or parabolic interpolation for displacement but can use only the linear interpolation for the temperature in coupled temperature

displacement type elements. During machining, lots of heat is generated which affects the mechanical properties of the workpiece. Hence, coupled analysis is preferred.

6.2.4 Material model

For thermo-mechanical analysis of the work piece, Johnson-Cook constitutive equation is used which considers the effect of strain, strain rate and temperature on the flow stress behavior of the materials (Johnson et al., 1983). This model which is followed by most of the researchers, requires the value of the parameters to calculate the equivalent flow stress ($\bar{\sigma}$) which is given as

$$\bar{\sigma} = (A + B\bar{\varepsilon}^{n})\left[1 + C\ln\left(\frac{\dot{\bar{\varepsilon}}}{\dot{\bar{\varepsilon}}_0}\right)\right]\left[1 - \left(\frac{\theta - \theta_{room}}{\theta_{melting} - \theta_{room}}\right)^{m}\right] \tag{6.1}$$

where, A is initial yield stress, B is hardening modulus, C is strain rate dependency coefficient, n is work hardening coefficient, m is thermal softening coefficient, $\dot{\bar{\varepsilon}}$ is plastic strain rate, $\bar{\varepsilon}$ is equivalent plastic strain and $\dot{\bar{\varepsilon}}_0$ is reference strain rate, $\theta_{melting}$ is the melting temperature of the workpiece, θ is the process temperature and θ_{room} is the ambient temperature. An equivalent plastic strain criterion is adopted to formulate the chip. Material failure depends upon the critical value of the equivalent plastic strain. This cumulative law by (Johnson and Cook, 1985) is used and it is given as

$$D = \sum\left(\frac{\Delta\bar{\varepsilon}}{\bar{\varepsilon}_f}\right) \tag{6.2}$$

where, D is the damage parameter, $\Delta\bar{\varepsilon}$ is the increment of equivalent plastic strain and $\bar{\varepsilon}_f$ is the equivalent strain at failure. Equivalent plastic strain is given as

$$\bar{\varepsilon}_f = \left[D_1 + D_2\exp\left(D_3\frac{P}{\bar{\sigma}}\right)\right]\left[1 + D_4\ln\left(\frac{\dot{\bar{\varepsilon}}}{\dot{\bar{\varepsilon}}_0}\right)\right]\left[1 + D_5\left(\frac{\theta - \theta_{room}}{\theta_{melt} - \theta_{room}}\right)\right] \tag{6.3}$$

where, $\Delta\bar{\varepsilon}$ gets updated at every load step. P is the hydrostatic pressure. D_1, D_2, D_3, D_4, D_5 are the experimentally obtained failure constants. Material stiffness starts degrading after the element satisfies the damage initiation criterion. Failure is assumed to occur when the value of D exceeds 1. After the element is fully degraded, the element deletion in ABAQUS completely removes the element. Johnson-Cook parameters for the present workpiece are given in Table 6.2 (Ucun and Aslantas, 2010).

Table 6.2 Johnson-Cook parameters for AISI 4340 (Ucun and Aslantas, 2010)

A (MPa)	B (MPa)	n	C	m	D_1	D_2	D_3	D_4	D_5
950	725	0.375	0.015	0.625	–0.8	2.1	–0.5	0.002	0.61

For both workpiece and tool, thermo-mechanical properties are specified. Material properties of AISI 4340 workpiece and tungsten carbide cutting tool insert i.e. density (ρ), elastic modulus (*E*), poisson's ratio (ν), thermal expansion coefficient (α), melting temperature (θ_{melt}) and room temperature (θ_{room}) are provided in Table 6.3. Temperature-dependent thermal conductivity (*K*) values of carbide tool and Al_2O_3 coating are given Table 6.4.

Table 6.3 Material properties of AISI 4340 workpiece, carbide tool and Al_2O_3 coating (Ucun and Aslantas, 2010)

Material	Carbide tool	AISI 4340	Al_2O_3
C_p (J/kg-°C)	126	475	904
ρ (kg/m^3)	11900	7850	3780
E (N/m^2)	650 E9	205 E9	415E9
ν	0.25	0.3	0.22
α (μm/m-°C)	–	13.7	–
θ_{melt} (°C)	–	1520	–
$\theta room$ (°C)	25	25	25

Table 6.4 Thermal conductivity of carbide tool and Al_2O_3 coating (Ucun and Aslantas, 2010)

Material	Property						
Al_2O_3	Temperature (°C)	50	90	300	500	1000	1300
	*K** (W/m-°C)	33	28	19	13	7	7
Carbide tool	Temperature (°C)	30	100	300	500	1000	1300
	K (W/m-°C)	30	32	34	37	44	47.5

**K* – Thermal conductivity

6.2.5 Contact properties

A kinematic contact algorithm is used to establish contact between tool rake face and chip. Tangential behavior effect of frictional forces is taken into consideration. Penalty contact with a constant coefficient of friction is used to model the contact.

6.2.6 Explicit dynamic analysis

Explicit dynamic formulation is generally used for highly non-linear problems which involve large amount of deformations. Explicit dynamic is an integration technique which uses central difference method to move the solution further in time. Explicit analysis uses the information already it has for obtaining unknown information. It does not require any iteration or convergence check for obtaining the solution. It is designed to study highly nonlinear, discontinuous and high speed dynamic problems. It requires lesser disk space as compared to standard analysis.

6.2.7 Arbitrary Lagrangian Eulerian

Arbitrary Lagrangian Eulerian (ALE) meshing technique combines the advantages of both Lagrangian and Eulerian methods. In Lagrangian model, the mesh is locked on to the material. ALE combines the advantages of both Lagrangian and Eulerian model to fit the simulation criteria. ALE arbitrarily changes from Lagrangian or Eulerian model depending upon the need of the mesh at a point. This mean, in regions of huge plastic deformation, ALE acts more or less like the Eulerian model. While along the boundary of the material, ALE acts like Lagrangian model to facilitate easy implementation of boundary conditions. In Eulerian approach, the mesh elements are locked on to the spatial points. This means that mesh remains fixed while the material flows through the mesh.

6.3 Results and discussion

In this section, an in-depth discussion of the simulated results and further validation with experimental results are carried out.

6.3.1 Validation of cutting force model

Figure 6.3 shows the simulation results of the variation of main cutting and feed forces with time at 100 m/min cutting speed. The cutting and feed forces have reached steady-state condition at 0.00016 s with a certain variation as shown in Fig. 6.3. Figure 6.4 shows the comparison between simulated (a) main cutting and (b) feed forces at different cutting speed with experimentally measured forces.

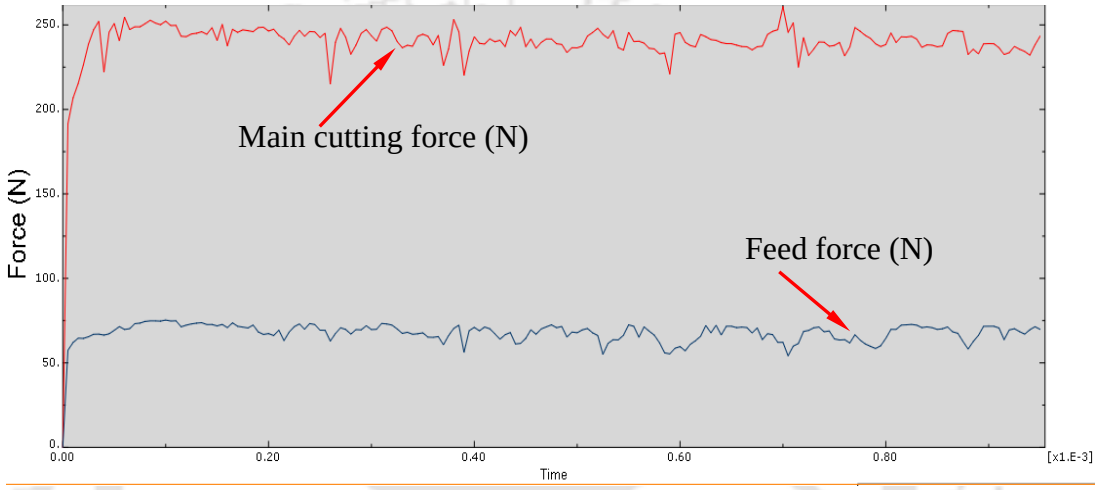

Fig. 6.3 Simulated main cutting and feed force plots with time at 100 m/min cutting speed

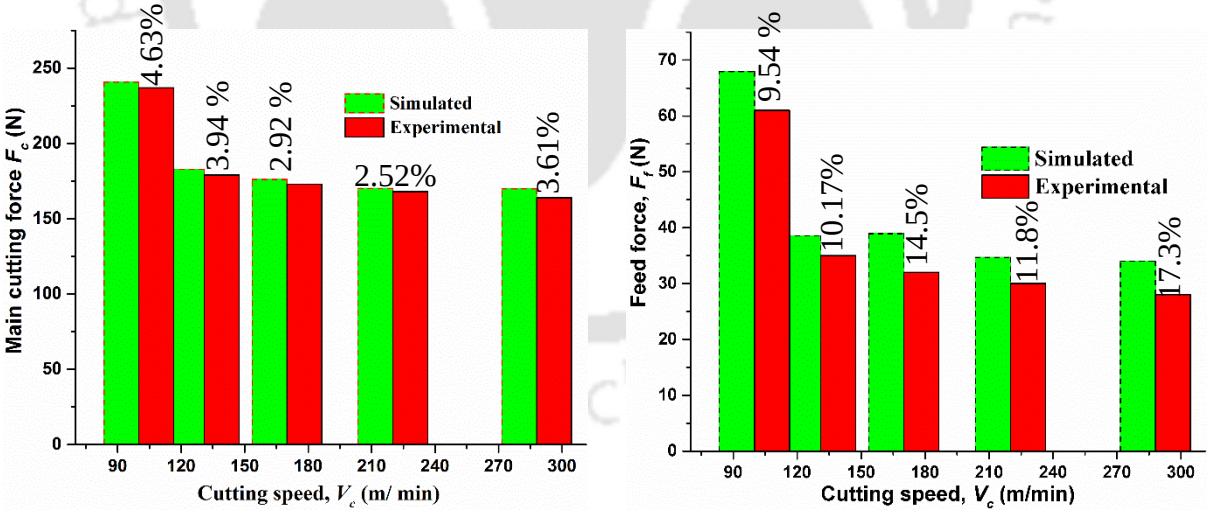

(a) (b)

Fig. 6.4 Effect of cutting speed on (a) main cutting force and (b) feed force

As the cutting speed increases from 100 to 288 m/min, the values of main cutting forces decrease gradually for both experimental (230 to 164 N) and simulated (240.67 to 169.93 N) results (Fig. 6.4(a)). Also, the feed forces decrease gradually for both experimental (61 to 28 N) and

simulated (67.93 to 34.03 N) results (Fig. 6.4(a)) with increased cutting speed. At higher cutting speed, cutting temperatures are significantly higher and the material becomes softer due to thermal softening which leads to reduced cutting force. From Fig. 6.5, it can be seen that both main cutting force and feed force increase with increasing feed. At higher feed, the area of interaction between cutting tool and work piece increases which results in both increased main cutting force and feed force. A good agreement between the measured and simulated forces at all cutting speed (with maximum error of 4.63% and 17.3 % for F_c and F_f, respectively) and feed (with maximum error of 5.6 % and 13.08 % for F_c and F_f, respectively) is observed as shown in Figs. 6.4 and 6.5, respectively.

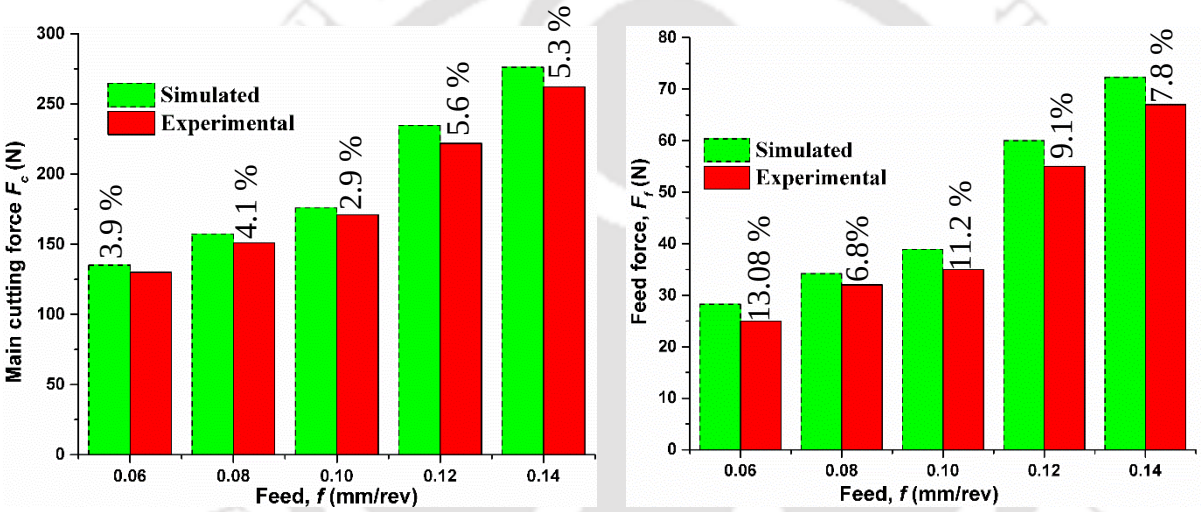

(a) (b)

Fig. 6.5 Effect of feed on (a) main cutting force and (b) feed force

6.4 Summary

The effect of Al_2O_3 coating on cutting force, feed force at different cutting speed and feed is carried out during 2D orthogonal simulation of hard turning while machining of AISI 4340 steel using a FEM based simulation package of ABAQUS®. The simulated results of cutting and feed forces are validated with experimental results with maximum error of 17.3 %. Hence, from above results it is clear that ABAQUS® can be used for the prediction of forces during hard turning operation.

Chapter 7 Conclusions and scope for future work

7.1 Conclusions

In the present thesis, a new type of coating material i.e. HSN^2 is introduced on carbide insert for machining hard AISI 52100 steel having hardness 55 HRC. Preliminary experimental investigation is carried out to select the main process parameters with their range and also, feasibility study of new coating material for hard machining. Also, coating thickness is determined. Further, the optimisation of cutting parameters using statistical design of experiments is conducted to select optimum cutting parameters. After that white layer analysis of the machined surface is carried out. Further, 2D orthogonal hard turning simulation using FEM based software package ABAQUS® is carried out and the simulated results are experimentally validated for AISI 4340 steel with Al_2O_3 coated tool. Following conclusions are drawn from the work reported in the thesis.

7.1.1 Preliminary experimetal investigation

In the present study, high speed machining of AISI 52100 grade steel is carried out using a newly developed coating (HSN^2) on carbide tool insert to observe the effect of process parameters on cutting forces, surface roughness and maximum flank wear. The following conclusions are observed.

- From physical-chemical characterization (DSC and TGA) of HSN^2 coating, the PVD coated carbide insert is found having high oxidation stability and better thermal behavior throughout the range of given temperature and also at elevated temperature.
- From preliminary experiments it is found that 8 µm thick coated inserts does not sustain at high cutting speed, however 12 µm thick coated inserts sustain.
- Experimentally it is observed that, feed and depth of cut are the major factors to affect the feed force, radial force, main cutting force during machining.
- Highest value among all three forces is observed for radial force due to ploughing effect.
- Flank wear is a very important aspect for hard turning. Experimentally, it is found that with increased cutting speed, flank wear also increases. Further, it reduces slightly at highest cutting speed due to chip embrittlement. Hence, low cutting speed is more suitable for

reducing flank wear. Most efficient machining for low surface roughness and low machining force are achieved at high cutting speed with low feed and depth of cut.

- It is found that improved surface roughness and low machining force are achieved at high cutting speed, low feed and depth of cut.
- From all experiments, the magnitude of the maximum flank wear is less than the standard acceptable maximum flank wear value of 0.4 mm for carbide tool. Hence, the selected new coating material (HSN^2) on the carbide tool can be successfully used for turning hardened AISI 52100 steel having hardness 55 HRC.
- From analysis of chip morphology, it is observed that the value of chip reduction ratio tends to 1 at higher cutting speed and lower feed. Hence, higher cutting speed and lower feed are favorable conditions while turning AISI 52100 steel with the present insert.
- The value of shear angle at higher cutting speed approaches to 45° which indicates smoother chip formation at higher cutting speed.

7.1.2 Statistical design of experiments

In the present study, hard turning based on statistical design of experiments is carried out to find out the influence of different input parameters on various responses while turning AISI 52100 steel. From the present study, the following conclusions are drawn.

- Comparing work by previous researchers, it is observed that the PVD coated HSN^2 carbide inserts are more effective in terms of achieved lesser value of flank wear and forces for dry hard turning within the selected range of process parameters.
- From ANOVA, it is observed that cutting speed is the most significant factor having contribution 89.13% followed by depth of cut (2.57%) and feed (2.28 %) while considering cutting force as the response parameter. Similarly, for radial force, cutting speed is the most effective factor (91.33 % contribution) following depth of cut (2.88 %) and feed (2.04 %).
- Also, for feed force, cutting speed is the most significant factor (92.83% contribution) followed by depth of cut (2.58%) and feed (2.21%).
- Reduction in all three forces is observed at higher cutting speed due to increased cutting temperature which leads to less shear strength of work piece material.
- The value of mesured radial force is observed greater than main cutting force unlike conventional turning process.

- For surface roughness, the most significant factor is cutting speed with 51.55% contribution followed by feed and depth of cut with 20.64% and 5.61% contribution, respectively. Higher cutting speed, lower feed and depth of cut are better option for achieving lower surface roughness.
- For maximum flank wear, the cutting speed has substantial effect (79.78%) followed by depth of cut (0.77 %) and feed (0.41 %). Increased cutting speed leads to higher temperature in the cutting zone. Hence, tool wear increases at higher cutting speed.
- Minimum tool wear can be achieved at lower value of all cutting parameters.
- According to ISO Standard 3685, the maximum flank wear observed at all cutting conditions are below 0.4 mm. Hence, HSN^2 coated carbide inserts are suitable for turning hard steel (AISI 52100) having hardness of 55 HRC.
- From confirmation test it is observed that at optimized cutting condition, the predicted responses calculated from regression models are very close to the experimental observations.

7.1.3 White layer analysis

- From experimental analysis, it can be concluded that the white layer thickness during hard turning can be controlled by carefully selecting suitable cutting parameters. A higher cutting speed should be used while machining brittle material with fresh edge of tool insert when discontinuous chips are generated.
- From temperature analysis, it is found that the thermal effect on the machined surface is the main reason for the generation of white layer. Also, machined surface temperature plays more significant role over chip temperature for higher thickness of the white layer.
- Experimentally, it is observed that white layer thickness decreases at higher cutting speed. Hence, it can be concluded that higher cutting speed should be chosen during high speed machining of AISI 52100 hard steel with HSN^2 coated carbide insert having fresh edge.
- The XRD results can be used very effectively for the analysis of white layer. From XRD analysis of the machined surface, it can be concluded that the retained austenite accumulates in the machined surface during formation of white layer.
- Microhardness variation is observed across the section (radially) of hard turned components. Maximum hardness value is observed at the top machined surface (i.e. white

layer), further its value decreases at the subsurface at plastically deformed zone and further reaches to the original hardness value at bulk material. The machined surface with white layer is harder than the base material.

7.1.4 Simulation of orthogonal hard turning operation

A finite element based simulation is carried out to model orthogonal cutting of hard steel with a single-layer coated carbide tool. The effect of coating on cutting force, thrust force at different cutting speed and feed during machining of AISI 4340 steel is studied. The experimental results are very close to the simulated results of cutting and thrust forces. Hence, from above results it is clear that ABAQUS® can be used for the prediction of forces for 2 D orthogonal hard turning operation.

7.2 Scope for future work

It is observed from preliminary experimental study that 12 µm thick HSN^2 coating on carbide insert is successfully used for hard turning of AISI 52100 hard steel having 55 HRC hardness. The following points can be incorporated as a scope for future work.

- HSN^2 coated carbide inserts can be attempted under near-dry cutting conditions while varying air pressure, oil concentration and simultaneous cooling of rake as well as flank faces of the tool for the same workpiece material.
- Further, experimental investigations to correlate the white layer thickness with residual stress of machined surface under dry and near-dry cutting conditions can be attempted using same tool and workpiece combination.
- HSN^2 coating material can be modified in terms of chemical composition for hard turning of workpiece material having hardness beyond 55 HRC.
- HSN^2 coated carbide inserts can be utilized to other machining processes like milling, drilling etc. where single point or multi-point cutting tools are used.
- In future environment-friendly cutting fluid can also be used to compare its performance with respect to dry turning for the same HSN^2 coated carbide inserts.

REFERENCES

[1] Adwani, M. (2012) 'High-end coatings for the Indian market', Customer magazine for coating technology FACTS, 37: 10–11.

[2] Afonasov, A. I. and Lasukov, A. A. (2014) 'Elementary chip formation in metal cutting', Russian Engineering Research. Allerton Press, 34(3), pp. 152–155. doi: 10.3103/S1068798X14030034.

[3] Akbar, F. et al. (2010) 'An experimental and coupled thermo-mechanical finite element study of heat partition effects in machining', The International Journal of Advanced Manufacturing Technology. Springer-Verlag, 46(5–8), pp. 491–507. doi: 10.1007/s00170-009-2117-5.

[4] Ali, M. Y. and Pan, J. (2015) 'Residual Stresses Due to Rigid Cylinder Indentation and Rolling at a Very High Rolling Load', Journal of Manufacturing Science and Engineering, 137(5), p. 51005. doi: 10.1115/1.4031067

[5] Aluspeed, C. C. (2012) 'CC800 ® /9 – the success model High-end coatings for nearly every purpose', (37), pp. 8–9.

[6] Alok, A. and Das, M. (2018) 'Cost-effective way of hard turning with newly developed HSN2-coated tool', Materials and Manufacturing Processes, 33(9). doi: 10.1080/10426914.2017.1388521.

[7] Alok, A. and Das, M. (2019) 'Multi-objective optimization of cutting parameters during sustainable dry hard turning of AISI 52100 steel with newly develop HSN2-coated carbide insert', Measurement. Elsevier, 133, pp. 288–302. doi: 10.1016/J.MEASUREMENT.2018.10.009.

[8] Aneiro, F. M. et al. (2008) 'Turning hardened steel using coated carbide at high cutting speeds', Journal of the Brazilian Society of Mechanical Sciences and Engineering. The Brazilian Society of Mechanical Sciences and Engineering, 30(2), pp. 104–109. doi: 10.1590/S1678-58782008000200002.

[9] Aramcharoen, A. et al. (2008) 'White layer formation and hardening effects in hard turning of H13 tool steel with CrTiAlN and CrTiAlN/MoST-coated carbide tools', The International Journal of Advanced Manufacturing Technology. Springer-Verlag, 36(7–8), pp. 650–657. doi: 10.1007/s00170-006-0899-2.

[10] Aouici, H. et al. (2012) 'Analysis of surface roughness and cutting force components in hard turning with CBN tool: Prediction model and cutting conditions optimization', Measurement. Elsevier, 45(3), pp. 344–353. doi: 10.1016/J.MEASUREMENT.2011.11.011.

[11] Asiltürk, İ. and Akkuş, H. (2011) 'Determining the effect of cutting parameters on surface roughness in hard turning using the Taguchi method', Measurement. Elsevier, 44(9), pp.

1697–1704. doi: 10.1016/J.MEASUREMENT.2011.07.003.

[12] Bagaber, S. A. and Yusoff, A. R. (2017) 'Multi-objective optimization of cutting parameters to minimize power consumption in dry turning of stainless steel 316', Journal of Cleaner Production. Elsevier, 157, pp. 30–46. doi: 10.1016/j.jclepro.2017.03.231.

[13] Bartarya, G. and Choudhury, S. K. (2014) 'Influence of machining parameters on forces and surface roughness during finish hard turning of EN 31 steel', Proceedings of the Institution of Mechanical Engineers, Part B: Journal of Engineering Manufacture. SAGE PublicationsSage UK: London, England, 228(9), pp. 1068–1080. doi: 10.1177/0954405413500492.

[14] Bartarya, G. and Choudhury, S. K. (2016) 'Effect of tool wear on white layer thickness and subsurface hardness on hard turned EN31 steel', International Journal of Machining and Machinability of Materials, 18(5/6), p. 483. doi: 10.1504/ijmmm.2016.078993.

[15] Bartarya, G. and Choudhury, S. K. (2012) 'Effect of Cutting Parameters on Cutting Force and Surface Roughness During Finish Hard Turning AISI52100 Grade Steel', Procedia CIRP. Elsevier, 1, pp. 651–656. doi: 10.1016/J.PROCIR.2012.05.016.

[16] Bensouilah, H. et al. (2016) 'Performance of coated and uncoated mixed ceramic tools in hard turning process', Measurement, 82, pp. 1–18. doi: 10.1016/j.measurement.2015.11.042.

[17] Bosheh, S. S. and Mativenga, P. T. (2006) 'White layer formation in hard turning of H13 tool steel at high cutting speeds using CBN tooling', International Journal of Machine Tools and Manufacture. Pergamon, 46(2), pp. 225–233. doi: 10.1016/J.IJMACHTOOLS.2005.04.009.

[18] Byrne, G. et al. (2003) UC Berkeley Consortium on Deburring and Edge Finishing Title Advancing Cutting Technology Permalink https://escholarship.org/uc/item/7hd8r1ft Publication Date Advancing Cutting Technology. Available at: https://escholarship.org/uc/item/7hd8r1ft (Accessed: 21 January 2019).

[19] Byrne, G. et al. (1995) 'Tool Condition Monitoring (TCM) — The Status of Research and Industrial Application', CIRP Annals, 44(2), pp. 541–567. doi: 10.1016/S0007-8506(07)60503-4.

[20] Cakir, M. C. et al. (2009) 'Mathematical modeling of surface roughness for evaluating the effects of cutting parameters and coating material', Journal of Materials Processing Technology. Elsevier, 209(1), pp. 102–109. doi: 10.1016/J.JMATPROTEC.2008.01.050.

[21] Chinchanikar, S. and Choudhury, S. K. (2014) 'Hard turning using HiPIMS-coated carbide tools: Wear behavior under dry and minimum quantity lubrication (MQL)', Measurement. Elsevier Ltd, 55, pp. 536–548. doi: 10.1016/j.measurement.2014.06.002.

[22] Chinchanikar, S. and Choudhury, S. K. (2013) 'Effect of work material hardness and cutting parameters on performance of coated carbide tool when turning hardened steel: An optimization approach', Measurement. Elsevier, 46(4), pp. 1572–1584. doi:

10.1016/J.MEASUREMENT.2012.11.032.

[23] Choudhury, S. and Kishore, K. (2000) 'Tool wear measurement in turning using force ratio', International Journal of Machine Tools and Manufacture, 40(6), pp. 899–909. doi: 10.1016/S0890-6955(99)00088-7.

[24] Chou, Y. K. and Evans, C. J. (1999) 'White layers and thermal modeling of hard turned surfaces', International Journal of Machine Tools and Manufacture. Pergamon, 39(12), pp. 1863–1881. doi: 10.1016/S0890-6955(99)00036-X.

[25] Ciftci, I. (2006) 'Machining of austenitic stainless steels using CVD multi-layer coated cemented carbide tools', Tribology International. Elsevier, 39(6), pp. 565–569. doi: 10.1016/J.TRIBOINT.2005.05.005.

[26] Cselle, T. et al. (2009) 'TripleCoatings - New generation of PVD-coatings for cutting tools', Journal of Machine Manufacturing, 49(E1), pp. 19–25.

[27] Cuppini, D. et al. (1990) 'Tool wear monitoring based on cutting power measurement', Wear. Elsevier, 139(2), pp. 303–311. doi: 10.1016/0043-1648(90)90052-C.

[28] Derringer, G. and Suich, R. (1980) 'Simultaneous Optimization of Several Response Variables', Journal of Quality Technology. Taylor & Francis, 12(4), pp. 214–219. doi: 10.1080/00224065.1980.11980968.

[29] Dhar, N. R. et al. (2006) 'Effect of minimum quantity lubrication (MQL) on tool wear and surface roughness in turning AISI-4340 steel', Journal of Materials Processing Technology. Elsevier, 172(2), pp. 299–304. doi: 10.1016/J.JMATPROTEC.2005.09.022.

[30] Dimla, D. E. (2000) 'Sensor signals for tool-wear monitoring in metal cutting operations—a review of methods', International Journal of Machine Tools and Manufacture. Pergamon, 40(8), pp. 1073–1098. doi: 10.1016/S0890-6955(99)00122-4.

[31] Dobrzański, L. A. et al. (2004) 'Structure and properties of the multi-component TiAlSiN coatings obtained in the PVD process in the nitride tool ceramics', Journal of Materials Processing Technology, 157, pp. 331–340. doi: 10.1016/j.jmatprotec.2004.09.052.

[32] Dobrzański, L. A. and Gołombek, K. (2005) 'Structure and properties of the cutting tools made from cemented carbides and cermets with the TiN + mono-, gradient- or multi(Ti, Al, Si)N + TiN nanocrystalline coatings', Journal of Materials Processing Technology. Elsevier, 164–165, pp. 805–815. doi: 10.1016/J.JMATPROTEC.2005.02.072.

[33] Dogra, M. et al. (2011) 'Performance evaluation of CBN, coated carbide, cryogenically treated uncoated/coated carbide inserts in finish-turning of hardened steel', The International Journal of Advanced Manufacturing Technology. Springer-Verlag, 57(5–8), pp. 541–553. doi: 10.1007/s00170-011-3320-8.

[34] Dogra, M. et al. (2012) 'Finish Hard Turning of Continuous and Interrupted Surfaces with Cubic Boron Nitride (CBN) and Coated Carbide Tools', Materials and Manufacturing Processes. Taylor & Francis Group , 27(5), pp. 523–530. doi:

10.1080/10426914.2011.593238.

[35] Dolinšek, S., Ekinović, S. and Kopač, J. (2004) 'A contribution to the understanding of chip formation mechanism in high-speed cutting of hardened steel', Journal of Materials Processing Technology. Elsevier, 157–158, pp. 485–490. doi: 10.1016/J.JMATPROTEC.2004.07.144.

[36] Ebrahimi, A. and Moshksar, M. M. (2009) 'Evaluation of machinability in turning of microalloyed and quenched-tempered steels: Tool wear, statistical analysis, chip morphology', Journal of Materials Processing Technology, 209(2), pp. 910–921. doi: 10.1016/j.jmatprotec.2008.02.067.

[37] Ezugwu, E. O. and Okeke, C. I. (2002) 'Behavior of Coated Carbide Tools in High Speed Machining of a Nickel Base Alloy', Tribology Transactions, 45(1), pp. 122–126. doi: 10.1080/10402000208982530.

[38] Faga, M. G. et al. (2007) 'AlSiTiN nanocomposite coatings developed via Arc Cathodic PVD: Evaluation of wear resistance via tribological analysis and high speed machining operations', Wear, 263(7–12), pp. 1306–1314. doi: 10.1016/j.wear.2007.01.109.

[39] Farrokhi, F. et al. (2015) 'Fiber Laser Welding of Direct-Quenched Ultrahigh Strength Steels: Evaluation of Hardness, Tensile Strength, and Toughness Properties at Subzero Temperatures', Journal of Manufacturing Science and Engineering. American Society of Mechanical Engineers, 137(6), p. 61012. doi: 10.1115/1.4030177.

[40] Famex Coating India Pvt. Ltd. (no date). Available at: http://www.famexcoating.com/hsn2.html (Accessed: 14 April 2017).

[41] Fang, N. et al. (2011) 'A comparative study of sharp and round-edge tools in machining with built-up edge formation: cutting forces, cutting vibrations, and neural network modeling', The International Journal of Advanced Manufacturing Technology. Springer-Verlag, 53(9–12), pp. 899–910. doi: 10.1007/s00170-010-2887-9.

[42] Fang, N., Pai, P. S. and Mosquea, S. (2011) 'A comparative study of sharp and round-edge tools in machining with built-up edge formation: cutting forces, cutting vibrations, and neural network modeling', The International Journal of Advanced Manufacturing Technology. Springer-Verlag, 53(9–12), pp. 899–910. doi: 10.1007/s00170-010-2887-9.

[43] Ferreira, R. et al. (2016) 'Surface roughness investigation in the hard turning of steel using ceramic tools', Materials and Manufacturing Processes. Taylor & Francis, 31(5), pp. 648–652. doi: 10.1080/10426914.2014.995051.

[44] Ferreira, R. et al. (2016) 'Analysis of the hard turning of AISI H13 steel with ceramic tools based on tool geometry: surface roughness, tool wear and their relation', Journal of the Brazilian Society of Mechanical Sciences and Engineering. Springer Berlin Heidelberg, 38(8), pp. 2413–2420. doi: 10.1007/s40430-016-0504-z.

[45] Ghani, J. A. et al. (2004) 'Wear mechanism of TiN coated carbide and uncoated cermets

tools at high cutting speed applications', Journal of Materials Processing Technology, 153, pp. 1067–1073. doi: 10.1016/j.jmatprotec.2004.04.352.

[46] Grzesik, W. and Zak, K. (2014) 'Characterization of Surface Integrity Produced by Sequential Dry Hard Turning and Ball Burnishing Operations', Journal of Manufacturing Science and Engineering. American Society of Mechanical Engineers, 136(3), p. 31017. doi: 10.1115/1.4026936.

[47] Griffiths, B. (2001) Manufacturing surface technology: surface integrity & functional performance. Penton. Available at: https://books.google.co.in/books?hl=en&lr=&id=oArJEllGi_0C&oi=fnd&pg=PP2&dq=B.J.+Griffiths+Manufacturing+Surface+Technology:+Surface+Integrity+and+Functional+Performance&ots=xebX_xSZ5A&sig=sSrZjbfrRANjiFBsQO1Qj2kKTtQ#v=onepage&q=B.J. Griffiths Manufacturing Surface Technology%3A Surface Integrity and Functional Performance & f = false (Accessed: 12 December 2018).

[48] Gupta, M. K. et al. (2016) 'Optimization of machining parameters and cutting fluids during nano-fluid based minimum quantity lubrication turning of titanium alloy by using evolutionary techniques', Journal of Cleaner Production. Elsevier, 135, pp. 1276–1288. doi: 10.1016/j.jclepro.2016.06.184.

[49] Hosseini, S. B. et al. (2015) 'Formation mechanisms of white layers induced by hard turning of AISI 52100 steel', Acta Materialia. Pergamon, 89, pp. 258–267. doi: 10.1016/J.ACTAMAT.2015.01.075.

[50] Ibrahim, G. A. et al.. (2009) 'The Effect of Dry Machining on Surface Integrity of Titanium Alloy Ti-6Al-4V ELI', Journal of Applied Sciences. Asian Network for Scientific Information, 9(1), pp. 121–127. doi: 10.3923/jas.2009.121.127.

[51] Isik, Y. (2007) 'Investigating the machinability of tool steels in turning operations', Materials & Design. Elsevier, 28(5), pp. 1417–1424. doi: 10.1016/J.MATDES.2006.03.025.

[52] Ichijo, K. et al. (2007) 'Microstructures of (Ti,Cr,Al,Si)N films synthesized by cathodic arc method', Surface and Coatings Technology, 201(9), pp. 5477–5480. doi: 10.1016/j.surfcoat.2006.07.016.

[53] Jawahir, I. S. (1988) 'The chip control factor in machinability assessments: Recent trends', Journal of Mechanical Working Technology. Elsevier, 17, pp. 213–224. doi: 10.1016/0378-3804(88)90023-X.

[54] Johnson, G. R. et al. (1983) 'A constitutive model and data for metals subjected to large strains, high strain rates and high temperatures', Proceedings of 7th International Symposium on Ballistics. Proceedings of the 7th International Symposium on Ballistics, pp. 541–547.

[55] Johnson, G. R. and Cook, W. H. (1985) 'Fracture characteristics of three metals subjected to various strains, strain rates, temperatures and pressures', Engineering Fracture Mechanics. Pergamon, 21(1), pp. 31–48. doi: 10.1016/0013-7944(85)90052-9.

[56] Kakade, S. et al. (1994) 'In-process tool wear and chip-form monitoring in face milling operation using acoustic emission.', Journal of Materials Processing Technology. Elsevier, 44(3–4), pp. 207–214. doi: 10.1016/0924-0136(94)90433-2.

[57] Kaynak, Y. et al. (2013) 'Tool-wear analysis in cryogenic machining of NiTi shape memory alloys: A comparison of tool-wear performance with dry and MQL machining', Wear. Elsevier, 306(1–2), pp. 51–63. doi: 10.1016/J.WEAR.2013.05.011.

[58] Khan, S. A. et al. (2018) 'Experimental investigations on wiper inserts' edge preparation, workpiece hardness and operating parameters in hard turning of AISI D2 steel', Journal of Manufacturing Processes. Elsevier, 34, pp. 187–196. doi: 10.1016/J.JMAPRO.2018.06.004.

[59] Kumar, R. et al. (2018) 'Comparative investigation towards machinability improvement in hard turning using coated and uncoated carbide inserts: part I experimental investigation', Advances in Manufacturing. Shanghai University, 6(1), pp. 52–70. doi: 10.1007/s40436-018-0215-z.

[60] Kumar, R. et al. (2017) 'Multi objective optimization using different methods of assigning weights to energy consumption responses, surface roughness and material removal rate during rough turning operation', Journal of Cleaner Production. Elsevier, 164, pp. 45–57. doi: 10.1016/J.JCLEPRO.2017.06.077.

[61] Khan, S. A. et al. (2017) 'High-feed turning of AISI D2 tool steel using multi-radii tool inserts: Tool life, material removed, and workpiece surface integrity evaluation', Materials and Manufacturing Processes. Taylor & Francis, 32(6), pp. 670–677. doi: 10.1080/10426914.2016.1232815.

[62] Klocke, F. and Eisenblätter, G. (1997) 'Dry Cutting', CIRP Annals. Elsevier, 46(2), pp. 519–526. doi: 10.1016/S0007-8506(07)60877-4.

[63] Ko, T. J. et al. (1999) 'Air-Oil Cooling Method for Turning of Hardened Material', The International Journal of Advanced Manufacturing Technology. Springer-Verlag London Limited, 15(7), pp. 470–477. doi: 10.1007/s001700050091.

[64] Kountanya, R. et al. (2009) 'Effect of tool edge geometry and cutting conditions on experimental and simulated chip morphology in orthogonal hard turning of 100Cr6 steel', Journal of Materials Processing Technology. Elsevier, 209(11), pp. 5068–5076. doi: 10.1016/J.JMATPROTEC.2009.02.011.

[65] Korkut, I. et al. (2011) 'Application of regression and artificial neural network analysis in modelling of tool–chip interface temperature in machining', Expert Systems with Applications. Pergamon, 38(9), pp. 11651–11656. doi: 10.1016/J.ESWA.2011.03.044.

[66] Krolczyk, G. M. et al. (2017) 'Dry cutting effect in turning of a duplex stainless steel as a key factor in clean production', Journal of Cleaner Production. Elsevier, 142, pp. 3343–3354. doi: 10.1016/j.jclepro.2016.10.136.

[67] Krolczyk, G. M. et al. (2018) 'Parametric and nonparametric description of the surface topography in the dry and MQCL cutting conditions', Measurement. Elsevier, 121, pp. 225–

239. doi: 10.1016/J.MEASUREMENT.2018.02.052.

[68] Kulkarni, A. P. and Sargade, V. G. (2015) 'Characterization and Performance of AlTiN, AlTiCrN, TiN/TiAlN PVD Coated Carbide Tools While Turning SS 304', Materials and Manufacturing Processes. Taylor & Francis, 30(6), pp. 748–755. doi: 10.1080/10426914.2014.984217.

[69] Kumar, T. S. et al. (2018) 'Comparative evaluation of performances of TiAlN, AlCrN, TiAlN/AlCrN coated carbide cutting tools and uncoated carbide cutting tools on turning Inconel 825 alloy using Grey Relational Analysis', Sensors and Actuators A: Physical. Elsevier, 279, pp. 331–342. doi: 10.1016/J.SNA.2018.06.041.

[70] Kupczyk, M. J. and Komolka, J. (2015) 'High durability of cutting insert edges made of nanocrystalline cemented carbides', International Journal of Refractory Metals and Hard Materials. Elsevier, 49, pp. 225–231. doi: 10.1016/J.IJRMHM.2014.07.003.

[71] Kruth, J. P. et al. (1995) 'Study of the White Layer of a Surface Machined by Die-Sinking Electro-Discharge Machining', CIRP Annals. Elsevier, 44(1), pp. 169–172. doi: 10.1016/S0007-8506(07)62299-9.

[72] Kupczyk, M. J. (2015) 'Cutting edges with high hardness made of nanocrystalline cemented carbides', International Journal of Refractory Metals and Hard Materials. Elsevier, 49, pp. 249–255. doi: 10.1016/J.IJRMHM.2014.07.041.

[73] Lalwani, D. I., Mehta, N. K. and Jain, P. K. (2008) 'Experimental investigations of cutting parameters influence on cutting forces and surface roughness in finish hard turning of MDN250 steel', Journal of Materials Processing Technology, 206(1–3), pp. 167–179. doi: 10.1016/j.jmatprotec.2007.12.018.

[74] Li, A. et al. (2012) 'Progressive tool failure in high-speed dry milling of Ti-6Al-4V alloy with coated carbide tools', The International Journal of Advanced Manufacturing Technology. Springer-Verlag, 58(5–8), pp. 465–478. doi: 10.1007/s00170-011-3408-1.

[75] Lima, J. G. et al. (2005) 'Hard turning: AISI 4340 high strength low alloy steel and AISI D2 cold work tool steel', Journal of Materials Processing Technology. Elsevier, 169(3), pp. 388–395. doi: 10.1016/J.JMATPROTEC.2005.04.082.

[76] Lin, J. (1995) 'Inverse estimation of the tool-work interface temperature in end milling', International Journal of Machine Tools and Manufacture. Pergamon, 35(5), pp. 751–760. doi: 10.1016/0890-6955(95)93043-6.

[77] Lotfi, M., Amini, S. and Aghaei, M. (2018) '3D FEM simulation of tool wear in ultrasonic assisted rotary turning', Ultrasonics, 88, pp. 106–114. doi: 10.1016/j.ultras.2018.03.013.

[78] Mabrouki, T. and Rigal, J.-F. (2006) 'A contribution to a qualitative understanding of thermo-mechanical effects during chip formation in hard turning', Journal of Materials Processing Technology. Elsevier, 176(1–3), pp. 214–221. doi: 10.1016/J.JMATPROTEC.2006.03.159.

[79] Mativenga, P. T. and Hon, K. K. B. (2003) 'A study of cutting forces and surface finish in high-speed machining of AISI H13 tool steel using carbide tools with TiAlN based coatings', Proceedings of the Institution of Mechanical Engineers, Part B: Journal of Engineering Manufacture. SAGE PublicationsSage UK: London, England, 217(2), pp. 143–151. doi: 10.1243/095440503321148786.

[80] Maruda, R. W. et al. (2017) 'Structural and Microhardness Changes After Turning of the AISI 1045 Steel for Minimum Quantity Cooling Lubrication', Journal of Materials Engineering and Performance. Springer US, 26(1), pp. 431–438. doi: 10.1007/s11665-016-2450-4.

[81] Maruda, R. W. et al. (2018) 'Effects of extreme pressure and anti-wear additives on surface topography and tool wear during MQCL turning of AISI 1045 steel', Journal of Mechanical Science and Technology. Korean Society of Mechanical Engineers, 32(4), pp. 1585–1591. doi: 10.1007/s12206-018-0313-7.

[82] Mia, M. et al. (2016) 'Modeling of Principal Flank Wear: An Empirical Approach Combining the Effect of Tool, Environment and Workpiece Hardness', Journal of The Institution of Engineers (India): Series C. Springer India, 97(4), pp. 517–526. doi: 10.1007/s40032-016-0262-9.

[83] Mia, M. and Dhar, N. R. (2017) 'Optimization of surface roughness and cutting temperature in high-pressure coolant-assisted hard turning using Taguchi method', The International Journal of Advanced Manufacturing Technology. Springer London, 88(1–4), pp. 739–753. doi: 10.1007/s00170-016-8810-2.

[84] Mia, M. et al. (2017) 'Effect of time-controlled MQL pulsing on surface roughness in hard turning by statistical analysis and artificial neural network', The International Journal of Advanced Manufacturing Technology. Springer London, 91(9–12), pp. 3211–3223. doi: 10.1007/s00170-016-9978-1.

[85] Mia, M. (2017) 'Multi-response optimization of end milling parameters under through-tool cryogenic cooling condition', Measurement. Elsevier, 111, pp. 134–145. doi: 10.1016/J.MEASUREMENT.2017.07.033.

[86] Mia, M. (2018) 'Mathematical modeling and optimization of MQL assisted end milling characteristics based on RSM and Taguchi method', Measurement. Elsevier, 121, pp. 249–260. doi: 10.1016/J.MEASUREMENT.2018.02.017.

[87] Mia, M. et al. (2018) 'Multi-objective optimization of chip-tool interaction parameters using Grey-Taguchi method in MQL-assisted turning', Measurement. Elsevier, 129, pp. 156–166. doi: 10.1016/J.MEASUREMENT.2018.07.014.

[88] Mia, M. et al. (2018) 'Taguchi S/N based optimization of machining parameters for surface roughness, tool wear and material removal rate in hard turning under MQL cutting condition', Measurement. Elsevier, 122, pp. 380–391. doi: 10.1016/J.MEASUREMENT.2018.02.016.

[89] Mia, M. and Dhar, N. R. (2018) 'Modeling of Surface Roughness Using RSM, FL and SA

in Dry Hard Turning', Arabian Journal for Science and Engineering. Springer Berlin Heidelberg, 43(3), pp. 1125–1136. doi: 10.1007/s13369-017-2754-1.

[90] Miguélez, H. et al. (2006) 'Numerical modelling of orthogonal cutting: Influence of cutting conditions and separation criterion', Journal de Physique IV (Proceedings). EDP Sciences, 134, pp. 417–422. doi: 10.1051/jp4:2006134064.

[91] Mohanty, A. et al. (2016) 'On applicability of multilayer coated tool in dry machining of aerospace grade stainless steel', Materials and Manufacturing Processes. Taylor & Francis, 31(7), pp. 869–879. doi: 10.1080/10426914.2015.1070413.

[92] Mondal, K. et al. (2016) 'An Investigation on Turning Hardened Steel Using Different Tool Inserts', Materials and Manufacturing Processes. Taylor & Francis, 31(13), pp. 1770–1781. doi: 10.1080/10426914.2015.1117634.

[93] Moreno, L. H. et al. (2010) 'Wear evaluation of WC inserts coated with TiN/TiAlN multinanolayers', Journal of the Brazilian Society of Mechanical Sciences and Engineering. The Brazilian Society of Mechanical Sciences and Engineering, 32(2), pp. 114–118. doi: 10.1590/S1678-58782010000200003.

[94] Mubarak, A. et al. (2008) 'Effect of coating thickness on the properties of tin coatings deposited on tool steels using cathodic arc pvd technique', Surface Review and Letters. World Scientific Publishing Company , 15(4), pp. 401–410. doi: 10.1142/S0218625X08011524.

[95] Musavi, S. H., Davoodi, B. and Niknam, S. A. (2018) 'Environmental-friendly turning of A286 superalloy', Journal of Manufacturing Processes. Elsevier, 32, pp. 734–743. doi: 10.1016/J.JMAPRO.2018.04.005.

[96] Noordin, M. Y. et al. (2007) 'Dry turning of tempered martensitic stainless tool steel using coated cermet and coated carbide tools', Journal of Materials Processing Technology, 185(1–3), pp. 83–90. doi: 10.1016/j.jmatprotec.2006.03.137.

[97] Noordin, M. . et al. (2004) 'Application of response surface methodology in describing the performance of coated carbide tools when turning AISI 1045 steel', Journal of Materials Processing Technology, 145(1), pp. 46–58. doi: 10.1016/S0924-0136(03)00861-6.

[98] Nouari, M. and Ginting, a. (2006) 'Wear characteristics and performance of multi-layer CVD-coated alloyed carbide tool in dry end milling of titanium alloy', Surface and Coatings Technology, 200(18–19), pp. 5663–5676. doi: 10.1016/j.surfcoat.2005.07.063.

[99] Oraby, S. E. and Hayhurst, D. R. (1991) 'Development of models for tool wear force relationships in metal cutting', International Journal of Mechanical Sciences. Pergamon, 33(2), pp. 125–138. doi: 10.1016/0020-7403(91)90062-8.

[100] Özel, T. (2006) 'The influence of friction models on finite element simulations of machining', International Journal of Machine Tools and Manufacture. Pergamon, 46(5), pp. 518–530. doi: 10.1016/J.IJMACHTOOLS.2005.07.001.

[101] Ozel, T. et al.. (2005) 'Effects of cutting edge geometry, workpiece hardness, feed rate and cutting speed on surface roughness and forces in finish turning of hardened AISI H13 steel', The International Journal of Advanced Manufacturing Technology. Springer-Verlag, 25(3–4), pp. 262–269. doi: 10.1007/s00170-003-1878-5.

[102] Özel, T. and Zeren, E. (2005) 'Finite Element Modeling of Stresses Induced by High Speed Machining With Round Edge Cutting Tools', in Manufacturing Engineering and Materials Handling, Parts A and B. ASME, pp. 1279–1287. doi: 10.1115/IMECE2005-81046.

[103] Pal, S. et al. (2011) 'Tool wear monitoring and selection of optimum cutting conditions with progressive tool wear effect and input uncertainties', Journal of Intelligent Manufacturing. Springer US, 22(4), pp. 491–504. doi: 10.1007/s10845-009-0310-x.

[104] Pal, S. and Deevi, S. . (2003) 'Single layer and multilayer wear resistant coatings of (Ti,Al)N: a review', Materials Science and Engineering: A, 342(1), pp. 58–79. doi: 10.1016/S0921-5093(02)00259-9.

[105] Panda, A. et al. (2018) 'Investigation of Flank Wear in Hard Turning of AISI 52100 Grade Steel Using Multilayer Coated Carbide and Mixed Ceramic Inserts', Procedia Manufacturing. Elsevier, 20, pp. 365–371. doi: 10.1016/J.PROMFG.2018.02.053.

[106] Pantalé, O. et al. (2004) '2D and 3D numerical models of metal cutting with damage effects', Computer Methods in Applied Mechanics and Engineering. North-Holland, 193(39–41), pp. 4383–4399. doi: 10.1016/J.CMA.2003.12.062.

[107] Park, K.-H. et al. (2015) 'The effect of cryogenic cooling and minimum quantity lubrication on end milling of titanium alloy Ti-6Al-4V †', Journal of Mechanical Science and Technology, 29(12), pp. 5121–5126. doi: 10.1007/s12206-015-1110-1.

[108] Pervaiz, S. et al. (2018) 'Exploring the influence of constitutive models and associated parameters for the orthogonal machining of Ti6Al4V', IOP Conference Series: Materials Science and Engineering. IOP Publishing, 346(1), p. 12058. doi: 10.1088/1757-899X/346/1/012058.

[109] Poulachon, G. et al. (2005) 'An experimental investigation of work material microstructure effects on white layer formation in PCBN hard turning', International Journal of Machine Tools and Manufacture. Pergamon, 45(2), pp. 211–218. doi: 10.1016/J.IJMACHTOOLS.2004.07.009.

[110] Poulachon, G. and Moisan, A. L. (2000) 'Hard Turning: Chip Formation Mechanisms and Metallurgical Aspects', Journal of Manufacturing Science and Engineering. American Society of Mechanical Engineers, 122(3), p. 406. doi: 10.1115/1.1285891.

[111] Priyadarshini, A. et al. (2012) 'Finite Element Modeling of Chip Formation in Orthogonal Machining', in Statistical and Computational Techniques in Manufacturing. Berlin, Heidelberg: Springer Berlin Heidelberg, pp. 101–144. doi: 10.1007/978-3-642-25859-6_3.

[112] Quiza, R. et al. (2008) 'Comparing statistical models and artificial neural networks on predicting the tool wear in hard machining D2 AISI steel', The International Journal of

Advanced Manufacturing Technology. Springer-Verlag, 37(7–8), pp. 641–648. doi: 10.1007/s00170-007-0999-7.

[113] Rabiei, F. et al. (2015) 'Performance improvement of minimum quantity lubrication (MQL) technique in surface grinding by modeling and optimization', Journal of Cleaner Production. Elsevier, 86, pp. 447–460. doi: 10.1016/J.JCLEPRO.2014.08.045.

[114] Rafaja, D. et al. (2007) 'Microstructure and hardness of nanocrystalline Ti1−x−yAlxSiyN thin films', Materials Science and Engineering: A, 462(1), pp. 279–282. doi: 10.1016/j.msea.2005.11.086.

[115] Ramesh, A. et al. (2005) 'Analysis of white layers formed in hard turning of AISI 52100 steel', Materials Science and Engineering: A. Elsevier, 390(1–2), pp. 88–97. doi: 10.1016/J.MSEA.2004.08.052.

[116] Ramesh, S. et al. (2009) 'Experimental study on machining of titanium alloy (Ti64) by CVD and PVD coated carbide inserts', International Journal of Manufacturing Technology and Management, 17(4), p. 373. doi: 10.1504/IJMTM.2009.023954.

[117] Rashid, W. Bin and Goel, S. (2016) 'Advances in the surface defect machining (SDM) of hard steels', Journal of Manufacturing Processes. Elsevier, 23, pp. 37–46. doi: 10.1016/J.JMAPRO.2016.05.007.

[118] Rech, J. and Moisan, A. (2003) 'Surface integrity in finish hard turning of case-hardened steels', International Journal of Machine Tools and Manufacture. Pergamon, 43(5), pp. 543–550. doi: 10.1016/S0890-6955(02)00141-4.

[119] Rocha, L. C. S. et al. (2017) 'Robust multiple criteria decision making applied to optimization of AISI H13 hardened steel turning with PCBN wiper tool', The International Journal of Advanced Manufacturing Technology. Springer London, 89(5–8), pp. 2251–2268. doi: 10.1007/s00170-016-9250-8.

[120] Rosa, G. C. et al. (2017) 'Wear analysis of ultra-fine grain coated carbide tools in hard turning of AISI 420C stainless steel', Wear, 376–377, pp. 172–177. doi: 10.1016/j.wear.2017.01.088.

[121] Roy, P. et al. (2009) 'Machinability study of pure aluminium and Al–12% Si alloys against uncoated and coated carbide inserts', International Journal of Refractory Metals and Hard Materials, 27(3), pp. 535–544. doi: 10.1016/j.ijrmhm.2008.04.008.

[122] Sadat, A. B. et al. (1991) 'Plastic deformation analysis in machining of Inconel-718 nickel-base superalloy using both experimental and numerical methods', International Journal of Mechanical Sciences, 33(10), pp. 829–842. doi: 10.1016/0020-7403(91)90005-N.

[123] Sahin, Y. and Motorcu, A. R. (2005) 'Surface roughness model for machining mild steel with coated carbide tool', Materials & Design. Elsevier, 26(4), pp. 321–326. doi: 10.1016/J.MATDES.2004.06.015.

[124] Sahoo, A. K. and Sahoo, B. (2012) 'Experimental investigations on machinability aspects

in finish hard turning of AISI 4340 steel using uncoated and multilayer coated carbide inserts', Measurement. Elsevier, 45(8), pp. 2153–2165. doi: 10.1016/J.Measurement.2012.05.015.

[125] Sargade, V. G. et al. (2011) 'Effect of Coating Thickness on the Characteristics and Dry Machining Performance of TiN Film Deposited on Cemented Carbide Inserts Using CFUBMS', Materials and Manufacturing Processes. Taylor & Francis Group , 26(8), pp. 1028–1033. doi: 10.1080/10426914.2010.526978.

[126] Sayuti, M. et al. (2014) 'Novel uses of SiO2 nano-lubrication system in hard turning process of hardened steel AISI4140 for less tool wear, surface roughness and oil consumption', Journal of Cleaner Production, 67, pp. 265–276. doi: 10.1016/j.jclepro.2013.12.052.

[127] Sencer, B. and Maulimov, M. (2018) 'A new turning system assisted by chip-pulling', Journal of Manufacturing Processes. Elsevier, 34, pp. 734–739. doi: 10.1016/J.JMAPRO.2018.03.044

[128] Shi, J. and Liu, C. R. (2004) 'The Influence of Material Models on Finite Element Simulation of Machining', Journal of Manufacturing Science and Engineering. American Society of Mechanical Engineers, 126(4), p. 849. doi: 10.1115/1.1813473.

[129] Shi, J. et al. (2006) 'Modelling White Layer Thickness Based on the Cutting Parameters of Hard Machining', Proceedings of the Institution of Mechanical Engineers, Part B: Journal of Engineering Manufacture. SAGE PublicationsSage UK: London, England, 220(2), pp. 119–128. doi: 10.1243/095440505X32977.

[130] Siller, H. R. et al. (2009) 'Study of face milling of hardened AISI D3 steel with a special design of carbide tools', The International Journal of Advanced Manufacturing Technology. Springer-Verlag, 40(1–2), pp. 12–25. doi: 10.1007/s00170-007-1309-0.

[131] Sikdar, S. K. and Chen, M. (2002) 'Relationship between tool flank wear area and component forces in single point turning', Journal of Materials Processing Technology. Elsevier, 128(1–3), pp. 210–215. doi: 10.1016/S0924-0136(02)00453-3.

[132] Sivaraman, V. and Prakash, S. (2017) 'Recent developments in turning hardened steels - A review', IOP Conference Series: Materials Science and Engineering, 197(1). doi: 10.1088/1757-899X/197/1/012009.

[133] Shaw, M. C. and Vyas, A. (1994) 'Heat-Affected Zones in Grinding Steel', CIRP Annals. Elsevier, 43(1), pp. 279–282. doi: 10.1016/S0007-8506(07)62213-6.

[134] Sharma, P. et al. (2015) 'Investigation of effects of nanofluids on turning of AISI D2 steel using minimum quantity lubrication', Journal of Cleaner Production, 108, pp. 72–79. doi: 10.1016/j.jclepro.2015.07.122.

[135] Su, G. and Liu, Z. (2012) 'Wear characteristics of nano TiAlN-coated carbide tools in ultra-high speed machining of AerMet100', Wear. Elsevier, 289, pp. 124–131. doi: 10.1016/j.wear.2012.04.005.

[136] Su, G. and Liu, Z. (2012) 'Analytical and experimental study on formation of concentrated shear band of saw tooth chip in high-speed machining', The International Journal of Advanced Manufacturing Technology, 65(9–12), pp. 1735–1740. doi: 10.1007/s00170-012-4295-9.

[137] Suresh, R. et al. (2012) 'Some studies on hard turning of AISI 4340 steel using multilayer coated carbide tool', Measurement. Elsevier Ltd, 45(7), pp. 1872–1884. doi: 10.1016/j.measurement.2012.03.024.

[138] Sutter, G. and List, G. (2013) 'Very high speed cutting of Ti–6Al–4V titanium alloy – change in morphology and mechanism of chip formation', International Journal of Machine Tools and Manufacture. Pergamon, 66, pp. 37–43. doi: 10.1016/J.IJMACHTOOLS.2012.11.004.

[139] Suresh, R. et al. (2012a) 'Machinability investigations on hardened AISI 4340 steel using coated carbide insert', International Journal of Refractory Metals and Hard Materials. Elsevier, 33, pp. 75–86. doi: 10.1016/J.IJRMHM.2012.02.019.

[140] Tang, B. T. et al. (2014) 'Influence of Temperature and Deformation on Phase Transformation and Vickers Hardness in Tailored Tempering Process: Numerical and Experimental Verifications', Journal of Manufacturing Science and Engineering, 136(5), p. 51018. doi: 10.1115/1.4027816.

[141] Takabi, J., Sadeghinia, H. and Razfar, M. R. (2007) Simulation of Orthogonal Cutting Process Using Arbitrary Lagrangian-Eulerian Approach. Available at: https://www.researchgate.net/publication/255610812

[142] Thakur, A. and Gangopadhyay, S. (2016) 'Dry machining of nickel-based super alloy as a sustainable alternative using TiN/TiAlN coated tool', Journal of Cleaner Production. Elsevier, 129, pp. 256–268. doi: 10.1016/J.JCLEPRO.2016.04.074.

[143] Trejo-Hernandez, M. et al. (2010) 'FPGA-Based Fused Smart-Sensor for Tool-Wear Area Quantitative Estimation in CNC Machine Inserts', Sensors, 10(4), pp. 3373–3388. doi: 10.3390/s100403373.

[144] Tuffy, K. et al. (2004) 'Determination of the optimum TiN coating thickness on WC inserts for machining carbon steels', Journal of Materials Processing Technology. Elsevier, 155–156, pp. 1861–1866. doi: 10.1016/J.JMATPROTEC.2004.04.277.

[145] Ucun, İ. and Aslantas, K. (2010) 'Numerical simulation of orthogonal machining process using multilayer and single-layer coated tools', The International Journal of Advanced Manufacturing Technology, 54(9–12), pp. 899–910. doi: 10.1007/s00170-010-3012-9.

[146] Umbrello, D. and Filice, L. (2009) 'Improving surface integrity in orthogonal machining of hardened AISI 52100 steel by modeling white and dark layers formation', CIRP Annals. Elsevier, 58(1), pp. 73–76. doi: 10.1016/J.CIRP.2009.03.106.

[147] Umbrello, D. and Rotella, G. (2012) 'Experimental analysis of mechanisms related to white layer formation during hard turning of AISI 52100 bearing steel', Materials Science and

Technology. Taylor & Francis, 28(2), pp. 205–212. doi: 10.1179/1743284711Y.0000000020.

[148] Unesco, S. et al. (1986) International journal of technology management = Journal international de la gestion technologique., International Journal of Manufacturing Technology and Management. Inderscience Enterprises. Available at: https://econpapers.repec.org/article/idsijmtma/v_3a17_3ay_3a2009_3ai_3a4_3ap_3a373-385.htm (Accessed: 21 February 2019)

[149] Vannan, R. R. R. M. et al. (2017) 'Effect of physical vapor deposited bilayer (AlCrN?+?TiAlN) coating on high-speed steel single point cutting tool', Materials and Manufacturing Processes. Taylor & Francis, 32(4), pp. 373–376. doi: 10.1080/10426914.2016.1176178.

[150] Wang, B. and Liu, Z. (2016) 'Evaluation on fracture locus of serrated chip generation with stress triaxiality in high speed machining of Ti6Al4V', Materials & Design. Elsevier, 98, pp. 68–78. doi: 10.1016/J.MATDES.2016.03.012.

[151] Xie, L. J. et al. (2005) '2D FEM estimate of tool wear in turning operation', Wear. Elsevier, 258(10), pp. 1479–1490. doi: 10.1016/J.WEAR.2004.11.004.

[152] Yallese, M. A. et al. (2009) 'Hard machining of hardened bearing steel using cubic boron nitride tool', Journal of Materials Processing Technology. Elsevier, 209(2), pp. 1092–1104. doi: 10.1016/J.JMATPROTEC.2008.03.014.

[153] Yan, D. et al. (1995) 'A multi-sensor strategy for tool failure detection in milling', International Journal of Machine Tools and Manufacture. Pergamon, 35(3), pp. 383–398. doi: 10.1016/0890-6955(94)E0021-A.

[154] Yigit, R. et al. (2008) 'Tool life performance of multilayer hard coatings produced by HTCVD for machining of nodular cast iron', International Journal of Refractory Metals and Hard Materials. Elsevier, 26(6), pp. 514–524. doi: 10.1016/J.IJRMHM.2007.12.003.

[155] Zhang, X.-M. et al. (2016) 'Effects of Process Parameters on White Layer Formation and Morphology in Hard Turning of AISI52100 Steel', Journal of Manufacturing Science and Engineering. American Society of Mechanical Engineers, 138(7), p. 74502. doi: 10.1115/1.4032769.

[156] Zhang, P. and Liu, Z. (2017) 'On sustainable manufacturing of Cr-Ni alloy coatings by laser cladding and high-efficiency turning process chain and consequent corrosion resistance', Journal of Cleaner Production. Elsevier, 161, pp. 676–687. doi: 10.1016/j.jclepro.2017.05.169.

[157] Zhang, F. et al. (2018) 'White and dark layer formation mechanism in hard cutting of AISI52100 steel', Journal of Manufacturing Processes. Elsevier, 32, pp. 878–887. doi: 10.1016/J.JMAPRO.2018.04.011.

[158] Zhou, J. M. et al. (2003) 'The monitoring of flank wear on the CBN tool in the hard turning process', The International Journal of Advanced Manufacturing Technology. Springer-

Verlag, 22(9–10), pp. 697–702. doi: 10.1007/s00170-003-1569-2.

[159] 4340 Steel | 36CrNiMo4 | 1.6511 | EN24 | SNCM439 - Otai Special Steel (no date). Available at: http://www.astmsteel.com/product/4340-steel-aisi/.

List of Publications

Papers published in Journals:

1. Alok, A. and Das, M. (2018) 'Cost-effective way of hard turning with newly developed HSN2-coated tool', Materials and Manufacturing Processes, 33(9). doi: 10.1080/10426914.2017.1388521
2. Alok, A. and Das, M. (2019) 'Multi-objective optimization of cutting parameters during sustainable dry hard turning of AISI 52100 steel with newly develop HSN2-coated carbide insert', Measurement. Elsevier, 133, pp. 288–302. doi: 10.1016/J.MEASUREMENT.2018.10.009.

Papers communicated to Journals:

1. Alok, A. and Das, M. 'White layer analysis of hard turned AISI 52100 steel with fresh tip of newly developed HSN^2 coated insert', journal of manufacturing process.

Papers published in conference proceedings:

1. Alok, A. and Das, M. (2017) 'Numerical simulation of orthogonal hard turning operation of AISI 4340 work piece using Al2O3 coated carbide tool', www.copen.ac.in/proceedings/copen10/copen/101.pdf(n.d.) 3–7, ISBN: 978-93-80689-28-9.
2. Alok, A. and Das, M. (2018) Analysis of chip formation of AISI 52100 steel during hard turning with newly developed HSN2 coated carbide insert, International Conference on Recent Innovations and Developments in Mechanical Engineering, NIT Meghalaya, Shillong, India, November 8 – 10.
3. Alok, A. and Das, M. (2019) 'A Finite element based simulation for hard turning operation of AISI 4340 work piece using Al_2O_3 coated carbide tool insert' International Conference on Computational Methods in Manufacturing, IIT Guwahati, India, March 8-9.